SYNTHESIS OF NEW TITANIUM COMPLEXES BEARING A BIDENTATE MONOANIONIC INVERSELY-POLARIZED PHOSPHAALKENE-ENOLATE LIGAND AND THEIR ACTIVITY IN OLEFIN POLYMERIZATION

MATTHEW ALEXANDER WIEBE

A THESIS SUBMITTED TO THE FACULTY OF GRADUATE STUDIES IN PARTIAL FULFULLMENT OF THE REQUIREMENTS FOR THE DEGREE OF

MASTER OF SCIENCE

GRADUATE PROGRAM IN CHEMISTRY
YORK UNIVERSITY
TORONTO, ONTARIO

October 2019

Abstract

The synthesis and characterization of several inversely-polarized phosphaalkenes, including the first ring-expanded inversely-polarized hydrido-phosphaalkene and imidazolidine-based inversely-polarized phosphaalkene-enolate ligand precursors, are herein reported. Coordination of the imidazolidine-based ligands to titanium was studied. Minimal decomposition (6%) of the isolated complex occurred over several days at 60 °C. The titanium complexes were explored computationally where it was revealed that there is evidence for the phosphorus atom of the bound ligand to donate an additional pair of electrons to Ti, resulting in a large stabilization of 18.2 kcal $\cdot$ mol^{-1}. Furthermore, the titanium complex has activity up to 5.64 kg$_{PE}$ $\cdot$ mol$^{-1}_{Ti}$ $\cdot$ h^{-1} in the polymerization of ethylene with little decomposition of the active species over several hours. The polymer produced was high-density polyethylene with an average molecular weight of 17.6 kDa and a T_m of 131 °C.

Acknowledgements

First of all, I would like to thank the National Science and Engineering Research Council of Canada, the Government of Ontario, and Indspire for scholarships and awards during my time at York University. I am also grateful for the time Professor Gino G. Lavoie has invested in my growth as scientist. Dr. Lavoie has challenged me over my years in his research group which has taught me a lot about how I wish to supervise my own group if I should have one in the future.

I am thankful for the input my committee members have provided. I am particularly grateful for the time Professor Chris Caputo has invested in the preparation of my thesis for defence and submission. I am indebted to Dr. Howard Hunter who has been instrumental in my understanding of the structural characteristics of the compounds I have prepared during my studies .

I am extremely thankful for my lab colleagues, especially Juan E. R. Villanueva and Brandon S. Khan. Juan and Brandon's work ethic has been an inspiration and I am extremely lucky to have studied with them. I am thankful for friendships made with several members of the Orellana and Caputo groups. I am also grateful for the community outside of the chemistry department at York University who have brought warmth and a welcoming environment to this concrete campus.

I am also grateful for the unconditional love from my parents and grandparents, who have supported me throughout my time far away from home. Lastly, I am grateful for the support from my elders and my community in Manitoba. This achievement is much more triumphant knowing I have my loved ones cheering me on from home.

Table of Contents

List of Tables

List of Figures

List of Schemes

List of Abbreviations

Ar	Aryl
B3LYP	Becke, 3-Parameter, Lee-Yang-Parr
BCF	Tris(pentafluorophenyl)borane
Cp	Cyclopentadienyl
DFT	Density Functional Theory
Dipp	2,6-Diisopropylphenyl
DMSO	Dimethyl sulfoxide
E	Electrophile
eq	Equation
equiv	Equivalent
HDPE	High Density Polyethylene
HMDS	Hexamethyldisilazide
ICI	Imperial Chemical Industries
IPP	Inversely-Polarized Phosphaalkene
IR	Infrared
L	Neutral Ligand
LDPE	Low Density Polyethylene
m	*meta*
MAO	Methylaluminoxane
Me	Methyl
Mes	2,4,6-Trimethylphenyl
MMAO-12	Modified Methylaluminoxane

NBO	Natural Bond Orbital
NHC	N-Heterocyclic Carbene
NMFRLP	Nitrosyl Mediated Free-Radical Living Polymerization
NMR	Nuclear Magnetic Resonance
Nu	Nucleophile
o	*ortho*
OTf⁻	Triflate anion
p	*para*
PE	Polyethylene
Ph	Phenyl
ppm	parts per million
PTFE	Polytetrafluoroethylene
R	Alkyl or aryl organic fragment
rt	Room Temperature
SHOP	Shell Higher Olefin Process
TEMPO	2,2,6,6-tetramethyl-1-piperidinyloxy
TBDMS	*tert*-Butyldimethylsilyl
THF	Tetrahydrofuran
TMS	Trimethylsilyl group

1. Introduction

1.1 Coordination Chemistry

Coordination chemistry is the study of compounds that consist of a central metal atom surrounded by either neutral or anionic electron donors called ligands.[1] Ligands are typically classified as L- or X-type for neutral or anionic donors. Formally, an L-type ligand will donate two electrons to the metal centre while the X-type will donate one electron to the metal atom bond and oxidize the metal by one electron, increasing its oxidation state by one (**Figure 1**, left and middle).[1,2] Additionally, ligands can have multiple donor atoms, denoted by denticity, that bind the metal and often result in a more stable species through the chelate effect. These ligands can be labelled using the donor atoms. For example, the monoanionic tridentate diarylamido selenium ligand could be labelled "SeNSe" as it binds metals through the two selenium atoms and the amido group (**Figure 1**, right).[3] Coordination compounds with metal–carbon bonds are further classified as organometallic complexes. These ligands can modulate the reactivity of the resulting coordination compound and facilitate chemical transformations that are otherwise difficult to achieve. If regenerated through the reaction, these complexes are called catalysts.
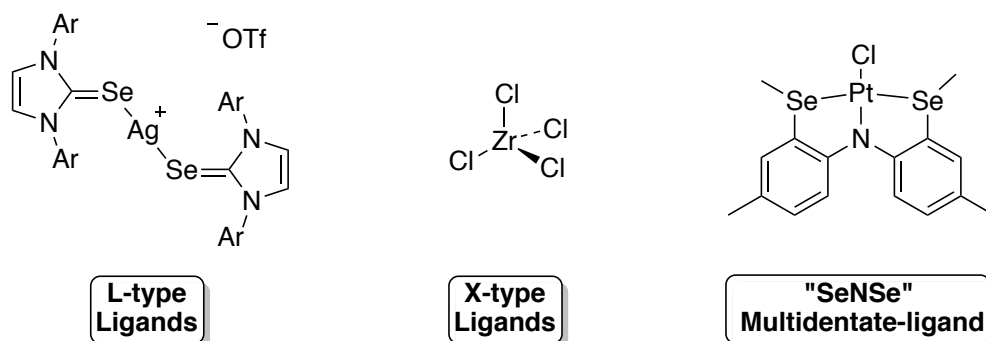
Figure 1: Examples of coordination compounds bearing L-type, X-type and multidentate ligands.

1.2 Inversely-Polarized Phosphaalkenes

Inversely-Polarized Phosphaalkenes (IPPs) are a structural motif in which the carbon–phosphorus bond has a polarization that is opposite to that predicted by Pauling electronegativity (**Figure 2**).[4] The inverse nature of the
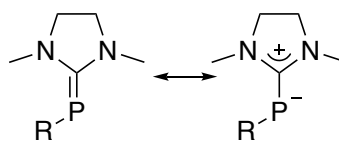
Figure 2: Two canonical forms of the inversely-polarized phosphaalkene.

polarity of this bond arises from the strongly σ-donating carbenoid carbon and the π-Lewis basic nitrogen atoms adjacent to the carbon centre of the phosphaalkene.[7,8] These IPPs are prepared from widely available N-heterocyclic carbenes (NHCs), which possess a broad range of steric and donor/acceptor properties.[7]

Typically, NHCs have poor π-acidity owing to the donation of the nitrogen lone pair of electrons into the p-orbital of the carbenoid carbon (**Figure 3**).[5] However, by carefully selecting the substituents on the nitrogen atoms (R^1), and the backbone, including the substituent X, the π-acidity of the carbene can be tuned (**Figure 3**).[6] For example, the presence of either aryl or alkyl groups flanking the nitrogen atoms can have a significant impact on the π-acidity of the carbenoid carbon. An electron withdrawing group (EWG) will increase the Lewis acidity of the p-orbital of the carbenoid carbon while an electron donating group (EDG) will decrease it.[10]
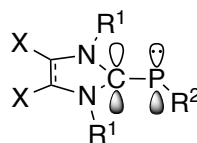
R[1]: Alkyl, Aryl
R[2]: Aryl, Hydride
X: EWG/EDG

Figure 3: C=P bond p-orbitals of an inversely polarized phosphaalkene.

The backbone of the NHC also provides ample opportunities for increasing the π-acidity of the carbenoid carbon through the addition of electron-withdrawing groups such as chloride or acyl groups (**Figure 3**). Furthermore, introduction of a saturated backbone or expansion of the backbone results in an increase of the π-acidity of the carbenoid

carbon. This has a direct influence on the local electron density of the phosphorus atom as a more π-acidic carbenoid carbon is capable of accepting more electron density from the "phosphinidene" resulting in more double-bond character.[7]

Since the local electron density at phosphorus of IPPs is dependent on the π-acidity of the carbenoid carbon, ^{31}P nuclear magnetic resonance (NMR) spectroscopy can be used to measure the level of shielding the phosphorus atom experiences (**Figure 4**).[7] Bertrand explored the use of the ^{31}P NMR spectra chemical shifts of IPPs to gauge the π-acidity of many carbenes and found that the IPPs of more π-acidic carbenes resonate at more positive (downfield) chemical shifts, while less π-acidic carbenes resonate at more negative (upfield) chemical shift values (**Figure 4**).
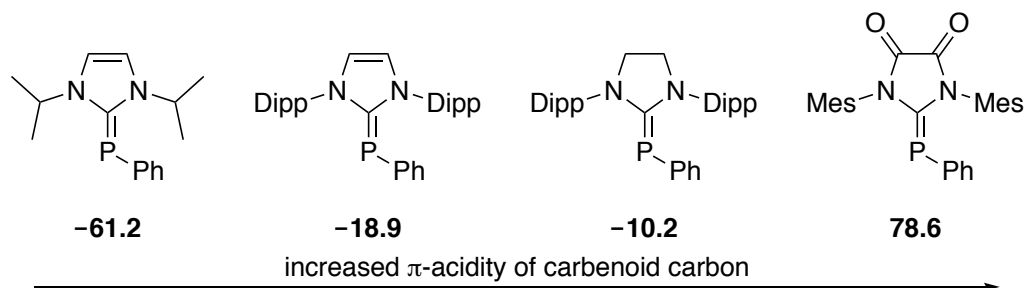
Figure 4: ^{31}P NMR chemical shifts (ppm) for selected inversely-polarized phosphaalkenes.

The structure of IPPs also allows for variation of the substituent on the phosphorus atom (**Figure 3**). In Figure 4, the structure of several IPPs are given with phenyl substituents. However inversely-polarized phosphaalkenes bearing a hydride (NHC=PH) have also been prepared.[7] Hydrido-IPPs resonate in the ^{31}P NMR spectrum at chemical shift values more upfield than their phenyl-bearing counterparts as they have a more electron-rich phosphorus atom.[8]

There are several strategies to prepare inversely-polarized phosphaalkenes (**Figure 5**). In the method described by Arduengo, a free carbene is reacted with an organocyclophosphane yielding the inversely-polarized phosphaalkene (i).[9] Alternatively, the reaction of a free carbene with dichlorophenylphosphine gives an intermediate salt that can be reduced to an inversely-polarized phosphaalkene (ii).[7]
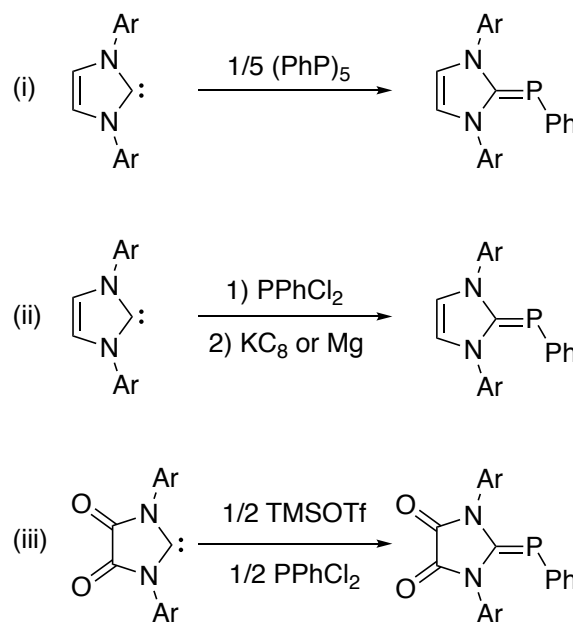
Figure 5: Synthetic strategies for accessing phenyl-substituted IPPs.

These reactions have shown to produce the IPPs of the archetypical NHCs; however, the IPPs of more π-acidic carbenes require a different strategy owing to their reduced nucleophilicity. Hudnall has addressed this issue by first increasing the electrophilicity of the tertiary phosphine through a reaction with trimethylsilyl triflate (TMSOTf), accessing chlorophenylphosphine triflate.[10] Then, the addition of this reactive species to two equivalents of free carbene, where one equivalent acts as the reducing agent, yields the inversely-polarized phosphaalkene (iii).[10]

An alternative synthetic route must be used for the synthesis of the more electron-rich hydrido-IPPs. Gudat has reported the synthesis of hydrido-IPPs of imidazolium and imidazolinium salts bearing either alkyl or aryl groups with Na_3P_7, a highly reactive phosphinidene source (**Scheme 1**).[11] These phosphaalkenes can also be accessed from their corresponding azole salt using sodium phosphaaethethynolate, Na(OCP).[8]

Scheme 1: Synthetic routes to Inversely-polarized phosphaalkenes from Imidazolium salts
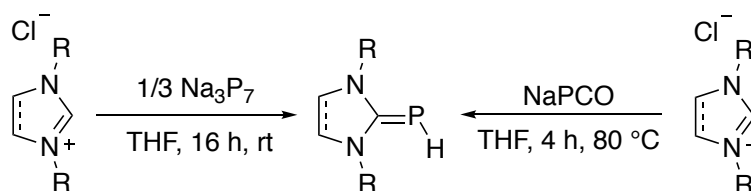
1.3 Coordination Chemistry of Inversely-Polarized Phosphaalkenes

The coordination chemistry of inversely-polarized phosphaalkenes is largely limited to examples of monodentate coordination, where the Lewis basic donor of the ligand is solely the phosphorus atom. The first example of a metal-bound inversely-polarized phosphaalkene was published by the Lavoie group in 2014 (**Scheme 2**, top).[12] The addition of a phenyl-substituted inversely-polarized phosphaalkene to the ruthenium-based Grubbs first-generation catalyst and its effect on olefin metathesis activity was studied (**Scheme 2**, bottom).

Scheme 2: Coordination of an IPP to ruthenium reported by Lavoie.[8]
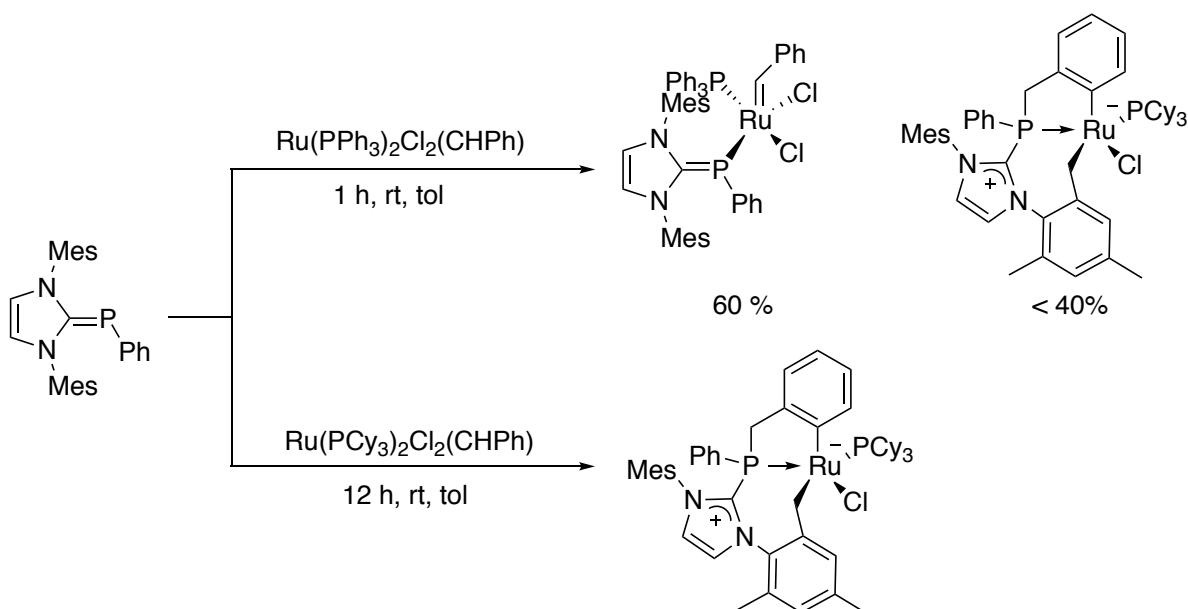
In the addition of one equivalent of IMes=PPh to $RuCl_2(PPh_3)_2(CHPh)$, η^1 coordination of the inversely-polarized phosphaalkene adopting a rare *cis*-chloride conformation was observed.[12] However, this compound was inactive in the ring-closing metathesis of diallylsulfide. The addition of the same IPP to $RuCl_2(PCy_3)_2(CHPh)$ exclusively yielded a product that had undergone two C-H activations. This unusual product was also observed as a minor product with the addition of IMes=PPh to $RuCl_2(PPh_3)_2(CHPh)$.

The coordination of inversely-polarized phosphaalkenes to coinage metals has been studied by the Tamm group (**Scheme 3**).[13] Due to the ability of the inversely-polarized phosphaalkene to access an additional lone pair at phosphorus depending on the canonical structure, both mono- and bimetallic complexes of the coinage metals have been observed.[7] Accessing the mono- or bimetallic complex can be controlled through stoichiometry of reagents as well as through the choice of the metal precursor. For example, the reaction of either CuCl or $AuCl(SMe_2)$ yields the mono- or bimetallic complex depending on the number of equivalents of IPP used (**Scheme 3**, top and centre), while the use of AgCl would result in exclusively a monometallic product (**Scheme 3**, top).[16] Alternatively, the reaction of Cu(OTf) would result in exclusively a bimetallic product (**Scheme 3**, bottom).[16]

Scheme 4: Coordination chemistry of IPPs to coinage metals observed by Tamm *et al.*[16]

The coordination of inversely-polarized phosphaalkenes to the metal carbonyl complexes of group 6 and 9 metals has also been probed by the Tamm group (**Scheme 4**).[14] In order to determine how strongly donating inversely-polarized phosphaalkenes are, the average infrared (IR) stretching frequencies of the carbonyl ligands of a complex bearing an IPP were obtained. It was found that the average carbonyl ligand stretching frequency for the rhodium, tungsten and molybdenum carbonyl complexes bearing an inversely polarized phosphaalkene were much lower than those for carbenes and phosphines. This further confirmed that inversely-polarized phosphaalkenes are overall stronger electron donors, producing a relatively electron-rich metal centre when coordinated.

Scheme 3: Carbonyl complexes bearing an IPP.
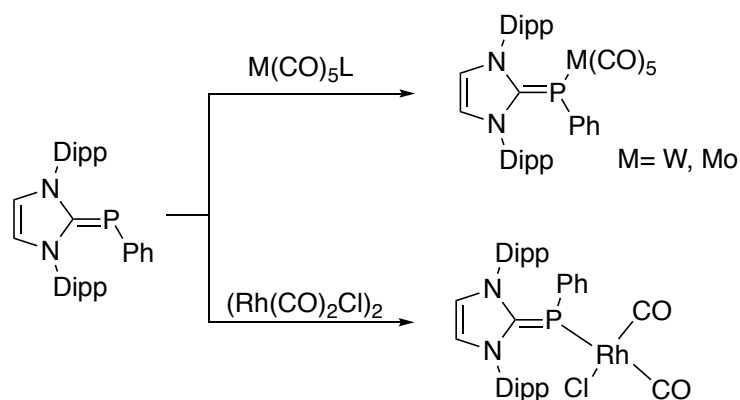
The limited coordination chemistry of inversely-polarized phosphalkenes studied thus far highlights the opportunity to incorporate them in new systems capable of useful

7

transformations. The Lavoie group has highlighted the ability of the inversely-polarized phosphaalkenes to access rare conformations of ruthenium-based complexes, while the Tamm group has shown the phosphorus of IPPs are capable of multiple coordination modes and strong donation to the metal centre. The electron-rich phosphorus centre is an attractive fragment for ligand design where an increase in Lewis basicity of the neutral donor atom results in either higher activity or control over the catalytic transformation.

1.4 Olefin Polymerization

Polymerization is the linkage of many smaller molecules containing functional groups allowing for their reaction with each other (**Scheme 5**).[15] These smaller molecules are known as monomers. Polymerization of olefins (ethylene, propylene, polar vinyl monomers, *etc.*) has allowed for the production of robust materials displaying a wide array of bulk properties such as tensile strength, impact resistance, and adhesive properties.[15] Accessing these olefin-based synthetic materials has been studied in depth since the 1930's, starting with radical chain-growth polymerization, and later ionic and coordination polymerization.[16]

Scheme 5: Polymerization of ethylene using a catalyst.
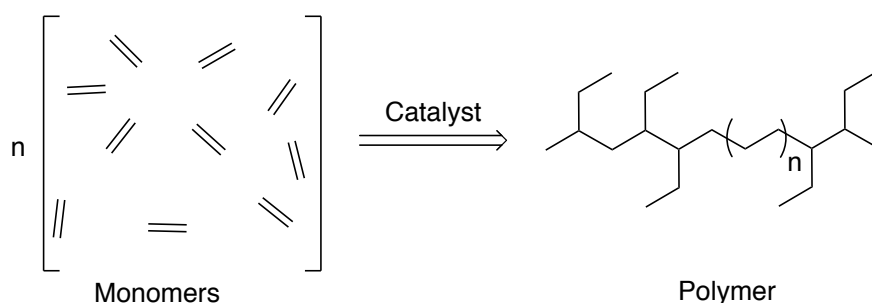
Types of Olefin Polymerization

Polymerization of olefins is typically accessed through a chain-growth mechanism in which the molecular weight of the polymer is increased as monomeric units are added to an activated polymer chain.[15] This is achieved through either a radical, ionic or coordination mechanism. In all three methods there is an initiation, propagation, and termination step. Notably, not all olefins will polymerize under all conditions, each of which offer a set of disadvantages and advantages.

Radical polymerization of olefins was first explored in the 1930's by the Imperial Chemical Industries (ICI), where they accessed low-density polyethylene (LDPE).[16] In radical polymerization, a radical reacts with the monomer yielding a new radical that can react with an additional monomeric unit.[17] In the case of 1,1-disubstitued olefins, this reaction normally occurs in a "head-to-tail" fashion where the radical will selectively react with one end of the olefin over the other (**Scheme 6**). The alternative, "head-to-head" or "tail-to-tail", is disfavoured due to steric hindrance and potential stabilization of radical from the substituents off the 1-carbon of the monomeric unit.[17]

Scheme 6: Initiation and propagation steps of radical polymerization
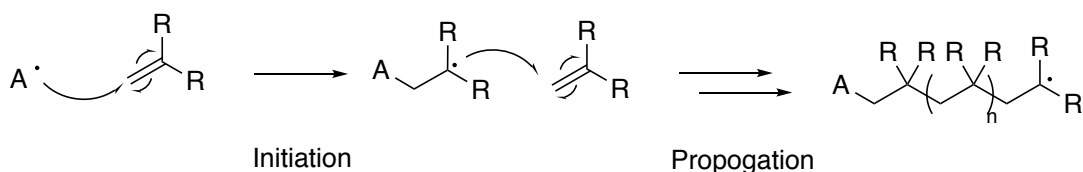
Polymerization initiated by a radical species can be disadvantageous as there is little control over the degree of branching, molecular weight and molecular weight distribution. During the polymerization, a growing polymer can react with another polymer

(**A**), monomer (**B**), initiator (**C**) or solvent (**D**) (**Scheme 7**).[15] This terminates the polymerization process for that chain and produces a new radical for further reaction. Chain transfer reactions are especially detrimental in the radical-initiated polymerization of propylene, as the chain transfer reaction produces a resonance-stabilized allylic radical.[15]

Scheme 7: Types of chain transfer reactions observed in radical polymerization.
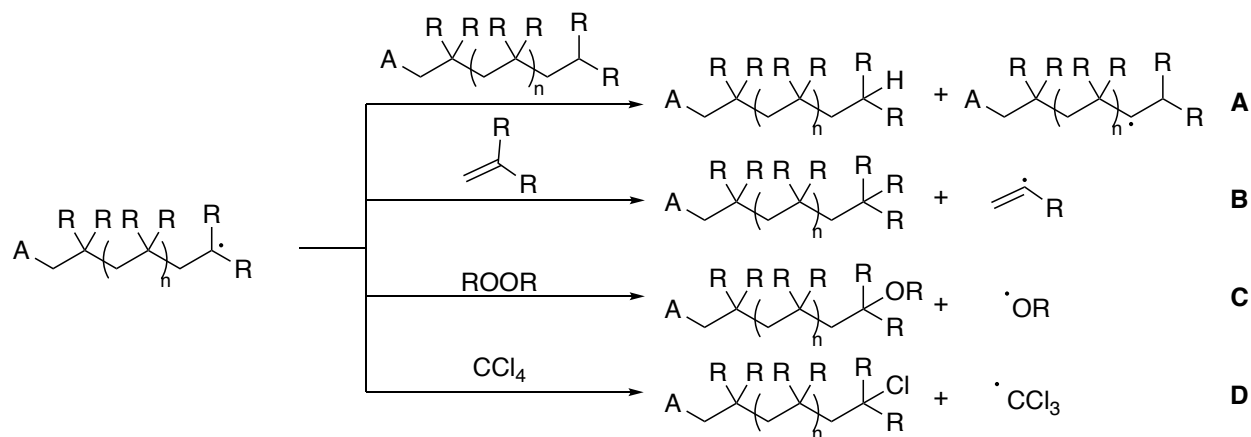
With some monomers, such as tetrafluoroethylene, chain transfer does not occur.[15] In these cases, radical polymerization is advantageous in accessing high molecular weight polymers.[17] Polytetrafluoroethylene (PTFE) is a highly inert material that has found many uses, from non-stick surfaces on cooking pans to valve oil in musical instruments.

Through the use of a stable nitrosyl radical, such as 2,2,6,6-tetramethyl-1-piperidinyloxy (TEMPO), nitrosyl mediated living free-radical polymerization (NMLFRP) of certain monomers can be achieved.[18] Living polymerization is obtained when a growing polymer does not undergo a termination reaction, allowing for the production of polymers with controlled molecular weights and of block copolymers. Under NMLFRP conditions, TEMPO can reversibly terminate a growing polymer chain by trapping the radical of the

terminal unit.[19] The labile monomer–TEMPO bond in the dormant species regenerates the necessary radical allowing polymer growth.[19] Therefore, radical polymerization can produce useful polymers and in some cases, in a living manner.

Alternatively, polymerization of olefins can be mediated by either cationic or anionic polymerization.[15] Similar to radical polymerization, ionic polymerization requires an initiation step. In ionic polymerization a species reacts with a monomeric unit forming an ion that will react with another monomer (**Figure 6**).[15] This initiation species is often a Lewis or Brønsted acid for cationic polymerization and an organolithium for anionic polymerization.[20]
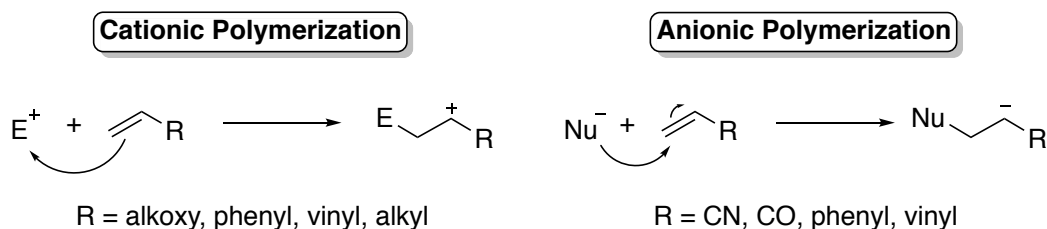
Figure 6: Initiation step of cationic and anionic polymerization.

Where radical polymerization will yield polymers of most monomers, ionic polymerization is more selective and only works with monomers bearing either cation-stabilizing electron donating groups, or anion-stabilizing electron withdrawing groups.[15] Furthermore, cationic polymerization relies on solvation and low temperatures to stabilize the ionic species and limit terminating reactions to access high-molecular weight polymers.[15] Chain transfer reactions are also prevalent in ionic polymerization, often leading to termination of the polymerization process.[20] Ionic polymerization has found use in the preparation of useful synthetic rubbers for gaskets and hosing from isobutylene and isoprene.[21]

Ionic polymerization can however produce a living polymer.[21] With subsequent addition of monomer, the polymer chain can grow, further increasing the number of repeating units and its molecular weight. Living polymers are useful in the production of block-copolymers and offer additional control over the properties of the bulk material.[15] One method of accessing a block-copolymer is through the addition of a new monomer to a living polymer, growing the polymer chain (**Scheme 8**).[22]

Scheme 8: Block Copolymer accessed through anionic living polymerization.
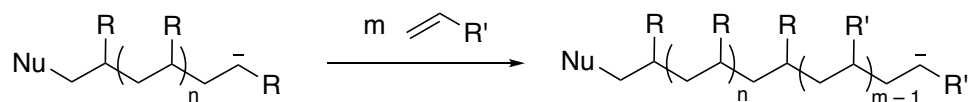
In radical and ionic polymerization, control over the structure of the resulting polymer is dictated by the reactivity of the monomeric units. Through coordination polymerization, control is obtained over the resulting material as it is influenced by the coordination sphere around the metal.[23] Coordination-mediated polymerization was first discovered using group 4 metals by Karl Ziegler in the 1940's.[16] Since then, studies of metal-mediated polymerization have expanded to obtain stereoregular polymers, giving high-performance catalysts and tailored materials.

Metal-Mediated Olefin Polymerization

Coordination polymerization mediated by a metal complex involves coordination and subsequent insertion of the monomer into the growing polymer chain, and then chain termination.[15] This is distinct from polymerization through radical or ionic-initiated systems as the metal centre is actively participating in the growth of the polymer chain throughout. This characteristic is highly advantageous as control can be extended onto the growing polymer chain.

Unlike polyethylene produced through radical polymerization which is highly branched due to chain-transfer reactions, polyethylene produced through a coordination mechanism with group 4 metals is highly linear.[16] Due to the lack of random branching, these polymers are denser, have higher melting points, and are known as high-density polyethylene (HDPE).[15] This linearity is a result of the coordination-insertion process during the propagation of the polymer chain.

Metal-mediated polymerization has also allowed for the production of stereoregular polymers of larger olefins such as propylene or butylene. A polymer of a larger olefin that has no repeating stereochemical pattern between units is known as an atactic polymer (**Figure 7, A**).[15] However, through metal-bound ancillary
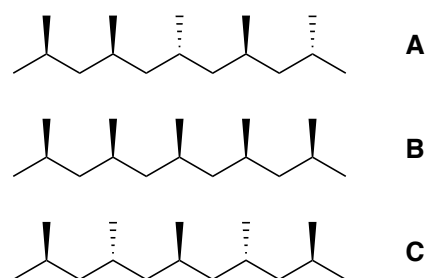
Figure 7: Atactic (**A**), isotactic (**B**), and syndiotactic (**C**) patterns in polypropylene.

ligands stereochemical control over the polymer can be obtained yielding either an isotactic polymer (**Figure 7, B**), where the stereochemistry of each stereocenter is constant throughout the chain, or a syndiotactic polymer, where the stereochemistry of each stereocenter alternates throughout the chain (**Figure 7, C**).[15] This control over the structure of the polymer can yield even more control over the properties of the bulk material. Atactic polymers will yield polymers that have lower melting points and densities than polymers that have a degree of stereoregularity such as isotactic and syndiotactic polymers.[20]

Mechanism and Kinetics of Olefin Coordination Polymerization

The general pathway of coordination polymerization follows a chain-growth mechanism in which there is activation of the precatalyst, coordination of the olefin,

insertion into a metal-carbon bond, propagation of the polymer and then termination (**Scheme 9**).[15] These steps produce a kinetic pathway that is relatively complex as each step has a separate activation barrier.[24]

Scheme 9: General Mechanism for Coordination Polymerization of Olefins

The first step in olefin coordination polymerization is activation of the metal centre initiating the polymerization process. Often the activator for group 4 catalysts is an alkyl aluminum species such as methylaluminoxane (MAO).[16] However, for catalysts of later metals the activation step can be a simple dissociation of a ligand bound to the pre-catalyst and coordination of the monomer.[25] In terms of kinetics, the activation of a metal centre involves two steps: production of the active species (K_1) and reaction of the monomer with the active species to produce the propagating species (K_2).[26] These two steps dictate the rate of the initiation of the polymerization process.

After the polymerization process is initiated, the polymer grows through addition of monomer units to the chain. In coordination polymerization, this step proceeds through coordination of the olefin and subsequent insertion in the metal-carbon bond of the growing polymer chain. Since the reaction is the same for each propagation step, the rate of the reaction is assumed to be constant (k_p).[24] The rate law (R_p) is first order with respect to both the propagating species ($[M^*]_C$) and the monomer (m) as the reaction is bimolecular (eq. 1).[24]

14

$$R_p = k_p[m][[M^*]_C] \qquad (1)$$

The overall rate of reaction (R_{poly}) for polymerization mediated by a single-site group 4 catalyst is first order with respect to the concentration of precatalyst, initiator, and monomer in solution (eq. 2).[26] This is because the concentration of the propagating species is taken to be equivalent to the concentration of activated metal centres in solution as the reaction represented by K_2 is assumed to be irreversible and fast.

$$R_{poly} = K_1 k_p[[M]_P][I][m] \qquad (2)$$

However, in the case that the conversion of the activated metal centre ($[M]_C$) is reversible and slow, the rate of polymerization (R_{poly}) is second order in monomer, and first in initiator and propagating species (eq. 3).

$$R_{poly} = K_1 K_2 k_p[[M]_P][I][m]^2 \qquad (3)$$

The polymer chain is liberated from the active centre during the termination step, regenerating the active species for further polymerizations.[15] Termination occurs either through β-hydride elimination producing an α-olefin product or through a reaction of the metal-bound polymer with either hydrogen or other organic species.[17]

1.2.1 Group 4 Olefin Polymerization Catalysts

Polymerization of olefins using titanium/aluminoxane systems has allowed access to polyolefins using relatively low temperature and pressure conditions.[27] In particular, Ziegler-Natta catalysts, group 4 metallocenes, and titanium-bound phenoxy-imine catalysts have are effective catalysts for the production of polyolefins (**Figure 8**).[28,23,29] Additionally, the Lavoie group has highlighted the ability of titanium complexes bearing an imine-ethenolate ligand to produce linear polyethylene at moderate rates (**Figure 8**).[30]
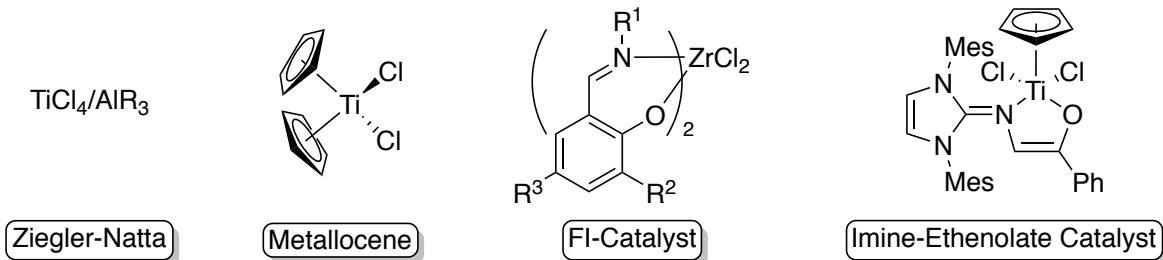
Figure 8: Group 4 catalysts capable of olefin polymerization.

Ziegler-Natta Catalysts

Ziegler-Natta catalysts have had an immense impact on the production of polyolefins. Karl Ziegler and Giulio Natta were awarded the Nobel prize for their work in the development of polymerization catalysts.[28] Before their discovery, polyolefins produced from radical polymerization would be highly branched due to chain-transfer reactions and accessing polymers of α-olefins such as propylene and butylene would be highly challenging.[15] Coordination polymerization using Ziegler-Natta catalysts produced new classes of polyethylene with higher melting points and densities and polymers of larger α-olefins. These catalysts consist of a group 4 metal that acts as the active site in the polymerization and a group 13 cocatalyst (eq. 4).[28]

$$TiCl_4/AlR_3 + n\ C_2H_4 \rightarrow (C_2H_4)_n \qquad (4)$$

The role of the cocatalyst in these systems is to alkylate the precatalyst, stabilize the cationic metal alkyl and scavenge any impurities in the solvent and feed, including water.[31] Therefore, a large excess of the cocatalyst is normally used. In early systems, trialkyl aluminum compounds or dialkyl aluminum halides were used. These cocatalysts are suitable for heterogeneous Ziegler-Natta catalysts. However homogeneous analogs exhibited low activity when these cocatalysts were used. It was found that introduction of

water to the reaction mixture using homogenous Ziegler-Natta catalysts greatly increased their reactivity. It was later discovered that this increase is due to the reaction of the aluminum species with water forming an alkylaluminoxane that proved to be an efficient cocatalyst and gave high activity with homogenous catalysts.[32] Methylaluminoxane (MAO) is an aluminoxane that is commonly used as the cocatalyst and is produced by controlled hydrolysis of trimethylaluminum.[31]

Group 4 Metallocene Catalysts

Group 4 metallocene catalysts are a class of Ziegler-Natta catalysts that have allowed for the production of highly stereoregular polymers while maintaining high catalytic activity.[33] A stereoregular polymer is a polymer that has a repeating pattern of stereochemistry between each unit. A polymer without a repeating pattern is an atactic polymer. These catalysts also yield polymers with smaller polymer dispersity index (PDI) values, a value measuring how consistent the polymer sizes are, and give higher activities than the earlier heterogeneous Ziegler-Natta catalysts.[15]

The ability of metallocene catalysts to produce stereoregular polymers stems from the structure of the catalyst used and the mechanism of coordination polymerization. Metallocene catalysts bearing two separate cyclopentadienyl ligands (**Figure 9**, **A**) will produce an atactic polymer as they are incapable of influencing how monomers will be incorporated into the polymer chain. Alternatively, group 4 metals bearing cyclopentadienyl rings with an organic bridge connecting the two rings yields a scaffold allowing for the production of isotactic (**Figure 9**, **B**) and syndiotactic (**Figure 9**, **C**)

polymers.[34,35] These *ansa*-metallocenes provide a rigid structure where stereochemical control over the polymerization of olefins is achieved.
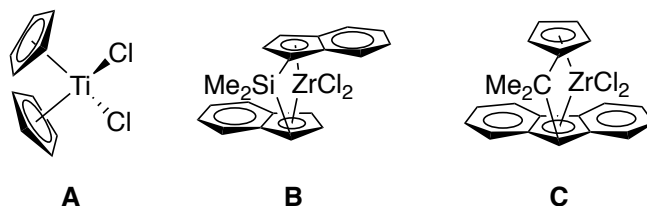
Figure 9: Group 4 Metallocene catalysts that will produce an atactic (**A**), isotactic (**B**), and syndiotactic (**C**) polymer.

Phenoxy-Imine Group 4 Catalysts

Following the success of group 4 metallocene catalysts to produce new olefinic materials, Fujita sought new single-site catalysts to develop tailored polyolefins. In seminal work at Mitsui Chemicals, Fujita developed a new class of group 4 metals bearing phenoxy-imine ligands that were able to produce polyolefins when activated by MAO.[25] Catalysts of this type have since been named FI-catalysts. The advantages of these catalysts are their tunable ligand structure, straightforward synthesis, high activity, and ability to accommodate the incorporation of polar vinylic monomers into the polymer chain in special cases.

These ligands are typically accessed through a Schiff base condensation between an amine and the corresponding 2-hydroxy benzaldehyde (**Scheme 10**). Since many amines and 2-hydroxy benzaldehydes are commercially available or easily accessed, a large array of phenoxy-imine ligands and their complexes have been prepared.[25] The substituent on the imine nitrogen as well as the substituents on the *para-* and *ortho-* positions of the phenyl ring tune the catalytic activity of their group 4 complexes in olefin polymerization. Generally, addition of bulky substituents at nitrogen, the *ortho-*position of

the phenol ring, and addition of electron withdrawing groups at the *para*-position of the phenol ring will yield a more active catalyst.[36,37]

Scheme 10: Synthesis of Group 4 complexes bearing a Phenoxy-Imine ligand.
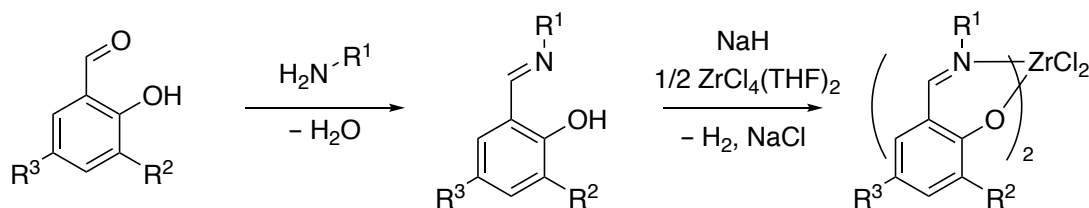
FI-catalysts have shown promising results in incorporating polar vinyl monomers into polyolefin chains through copolymerization when the polar moiety is separated by several carbon atoms from the olefinic group.[38] Copolymerization is the act of polymerizing two or more monomers together forming a copolymer. Copolymerization offers another method for the production of tailored materials with varying characteristics. The ethylene/5-hexene-1-yl-acetate copolymer was accessed using a FI-catalyst when 250 equivalents of the aluminum cocatalyst and 50 equivalents of the polar monomer were used and activities as high as 515 $kg_{polymer} \bullet mol_{catalyst}^{-1} \bullet h^{-1}$ were observed.[38] However, the incorporation of the monomer remained low at below 1% incorporation.[36] Metallocene catalysts exhibited no activity in either ethylene polymerization or copolymerization of ethylene with a polar monomer under the same conditions.[38]

Imine-Ethenolate Group 4 Catalysts

In the Lavoie group, a series of imine ethenolate complexes of titanium and zirconium have been prepared and their polymerization of ethylene with MAO as a cocatalyst was studied (**Scheme 11**).[30] The ligand precursors were accessed through an S_N2 reaction of 1,3-bis(2,4,6-trimethylphenyl)imidazol-2-imine with the corresponding 2-haloacetophenone yielding a ligand precursor with the same monoanionic N^O fragment as the FI-catalysts. The complexes were accessed through the addition of ligand to either $ZrCl_4(THF)_2$ or $CpMCl_3$ (M = Ti, Zr) (**Scheme 11**).

Scheme 11: Synthesis and utility of imine ethenolate complexes of group 4 metals.[14]
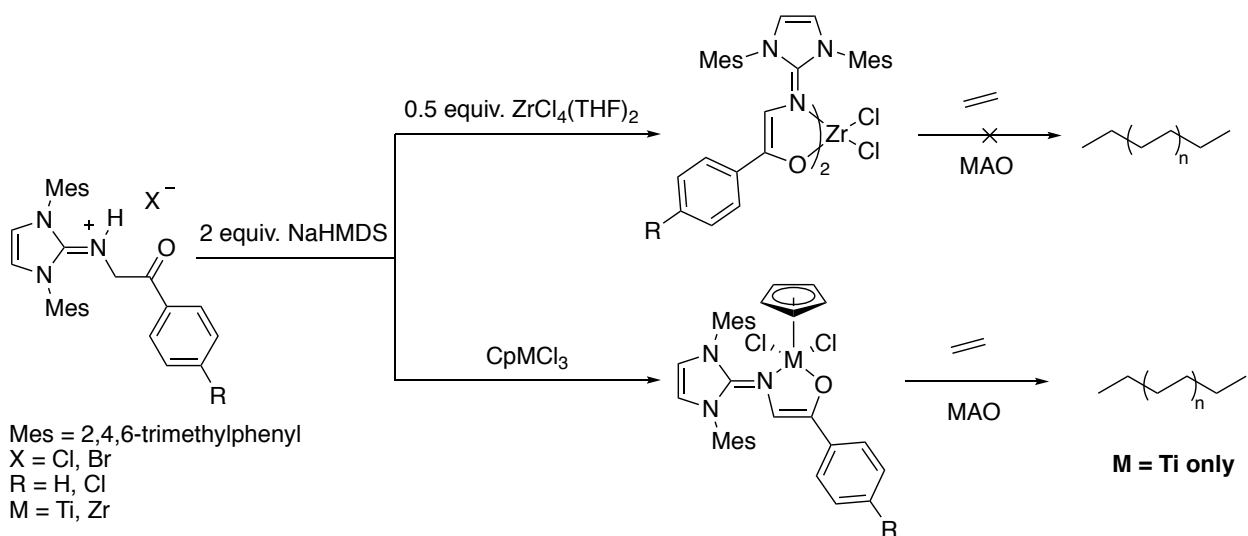
It was found that the zirconium complexes only produced trace amounts of polymer when tested in the polymerization of ethylene with MAO. In contrast, the titanium complexes produced polyethylene at a moderate rate, warranting further variations on the ligand structure.[30] As such, the replacement of the *p*-H of the phenyl ring with the more electronegative chlorine atom led to enhanced catalyst reactivity.[30] This increase was attributed to increasing the electron-withdrawing character of the ligand structure, producing a more electron poor metal centre relative to the *p*-H analogue.[30]

1.2.2 Group 10 Olefin Polymerization Catalysts

Polymerization using group 10 metal centres has allowed for the efficient production of oligomeric α-olefins, polyolefins, as well as copolymers of ethylene and polar vinyl monomers.[39–41] Group 10 metal catalysts (**Figure 10**) of monoanionic bidentate ligands typically do not require an aluminum cocatalyst as the active species is accessed through dissociation of a labile ligand. However, a scavenging agent such as tris(pentafluorophenyl)borane (BCF) or bis(1,4-cyclooctadiene)nickel(0) (Ni(COD)$_2$) can be used to assist in the activation of the catalyst.[25] Additionally, β-hydrogen elimination of the growing chain can limit the catalysts ability to grow polymers with greater than a few units.[39] Otherwise olefin polymerization follows the same general coordination polymerization mechanism. Notably, catalysts based on heavier group 10 metals (Pd and Pt) are more expensive than group 4 catalysts as platinum and palladium are less abundant metals.

SHOP catalyst   Salicylaldiminato Catalyst   Drent Catalyst
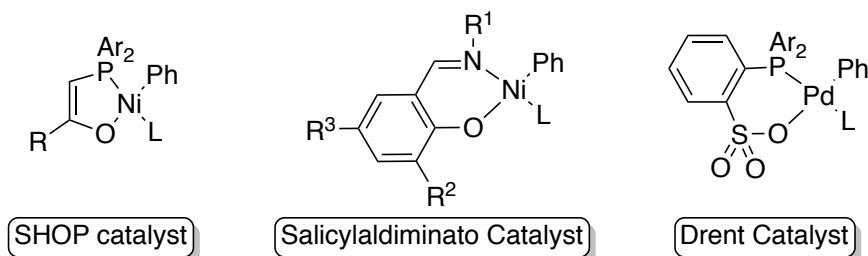
Figure 10: Group 10 Catalyst capable of producing polyethylene and copolymers

SHOP-type Catalyst

In the 1970's, complexes bearing a bidentate monoanionic phosphanylenolato ligand were shown to efficiently produce oligomeric α-olefins with low molecular weight.[39] In the presence of a phosphine scavenging agent, these activated systems can produce a heavier polymeric α-olefin.[39] Catalysts of this type are called Shell higher olefin process (SHOP) catalysts.

SHOP-type catalysts follow a general polymerization mechanism (**Scheme 12**) in

Scheme 12: Production of α-olefins using a generic SHOP catalyst.

which the tertiary phosphine first dissociates from the precatalyst, thereby yielding an open coordination site, followed by coordination and insertion of ethylene into the Ni-Ph bond. The complex subsequently undergoes β-hydride elimination, with loss of styrene, to give the three-coordinate active catalyst. The active species can also be accessed through oxidative addition of a keto-stabilized phosphorus ylide, followed by reaction with ethylene. Subsequent (i) coordination and (ii) insertions of ethylene allows for (iii) the oligomerization of the olefin (**Scheme 12**). This cycle continues until elimination occurs, normally through (iv) β-hydride elimination of the alkyl chain yielding an α-olefin.[5] Decomposition of these catalysts normally follows coordination of a second (P^O) bidentate ligand, supported by the isolation of Ni(P^O)$_2$.[39]

One postulated method to avoid the formation of catalytically inactive Ni(P^O)$_2$ is to increase the overall steric bulk of the (P^O) bidentate ligand.[40] The increase in the sterics reduces the propensity of the chelation of a second (P^O) ligand. Furthermore, these systems are primarily used in the oligomerization of non-polar olefins, limiting their applications in the production of more tailored materials.[39]

Salicylaldiminato Group 10 Catalysts

Group 10 metals bearing salicylimine (phenoxy-imine) ligands have shown promising results in the polymerization and copolymerization of olefins. Grubbs first explored the ability of group 10 complexes bearing these phenoxy-imine ligands to polymerize ethylene in 1998, where he found the addition of bulky groups to the phenolic ring at the R^2 position and electron withdrawing groups at the R^3 position increased catalytic activity (**Scheme 13**, **A**).[40] However, activity of these nickel complexes is generally lower than the titanium complexes bearing a phenoxy-imine ligand reported by Fujita.

Scheme 13: Types of Polymerizations performed using the salicylaldimine catalyst reported by Grubbs.
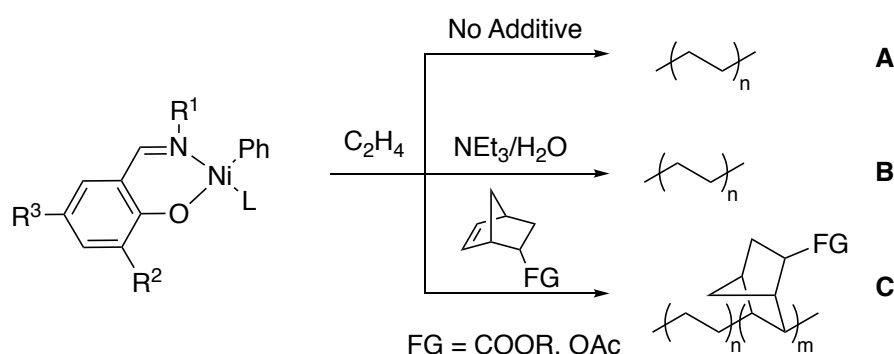
As salicylaldiminato group 10 catalysts have a neutral active species in olefin polymerization, they are considered to be more compatible for the polymerization and copolymerization of polar vinyl monomers.[42] Grubbs first demonstrated the ability of these complexes to have moderate activity in the polymerization of ethylene even when polar

additives such as water or tertiary amines were added which would readily deactivate the analogous group 4 systems (**Scheme 13, B**).[42] Then copolymerizations were performed with ethylene and a variety of olefins with polar functional groups accessing a variety of copolymers (**Scheme 13**, **C**).[42] Grubbs demonstrated that bicyclic olefins were more easily incorporated into the polymer chain than α-olefins due to the ring strain increasing reactivity of the olefin. However, the incorporation of the polar monomer into the polymer chain is typically below 5% which is considered a low value.

Drent-Type Catalysts

Palladium complexes of phosphinato-sulfonate ligands, classified as Drent-type catalysts, are a group of catalysts capable of performing copolymerization of polar olefins with ethylene. [43–45,] The substrate scope of these complexes include the copolymerization of ethylene with acrylates, acrylonitrile, acrylamides, acrylic acid, vinyl acetate, vinyl halides, vinyl ethers, and allyl monomers.[46] However, these systems suffer from a lack of regio- and stereoselectivity, and low reactions rates due to formation of strong σ-bonds between the metal and the functional group.[46] Furthermore, depending on the mode of insertion of the polar monomer into the coordinated polymer chain, β-elimination of the functional group can deactivate the complex (**Scheme 14**).[41]

Scheme 14: Possible modes of insertion of vinyl acrylate into polymer chain, one leading to polymer growth the other to deactivation.
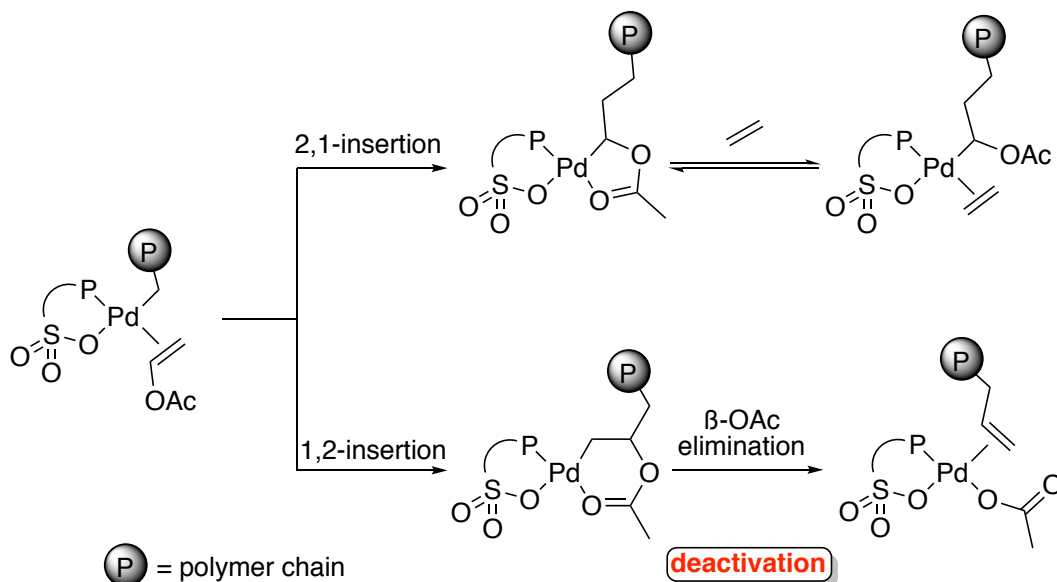
Despite these shortcomings, efforts have been made into gaining regio- and stereoselective transformations with bulky ancillary phosphine-sulfonate ligands. Increasing the sterics around phosphorus increases selectivity for 1,2-insertion over 2,1-insertion of methyl acrylate. This is due to the unfavorable formation of the intermediate that includes repulsion between the phosphorus substituents and the ester of the monomer. In this case, the product of 1,2-insertion allows for further propagation of the polymer chain but 2,1-insertion leads to β-elimination of the functional group and deactivation of catalyst.[7] However, when the catalyst is regioselective it does not incorporate methyl acrylate at an acceptable rate.[41]

In order to overcome these issues in Drent-type systems, Nozaki[47] and Jordan[48] have researched the effects of replacing the phosphorus atom in these ligands with a NHC, yielding palladium complexes of NHC-sulfonate ligands (**Figure 11**). The σ-donating ability of NHCs has been taken advantage of in the past to stabilize metal complexes yielding more active catalysts.[47] However, it was found that in the case of the palladium complex of the NHC-sulfonate prepared by Jordan *et al.* that the complex was inactive in the polymerization of olefins.[10] This change in reactivity was attributed to the observed increase in the lability of the seven-membered ring of the (C^O) ligand, over that of the 6-membered ring of the (P^O) system employed in Drent-type catalysts.[48] The increase of lability of the (C^O)

Figure 11: Palladium complexes of NHC-sulfonates prepared by Nozaki and Jordan.

ligand allows for reductive elimination from the propagating species where the methylated azole ring and palladium(0) are produced.[48] In the case of the (C^O) ligand prepared by Nozaki, the resulting 6-membered metallocycle is more stable and therefore less labile. However, polymerization studies for this complex were not reported.[47]

1.5 Proposed Work by the Lavoie Group

The incorporation of inversely-polarized phosphaalkenes in bidentate ligands has remained largely unexplored. Due to the ability to tune the electronics and sterics of the phosphorus centre, the Lavoie group is highly interested in exploring the potential of inversely-polarized phosphaalkenes in metal-mediated transformations. Using the ligand-design employed in SHOP, Drent-type, imine-ethenolate, FI-catalyst systems we aim to prepare the related inversely-polarized phosphaalkene containing ligand, their metal complexes, and test their ability to perform olefin polymerization (**Scheme 15,** top, middle, and bottom). The inversely-polarized phosphaalkene fragment may be useful in future ligand design where an electron-rich donor atom yields control over the desired transformation. Ideally, the inversely-polarized phosphaalkene-based ligand will yield an electron-rich metal centre that disfavors unwanted reactions with polar vinyl monomers and react exclusively with the vinylic moiety.

Scheme 15: Proposed work by the Lavoie group for developing new olefin polymerization catalysts.
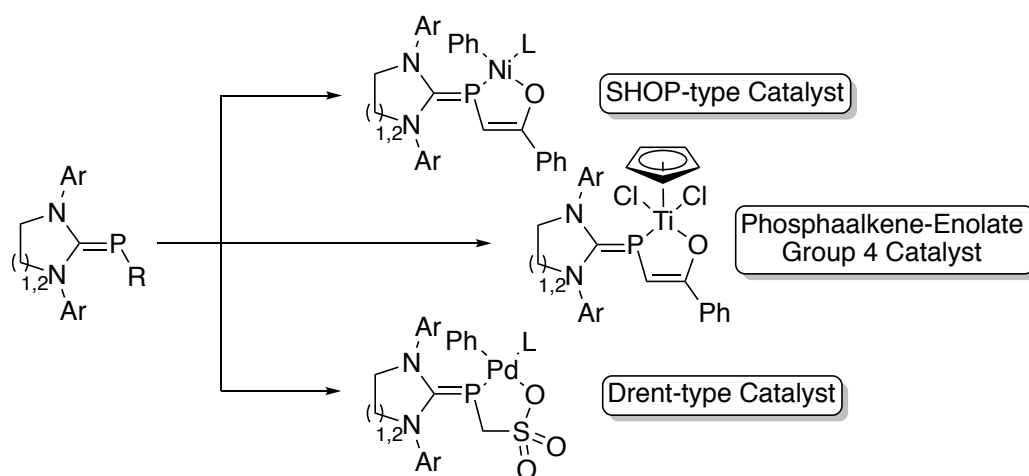
2. Results and Discussion

The goal of this research is to advance the knowledge of inversely-polarized phosphaalkenes and assess their utility and potential as ancillary ligands in the metal-mediated polymerization of olefins and polar vinyl monomers. Particularly, this work focusses on the synthesis of new monoanionic bidentate ligand precursors bearing an inversely-polarized phosphaalkene fragment, the coordination chemistry of inversely-polarized phosphaalkene-enolate ligands to titanium and the activity of the resulting complexes in olefin polymerization.

2.1 Synthesis of the First Inversely-Polarized Hydrido-Phosphaalkene of a 6-Membered Cyclic Amidine

The synthesis of hydrido-phosphaalkenes has been previously reported to be successful with various imidazolium and imidazolinium salts using Na_3P_7, a reactive cage-type phosphorus species.[11] However, the same reaction has yet to be reported for 6-membered cyclic amidines which have a corresponding carbenoid carbon with reduced σ-donating and increased π-accepting character. Thus, the hydrido-phosphaalkenes of these 6-membered cyclic amidines should have a less electron-rich phosphorus atom than their 5-membered counterparts as a result of the increased π-acidity of the carbenoid carbon in the former. Therefore, the coordinated phosphaalkene will produce a less electron-rich metal.

The reaction of Na_3P_7 with the cyclic amidine provided convincing spectroscopic evidence for the production of the desired phosphaalkene **1** (**Scheme 16**). The observed doublet at −99.7 ppm in the ^{31}P NMR spectrum with a $^1J_{PH}$ of 161 Hz is consistent with the desired phosphaalkene.[11] This presumption is based on the pyrimidine ring used

which is capable of accepting more electron density from the phosphorus atom than the corresponding imidazolium-based phosphaalkenes, which have a phosphorus chemical shift around −140 ppm.[11] The change in chemical shift confirms that the phosphorus is less electron-rich in the IPP bearing a 6-membered carbene fragment. However, when attempting to isolate the single species observed in the ^{31}P NMR spectrum, some

Scheme 16: Pyridinium salts used for the synthesis of a ring-expanded hydrido-IPP

X= Br, BF$_4$

1
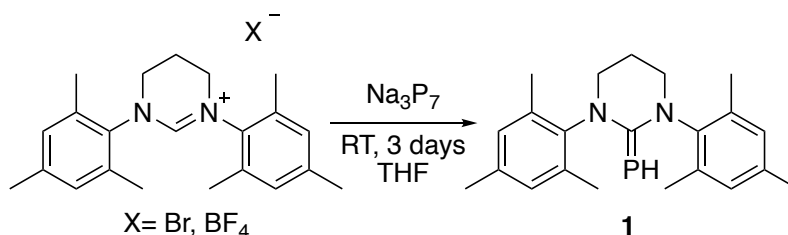
challenges were encountered in the removal of the side-products of the reaction.

In attempts to change the solubility of the side products of this reaction, the amidinium tetrafluoroborate salt was used in place of the bromide salt. The reaction occurred in a similar manner to the bromide salt, but the isolation of the phosphaalkene was more successful with this reagent. The product was isolated by an initial extraction using THF, removal of THF *in vacuo*, and a subsequent extraction using toluene. The dried toluene-soluble fraction was then washed with pentane. The remaining solids contain the desired IPP and around 15 percent of the free carbene (compound **1'**) as determined by ^{1}H NMR spectroscopy (**Scheme 17**). The pentane soluble layer contains the product of the *ortho* position CH activation: a five- and six-membered fused ring heterocyclic system (compound **1"**) in 56 mol%.

Scheme 17: Identified products from the toluene soluble fraction of the reaction of the tetrafluoroborate pyridinium salt with Na_3P_7.
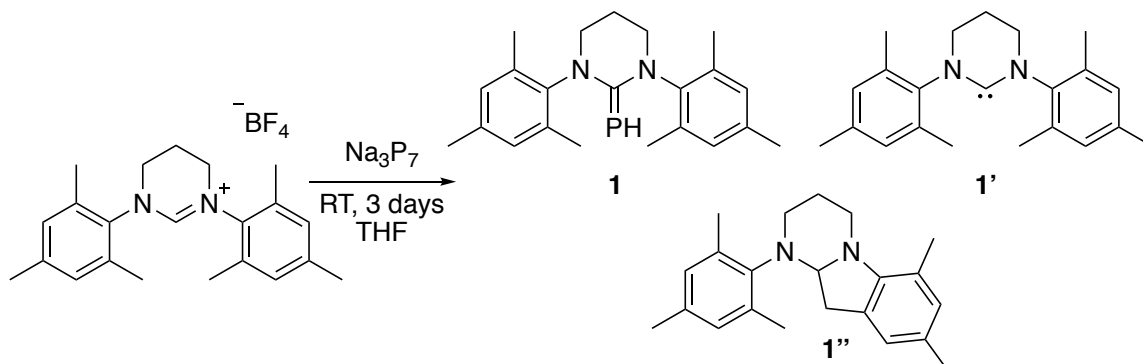
The formation of compound **1"** has been previously reported by Whittlesey, et al.[49] They discovered C–H activation had occurred with the six- and seven-membered dimesityl-substituted carbenes and not with the five-membered analogs. The authors hypothesized that this is in part due to the N–C–N bond angle of the six- and seven-membered rings, yielding a carbenoid carbon that is more basic than the 5-membered rings.[49] This conclusion arose from the lack of reactivity observed for the related 5-membered ring carbenes.[49]

To access pure phosphaalkene, remaining free carbene (**1'**) can be transformed to the CH-activated product (**1"**) by allowing the toluene soluble fraction to react at room temperature for 3 days. Removing volatiles and washing the solids with pentane yields pure phosphaalkene in 19% yield with respect to the amidinium salt. The hydride of **1** is observed as a doublet with $^1J_{HP}$ = 161 Hz at 2.29 ppm in the ^1H NMR spectrum (**Figure 12**). Additionally, the ^1H NMR spectrum of **1** shows broad signals for the atoms in the mesityl rings due to restricted rotation about the C–P bond at 6.80 ppm and 2.35 ppm. The remaining broad signal at 2.90 ppm belongs to the methylene groups adjacent to the nitrogen atoms.
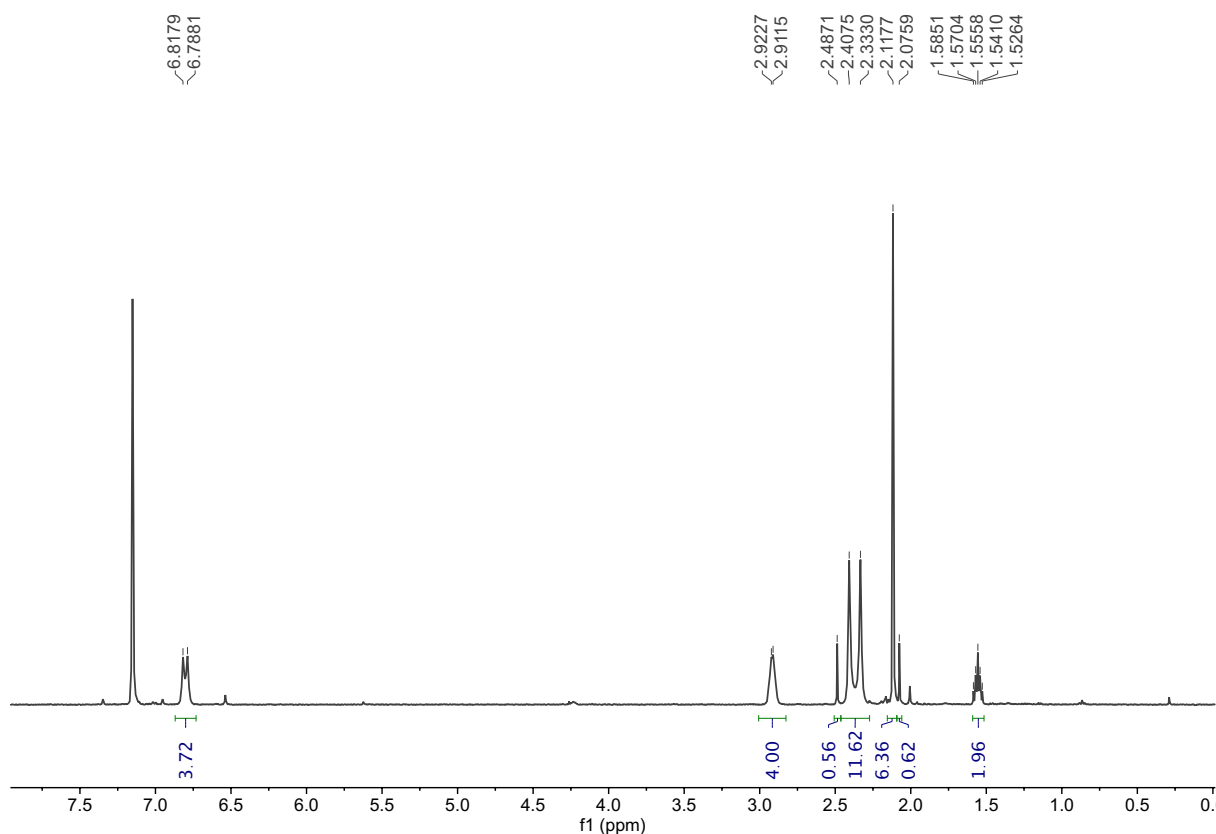
Figure 12: ^{1}H NMR spectrum of **1** in C_6D_6 taken at a frequency of 400 MHz.

The spectroscopic data of **1** suggests that the phosphorus atom is less electron-rich when compared to the 5-membered analogs. Thus, when coordinated, these phosphaalkenes will produce a more electron-poor metal centre in relation to the imidazole- and imidazolidine-based phosphaalkenes. In theory, the resulting coordination compound bearing this 6-membered inversely-polarized phosphaalkene will have higher activities in the polymerization of olefins as the more electropositive metal centre will bind units of ethylene more readily and insert them into the growing polymer chain.

2.2 Attempted Synthesis of Drent-Type Ligand Precursors

The synthesis of a Drent-type ligand precursor was attempted through the reaction of the imidazolium sulfonate with Na_3P_7. The NHC-sulfonate precursor was accessed using a procedure reported previously by Nozaki et $al.$[47] This synthetic route involves the S_N2 reaction of mesityl imidazole with chloroiodomethane, producing a mixed salt (**Scheme 18**). To exclusively obtain the more reactive iodo iodide product, reaction with excess sodium iodide in acetone is performed. An additional S_N2 reaction with the iodo iodide salt and sodium sulfite yields the NHC-sulfonate zwitterion (**Scheme 18**).[47]

Scheme 18: Synthesis of NHC-sulfonate with alkyl-spacer described by Nozaki et al.[9]
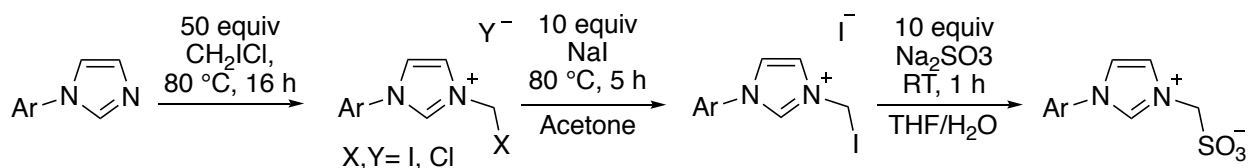
To access the inversely-polarized phosphaalkene a reaction with the NHC-sulfonate and Na_3P_7 was attempted (**Scheme 19**). As the NHC-sulfonate is insoluble in ethereal solvents, the reaction was performed in dimethyl sulfoxide (DMSO). After one day at room temperature, monitoring the reaction by ^{31}P NMR reveals a doublet at -145 ppm with a coupling constant of 169 Hz. This resonance is consistent with other IPPs of 5-membered ring carbenes. It was thus hypothesized that this signal arose from the targeted sodium IPP-sulfonate salt, **2**. However, this species was a minor product among many other phosphorus containing-species identified by ^{31}P NMR spectroscopy of the reaction mixture in DMSO. In an attempt to isolate this species the less polar solvent, THF, was added to the solution in DMSO in order to precipitate the desired phosphorus containing species. This was determined to be unsuccessful as ^{31}P NMR spectroscopy

of the soluble fraction revealed the doublet was still present in the soluble fraction and not in the precipitate. Since multiple additional phosphorus containing species were generated from the reaction of the NHC-sulfonate with Na_3P_7 and the isolation of the single species with a promising ^{31}P chemical shift value was unsuccessful an alternate route was attempted for the synthesis of an IPP-sulfonate.

Scheme 19: Attempted synthesis of an Inversely-Polarized Phosphaalkene-Sulfonate Ligand Precursor
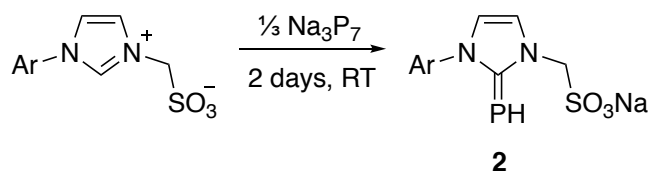
In the first attempted route the goal was to add the inversely-polarized phosphaalkene fragment to the imidazolium sulfonate. However, as this was not successful, an alternate route was attempted where an inversely-polarized phosphaalkene would be used as a nucleophile similar to the first step of the synthetic route employed by Nozaki (**Scheme 18**). Thus, Compound **1** was reacted with chloroidodomethane (**Scheme 20**). The product of this reaction yielded two doublets of triplets in the ^{31}P NMR spectrum at -59.9 ppm ($^1J_{PH}$ = 207 Hz, $^3J_{PH}$ = 45.0 Hz) and -66.4 ppm ($^1J_{PH}$ = 214 ppm, $^3J_{PH}$ = 37.7). These signals were assigned to the formation of a chloro iodide salt and an iodo chloride salt, as observed by Nozaki in the preparation of the NHC-sulfonate. The next step involved preparing the exclusively the more reactive iodo-iodide product through reaction with sodium iodide, which would then be reacted with sodium sulfite. However, the mixed salt product obtained from the reaction of **1** with chloroiodomethane is unreactive to excess sodium iodide (**Scheme 19**). Thus, the

reaction of the mixed salt, **3**, with sodium sulfite was not attempted as sulfite is a poorer

nucleophile than iodide and would likely not undergo the desired substitution reaction.

Scheme 20: Synthesis of IPP-sulfonate ligand precursor **3** and subsequent reaction with NaI
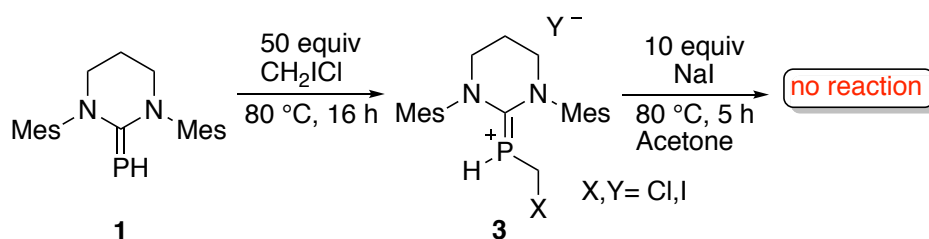
2.3 Synthesis of New Imidazolidine- and Pyrimidine-based Inversely-Polarized Phosphaalkene-Enolate Precursors

The strategy for the synthesis of the monoanionic-bidentate ligand was selected

based on current work within the Lavoie Group. In this unpublished work by Juan E. R.

Villanueva, the hydrido-IPP of the 1,3-bis(diisopropylphenyl)imidazole-2-ylidene reacts

with bromoacetophenone as the S_N2 reaction product to give the precursor to the

monoanionic bidentate ligand (**Scheme 21**). Subsequent deprotonations and reaction

with trimethylsilyl chloride yields a silyl vinyl ether that can be used for coordination to a

transition metal.

Scheme 21: Synthesis of a monoanionic bidentate inversely-polarized phosphaalkene ligand precursor.
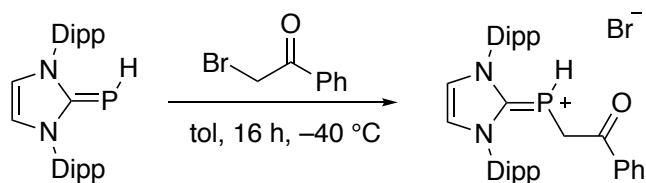
The analogous reaction between compound **1** and bromoacetophenone was attempted (**Scheme 22**). After addition of **1** to bromoacetophenone, evidence of the production of the IPP-enolate precursor, **4**, was obtained by ^{1}H NMR and ^{31}P NMR spectroscopy. Precipitating the salt out of a solution of DCM with pentane yields the salt in 48% yield. The ^{31}P NMR spectrum of **4** yields a doublet with $^1J_{PH}$ = 252 Hz with further splitting of the doublet due to the protons of the adjacent methylene spacer. The ^{1}H NMR spectrum yields a doublet of triplets for the proton bound to phosphorus with $^1J_{HP}$ = 252 Hz and $^3J_{HH}$ = 7.5 Hz. However, as the yield of compound **1** is relatively poor, this route towards the synthesis of a new inversely-polarized phosphaalkene-enolate ligand was withdrawn in favor of higher yielding inversely-polarized phosphaalkenes.

Scheme 22*: Synthesis of the pyrimidine-based IPP-enolate precursor.*
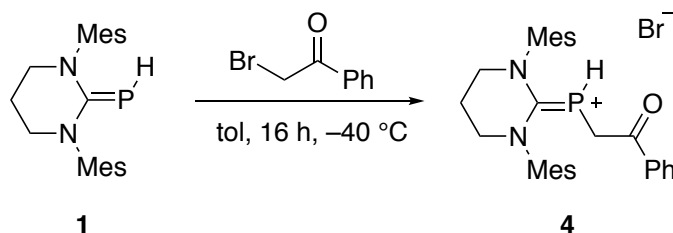
The synthesis of the imidazolidine-based hydrido-phosphaalkene has been reported by Gudat.[11] This route involves the reaction of the imidazolinium chloride salt with Na_3P_7 in THF at room temperature for 16 hours. After removing the THF-insoluble solids and extracting the product with toluene, moderate yields of the inversely-polarized phosphaalkene are obtained (*ca.* 60%).[11]

The imidazolidine fragment is distinct from its imidazole counterpart by its saturated backbone. Thus, in their NHC analogs, imidazolidine-based carbenes are not aromatic with respect to the cyclic amidine while imidazole-based carbenes are. The two sp^3-carbon atoms of the backbone in imidazolidine carbenes are less capable of donation

of electron density to the sp^2-nitrogen atoms of the aminal group compared to the two sp^2-carbons of the imidazole carbene. Thus, the p-orbital of the carbenoid carbon in the imidazolidinyl phosphinidene will be able to accept more electron density from the phosphinidene fragment, resulting in a shorter C–P bond. This is confirmed by the solid-state molecular structures of the phosphaalkenes bearing diisopropylphenyl rings on the nitrogen atoms where the imidazoyl phosphinidene has a C–P bond length of 1.752(1) Å and the imidazolidinyl phosphinidene has a slightly shorter bond length of 1.743(2) Å.[8,7] Furthermore, the phosphorus atom of the saturated derivative has a chemical shift value of –116.7 ppm while the unsaturated has a chemical shift of –136.7 ppm.[11] These chemical shifts are consistent with a less shielded phosphorus atom in the imidazolidinyl phosphinidene.

The reaction of the imidazolidinyl phosphinidene with bromoacetophenone yields the phosphonium salt in 82% yield. Despite the reduced nucleophilicity of the phosphinidene centre, the reaction is complete after 3 hours at –40 °C in toluene (**Scheme 23**). The isolation of **5** is achieved by removal of the toluene supernatant from the reaction mixture, then the solids are dissolved in dichloromethane and the product is precipitated out of solution with pentane yielding **5**.

Scheme 23: Synthesis of imidazolidine-based IPP-enolate precursor.

5
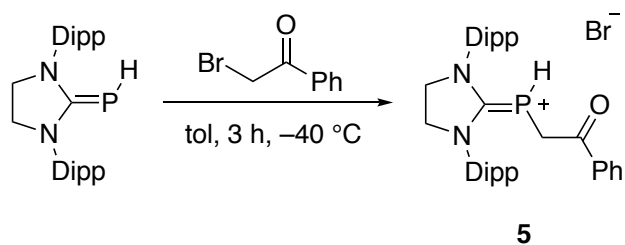
Characterization by ¹H NMR spectroscopy reveals multiple complex splitting patterns for the protons of **5** (**Figure 13**). The methylene-protons adjacent to the phosphorus atom of **5** show a complex splitting pattern. These protons show coupling to the phosphorus centre as well as to the proton bound to phosphorus. The protons of the backbone are also all inequivalent, evident by geminal splitting. The signals for the isopropyl groups belonging to the diisopropylphenyl rings are all inequivalent with four sets of distinct doublets. The ³¹P NMR signal for the product is a doublet of doublets with $^1J_{PH}$ = 241 Hz and $^2J_{PH}$ = 10.4 Hz at −95.8 ppm.
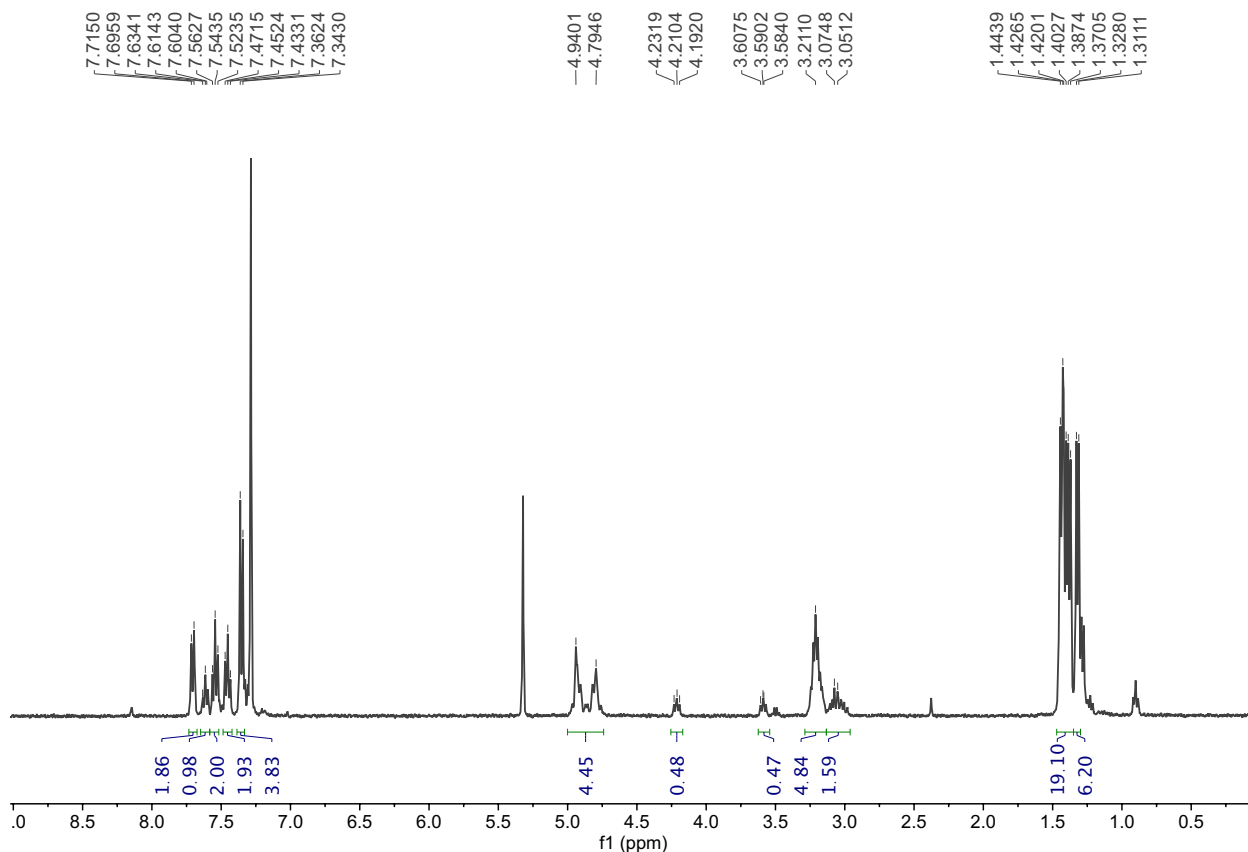
Figure 13: ¹H NMR spectrum of **5** taken in CDCl₃ taken at a frequency of 400 MHz.

The synthesis of a ligand precursor bearing an additional withdrawing group at the *para* position of the phenyl group was also attempted to showcase the modularity of the

ligand structure. It is expected that the addition of a chloride at the para position of the phenyl group will increase the activity of the resulting complex as observed with work on the imine-ethenolate titanium complexes as a result of increased electropositivity of the metal centre.[30] To access the appropriate ligand precursor, the reaction of the imidazolidinyl phosphinidene with three different 2-halo-4′-chloroacetophenone reagents were performed. The reaction of 2-chloro-4′-chloroacetophenone and the inversely-polarized phosphaalkene was performed at room temperature (**Scheme 24**, top). After 2 hours, a precipitate had formed and was identified to be the imidazolidinium salt by ^{1}H NMR spectroscopy.

Scheme 24: Recovered products from reactions of imidazolidinyl phosphinidene with 2-halo-4'-chloroacetephones.*x*

To increase the electrophilicity of the methylene carbon of the acetophenone, 2-iodo-4′-chloroacetophenone was prepared through a Finkelstein reaction with the chloro derivative.[50] Adding a solution of the phosphaalkene to a solution of the acetophenone in

Figure 14:^{31}P NMR spectrum (top) and ^{31}P{^{1}H} NMR spectrum (bottom) of major phosphorus containing products obtained from reaction using 2-iodo-4'-chloroacetophenone taken at 121 MHz.

toluene yields a green precipitate after two hours at room temperature (**Scheme 24**, bottom). The NMR spectra of the products revealed the presence of multiple species, including the protonated hydrido phosphaalkene, **6** and a species containing a P–P bond, **7**. These two species were identified by their ^{31}P NMR spectra (**Figure 14**). The protonated hydridophosphaalkene was identified by a triplet observed at –156.8 ppm with $^1J_{PH}$ of 233.6 Hz. This chemical shift is consistent with that reported by Pringle and coworkers when similar products were intentionally prepared.[51]

The second product **7**, was identified by an AB quartet centred at 91.6 ppm in the ^{31}P{^{1}H} NMR spectrum (**Figure 14**). This species has $^1J_{PP}$ = 241 Hz, and in the proton-coupled spectrum the downfield signals split into doublets with $^1J_{PH}$ = 214 Hz. The

formation of **7** is less clear, but the ^{31}P NMR is consistent with the products produced and characterized by Robinson and coworkers.[52]

The phosphonium salt **5Cl** was successfully accessed through the reaction of 2-bromo-4′-chloroacetophenone with the imidazolidinyl phosphaalkene (**Scheme 24**, middle). In toluene at room temperature, the reaction is complete after two hours. However, a small fraction of **6** and **7** can be observed in the ^{31}P NMR spectrum of the precipitate. The product can be purified by precipitating **5Cl** out of a solution of dichloromethane with pentane. However, performing the reaction at –40 °C over 5 hours reduces the amount of **6** and **7** produced with a yield of 86% of **5Cl** (**Scheme 25**).

Scheme 25: Synthesis of the neutral ligand precursors, **8**.
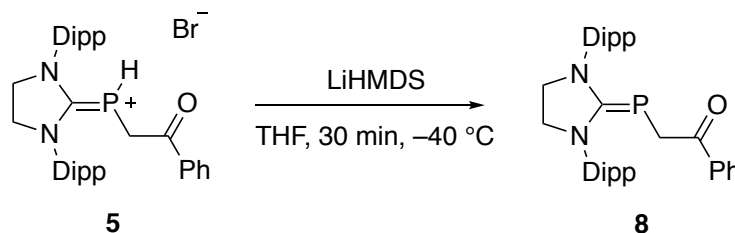
The neutral ligand precursor, **8**, is accessed in 85% yield through deprotonation of **5** in tetrahydrofuran (**Scheme 26**). This species can be accessed using either MHMDS (M=Li, Na, K), NaH, or KH as the base. In the case of NaH or KH, an excess of base is needed to accommodate their poor solubility in tetrahydrofuran. The ligand precursor is purified from the dried reaction mixture by filtration of the toluene soluble fraction through a Kimwipe plug and subsequent removal of volatiles. Washing the solids with pentane and removal of residual pentane *in vacuo* yields **8** as a yellow powder.

Scheme 26: Synthesis of imidazolidine-based ligand with an electron-withdrawing group on the phenyl ring.

5Cl
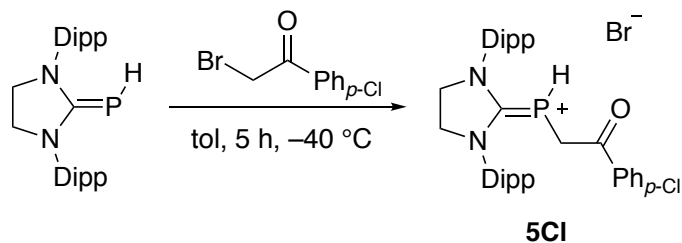
The ^{1}H NMR spectrum of **8** shows two distinct magnetic environments for the methine protons belonging to the diisopropylphenyl rings (**Figure 15**). There are also four distinct environments for the methyl groups belonging to the diisopropylphenyl rings, where one set of two doublets are more downfield than the other two doublets. The distinct environments result from the carbenoid carbon-phosphorus bond having double bond character, restricting rotation about the bond and yielding magnetically inequivalent protons on either side of the azole ring. Interestingly, the methylene protons between the acyl group and phosphaalkene is observed as a doublet at 2.96 ppm with fine splitting ($^2J_{HP}$ = 0.9 Hz). The assignment of this signal was supported by heteronuclear multiple-bond correlation spectroscopy, where couplings were observed to both the acyl group carbon and the carbenoid carbon. Coupling to the phosphorus atom can also be seen in multiple bond correlation spectroscopy between the phosphorus atom and these methylene protons.
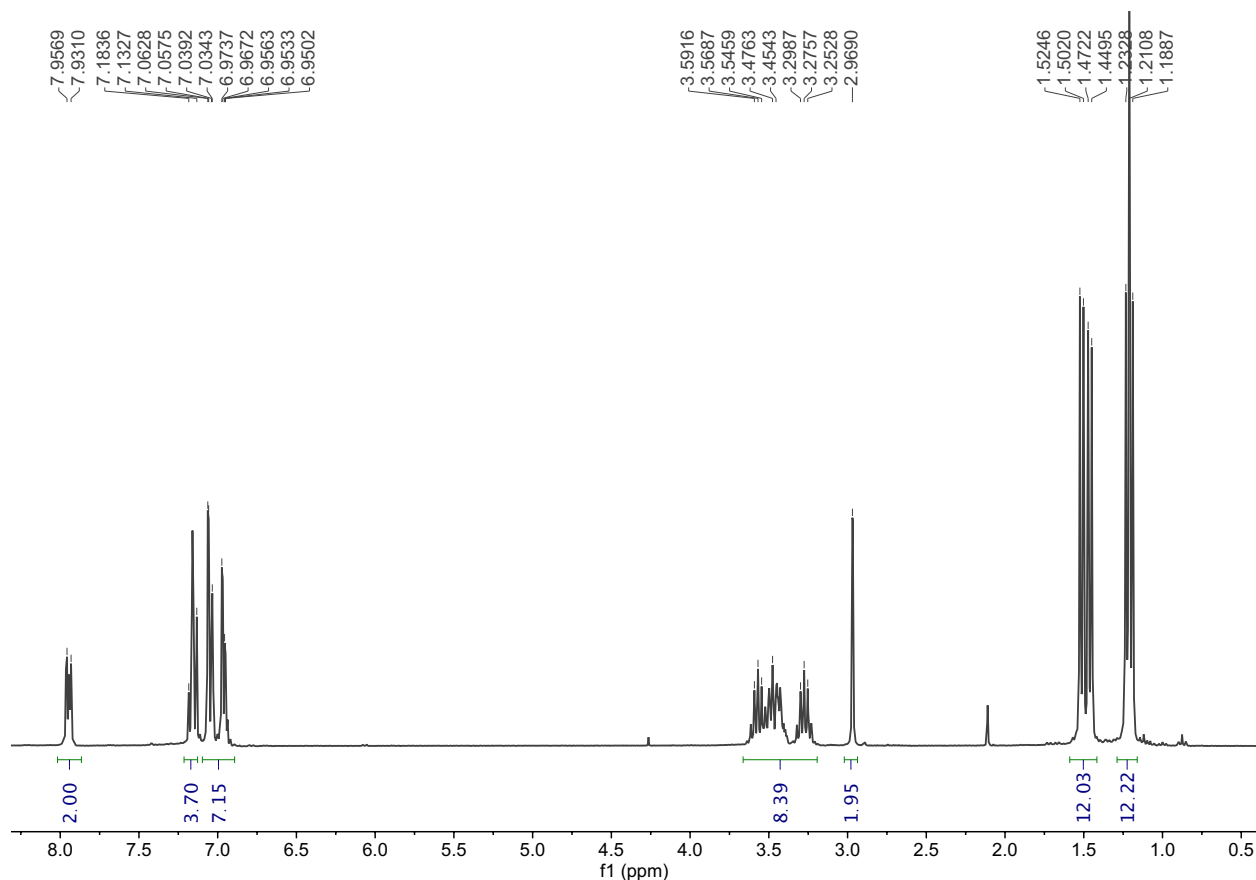
Figure 15: ^{1}H NMR spectrum of neutral ligand precursor, **8**, taken in C$_6$D$_6$ (300 MHz).

In solution, the keto-enol tautomerization of **8** to **8′** is observed (**Scheme 27**). The enol tautomer is observed slightly more downfield in the ^{31}P NMR spectrum at −26.5 ppm than the keto tautomer at −29.8 ppm. In the ^{1}H NMR spectrum, the vinylic proton of the enol tautomer is observed at 6.05 ppm with $^2J_{HP}$ = 6.0 Hz.

Scheme 27: Keto-enol tautomerization of IPP-enolate precursor, **8.**
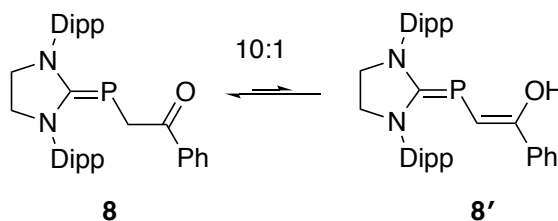
The isolation of the IPP-enolate as an alkali salt is desirable as the product would be a candidate for salt metathesis with transition metal halides. Salt metathesis is a commonly employed reaction as the desired product is typically accessed in good yields. The lithium IPP-enolate salt of the imidazolidine-based ligand **9** was accessed using LiHMDS (**Scheme 28**) in 84% yield. The product is obtained from the reaction mixture by removal of volatiles and washing the resulting solids with cold pentane.

Scheme 28: Synthesis of lithium enolate, **9**.
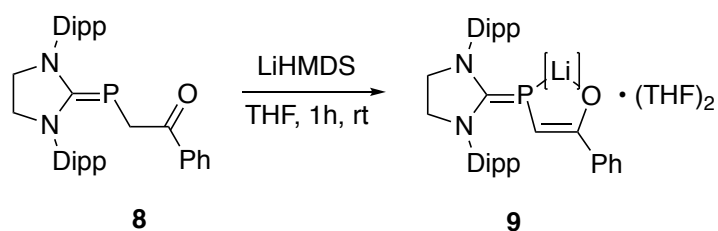
The isolation of a single species resembling **9** was not achieved, but the ¹H NMR spectrum of **9** is similar to the enol tautomer **8′** where the vinylic proton is observed as a doublet at 4.94 ppm with $^2J_{HP}$ = 5.1 Hz (**Figure 16**). There are however several vinyl environments observed, indicating several structural isomers. There are also two equivalents of THF observed in the spectrum at 3.50 and 1.50 ppm, even after drying the solids *in vacuo* for many hours. This is possibly due to the lithium cation binding THF atoms in a Lewis acid base interaction. The product was used in future transformations without further purification while maintaining high yields of the desired products.
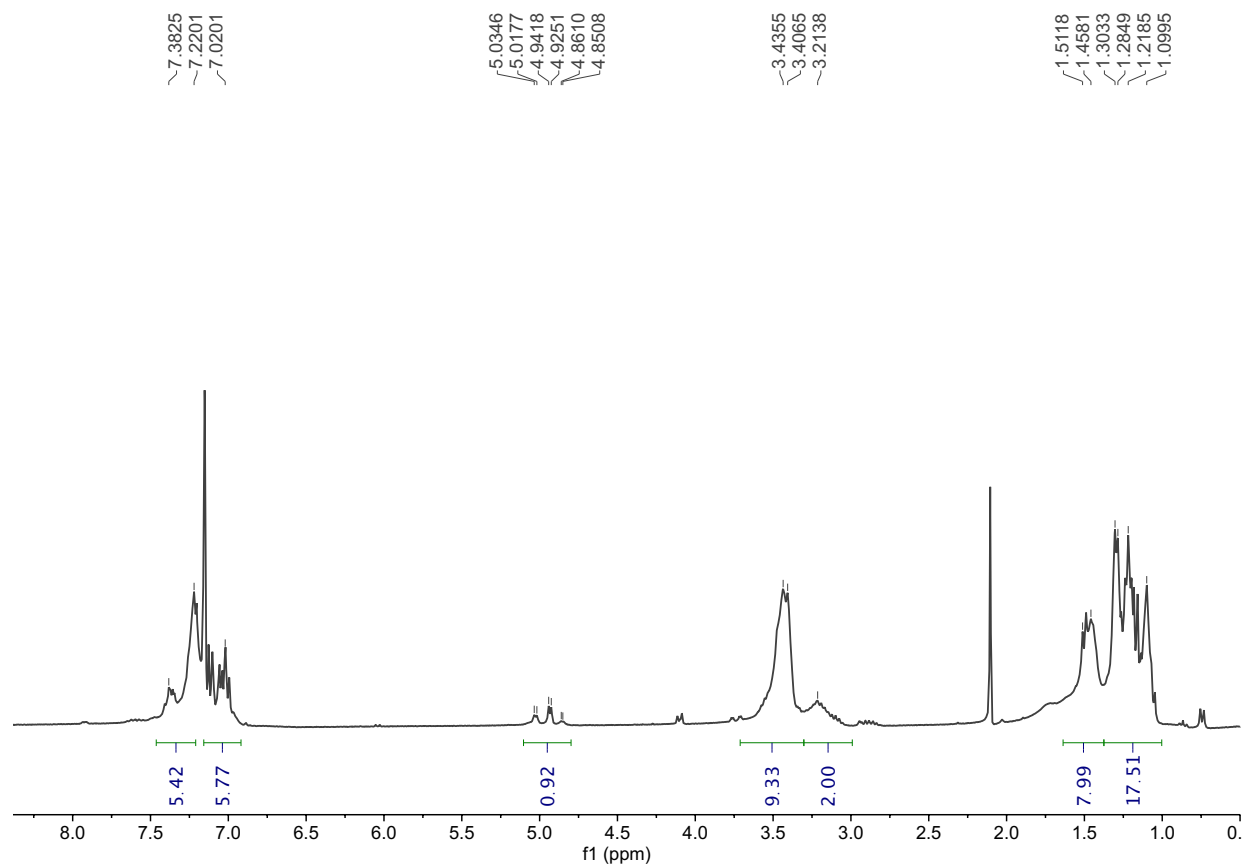
Figure 16: ^{1}H NMR spectrum of lithium enolate, **9**, taken in C$_6$D$_6$ (300 MHz).

The use of trialkylsilyl-protected enolates in coordination chemistry with metal chlorides is an alternate route to access metal complexes through liberation of trimethylsilyl chloride.[53] The more stable trialkylsilyl-protected enolates can provide control in reactivity of the ligand precursor and the resulting silyl chloride can be removed *in vacuo*, providing a convenient method of product isolation. These silyl vinyl ethers are accessed through the reaction of the enolate and a silyl chloride. Accessing **10** using the isolated lithium enolate and TMSCl produces LiCl as a side product, allowing for isolation by a simple filtration with a yield of 83% (**Scheme 29**).

Scheme 29: Synthesis of the silyl vinyl ether ligand precursor, **10**.
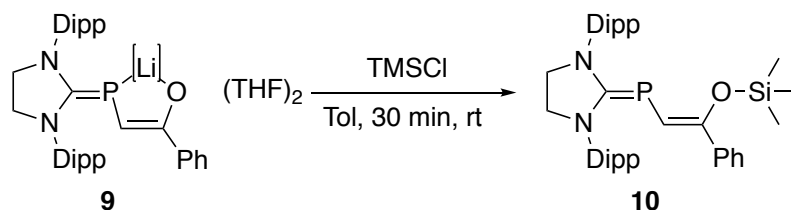
Characterization by NMR spectroscopy reveals the ^{31}P NMR chemical shift is similar to the chemical shift observed for the enol tautomer **9**, at –27.0 ppm. The ^{1}H NMR spectrum is similar to those of the other ligand precursors with two magnetically inequivalent methine protons and three resonances observed for the methyl groups of the diisopropylphenyl rings (**Figure 17**). The signal for the vinylic proton is observed at 6.06 ppm with $^2J_{HP}$ = 7.8 Hz. The broad peaks are due to the restricted rotation about the C–P bond, similar to the restricted rotation about the neutral ligand precursor, **8**.
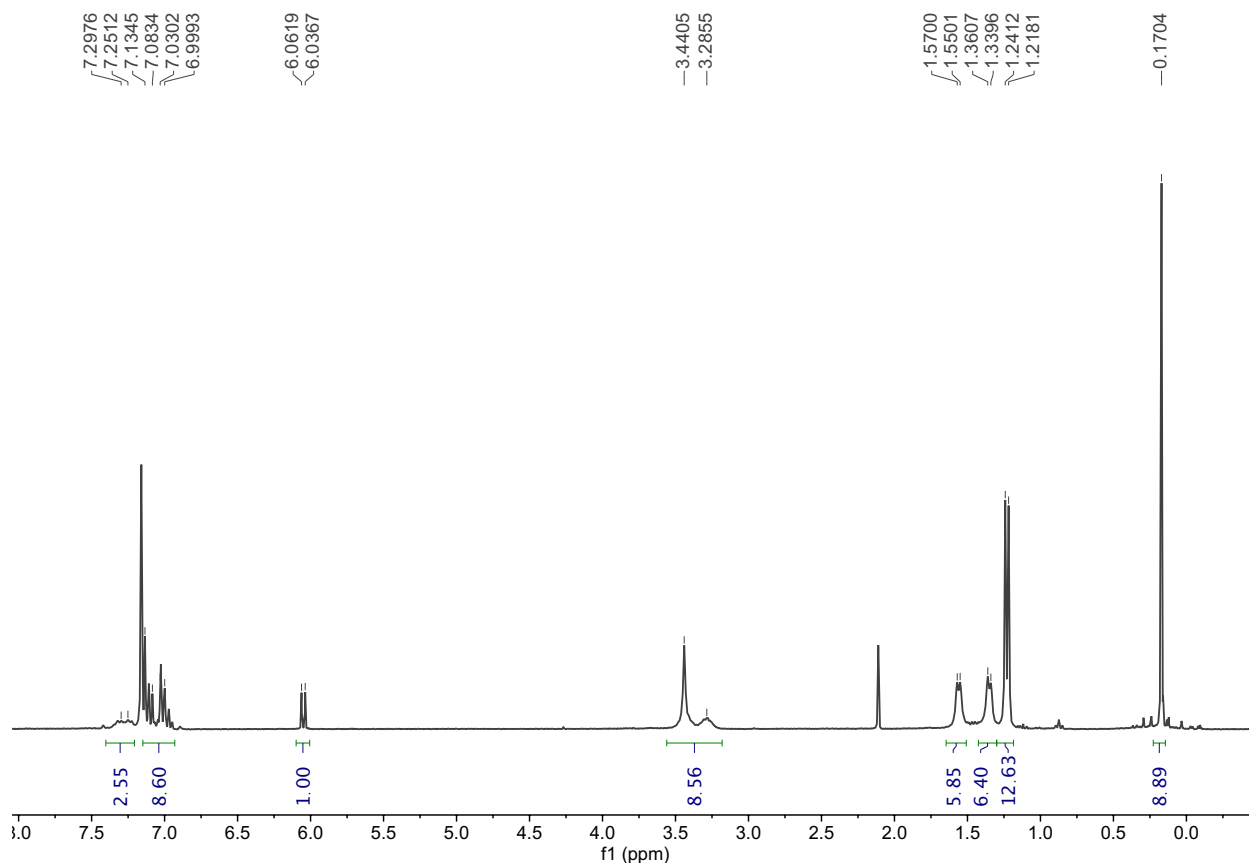
Figure 17: ^{1}H NMR spectrum of silyl vinyl ether, **10**, taken in C_6D_6 (300 MHz).

Starting from the ligand precursor bearing an electron-withdrawing group at the *para*-position of the phenyl ring, **5Cl**, the silyl vinyl ether **10Cl** was also prepared for coordination studies. The synthesis of **10Cl** was performed directly from **5Cl** through the use of two equivalents of LiHMDS and subsequent addition of TMSCl (**Scheme 30**). Isolation of the product is obtained by extracting the product with toluene from the crude reaction mixture with toluene and filtering through a Celite plug. Subsequent removal of volatiles yields a yellow solid that is then washed with cold pentane. Removal of residual pentane *in vacuo* yields the yellow solids in 96% yield.

Scheme 30: Synthesis of the silyl vinyl ether ligand precursor bearing an electron withdrawing group at the *para*-position of the phenyl ring.
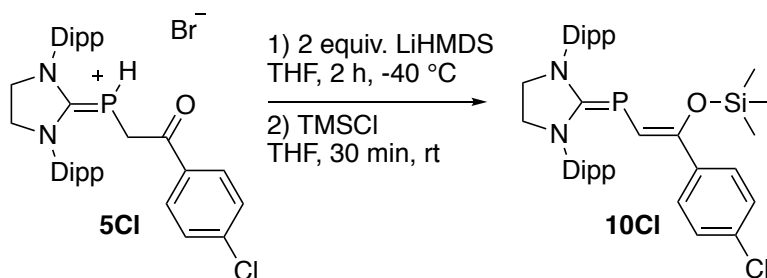
The ^{1}H NMR spectrum of **10Cl** is similar to the spectrum of **10** with the vinylic proton resonating at 6.03 ppm with $^2J_{PH}$ = 7.5 Hz (**Figure 18**). The protons at the *ortho* and *meta* positions of the phenyl ring are also observed as two sharp doublets while the protons of the diisopropylphenyl rings are observed as broad peaks. The rigid C–P double bond is maintained in this structure, resulting in broad peaks observed for the diisopropylphenyl rings.
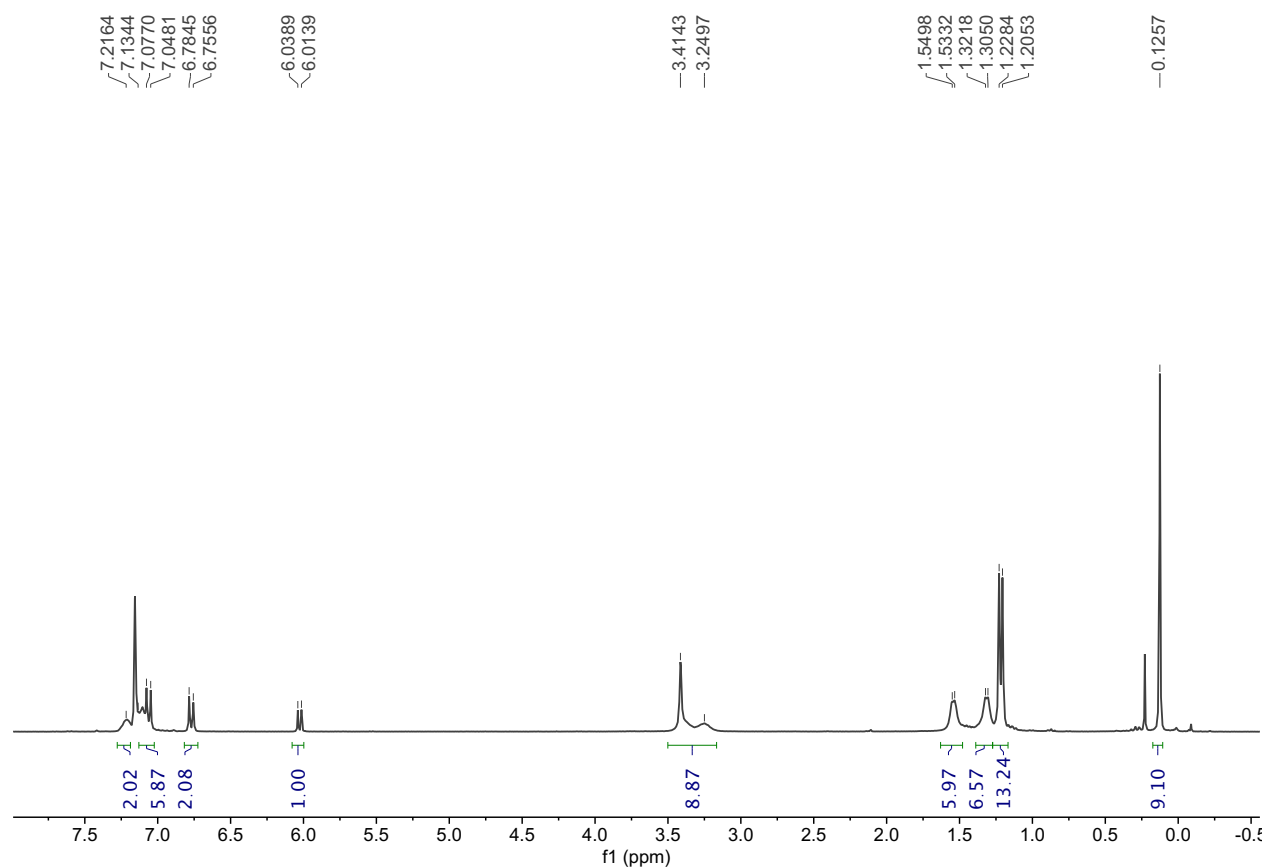
Figure 18: ^{1}H NMR spectrum of the silyl vinyl ether bearing an electron withdrawing group at the *para*-position of the phenyl ring, **10Cl**, taken in C_6D_6 (300 MHz).

The series of imidazolidine-based ligands show more unique signals for the methine and methyl protons of the diisopropylphenyl rings than the imidazole-based counterparts. This observation is due to the increased double bond character of the C–P bond, restricting rotation about that bond and yielding more unique environments for the protons of the diisopropylphenyl rings. This increase in double bond character is a result of the increased π-acidity of the carbenoid carbon, resulting in a less electron-rich phosphorus nucleus. Thus, this phosphorus atom of the imidazolidine-based ligand will have less donating capability to the metal centre in its respective complex. This will produce a more electropositive metal centre that should have greater activity in olefin

47

polymerization. Additionally, this increase in C–P double bond character may contribute to the formation of a more stable precatalyst and active catalyst for the polymerization of olefins. To obtain the rotational barrier, variable-temperature NMR studies were performed on the silyl vinyl ether, **10** (**Figure 19**).
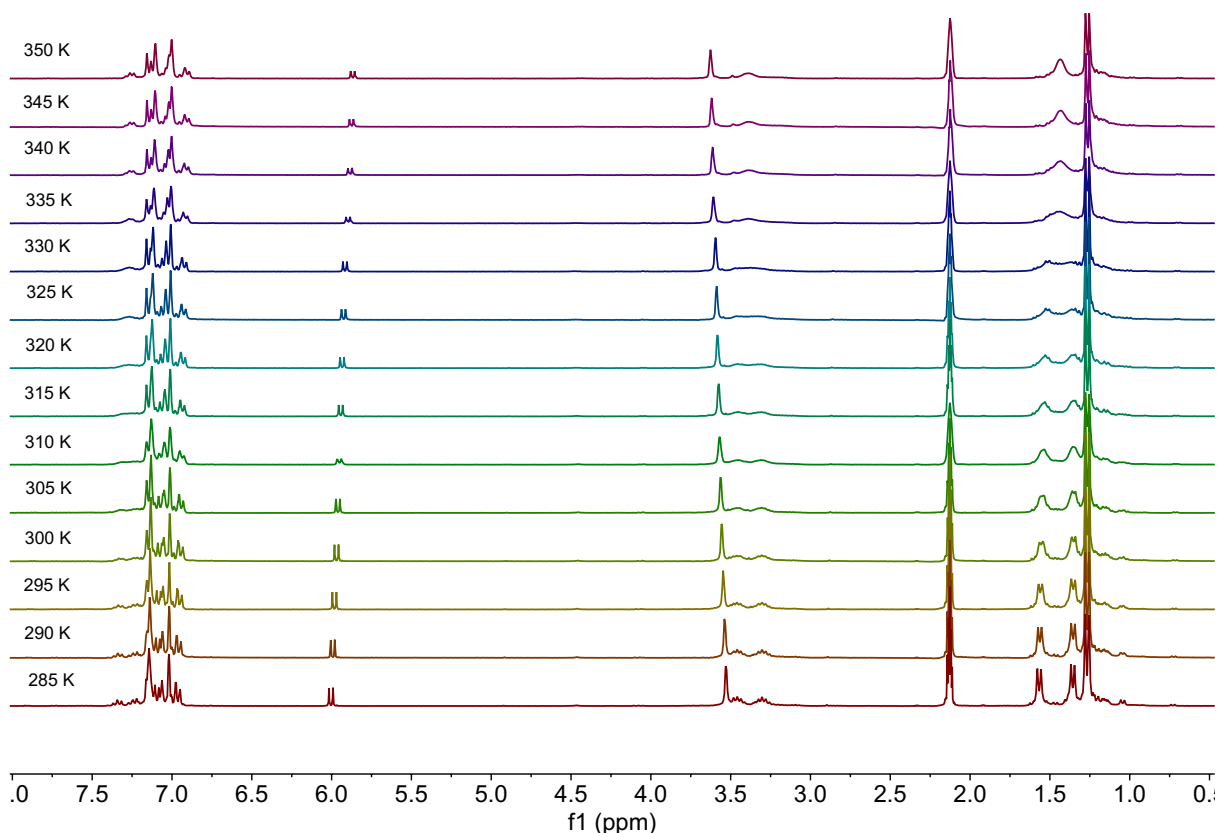
Figure 19: Variable temperature studies performed on **10** in toluene-d^8 (300 MHz).

Using the signals for the isopropyl groups of the diisopropylphenyl rings of **10** the coalescence temperature (T$_C$) is 335 K. Using the Eyring equation an $\Delta G^{\ddagger}$ value of 71 kJ•mol^{-1} was obtained for the rotation of the C–P double bond of **10** (**Figure 20**). Comparatively, the $\Delta G^{\ddagger}$ values of phenyl bearing imidazole (**11**) and imidazolidine (**12**) phosphaalkenes are 34 and 58 kJ•mol^{-1} respectively.[4] The increase in energy required to rotate the C–P bond for **12** over **11** confirms the increased π-acidity of the carbenoid

carbon in **12**, resulting in more double bond character. For the imidazole-based silyl vinyl

ether, **13**, only one methine and two methyl signals are observed at room temperature

meaning there is free rotation about the C–P bond at that temperature (**Figure 20**). This

means the energy needed for rotation of that bond is met at a lower temperature. Thus,

10 has more double bond character than the imidazole counterpart, **13**, which is

consistent with the observed rotation barriers for **11** and **12**. Therefore, the double bond

character of the C–P bond of the parent phosphaalkenes used in the synthesis of the

ligand precursors are carried on to the ligand precursors themselves. The increased

double bond character of the imidazolidine-based ligand precursor may contribute to a

more thermally stable and more active catalyst in olefin polymerization.

$\Delta G^{\ddagger}$ (kJ·mol^{-1}):	71	34	58	
T_C (K)	335	180	293	< 293
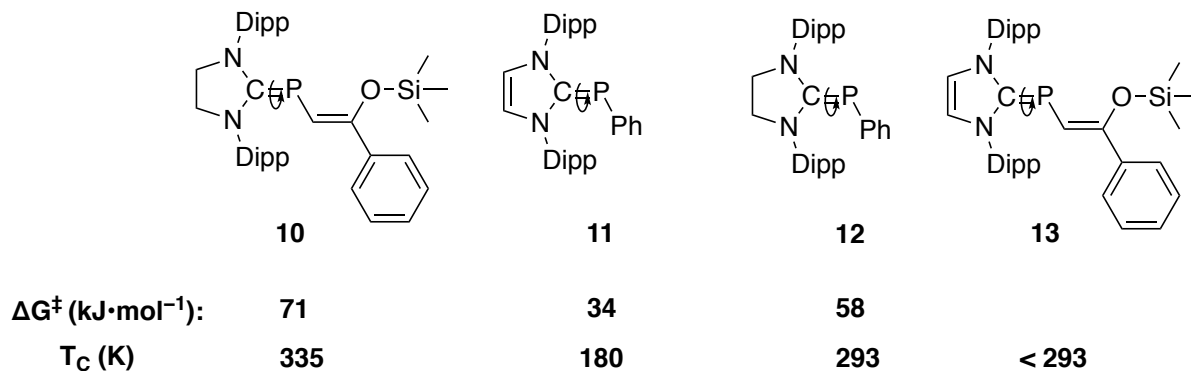
Figure 20: $\Delta G^{\ddagger}$ and T_c of rotation around the C–P bond of inversely-polarized phosphaalkenes **10**, **11**, **12**, and **13**.

2.4 Coordination Chemistry of Imidazolidine-Based Inversely-Polarized Phosphaalkene-Enolates

The coordination chemistry of the imidazolidine-based inversely-polarized

phosphaalkene-enolate ligand was explored with multiple metal precursors from groups

4 and 10. The intention of the coordination chemistry was to access precatalysts for olefin

polymerization of the SHOP-type, FI-type, and the heavier congener to the imine-

ethenolate titanium catalyst. However, coordination and isolation of the resulting complex was only successful with cyclopentadienyltitanium(IV) trichloride (CpTiCl$_3$).

Initially the reaction between the **9** and the metal precursor was attempted as it was expected this would yield the desired complex. However, it was observed that three phosphorus containing products, including **14**, were produced immediately after addition of **9** to a solution of CpTiCl$_3$ (**Scheme 31**). In order to gain more control over the distribution of products, the reaction was reattempted at −78 °C and another was heated to 60 °C. The reaction performed at −78 °C had little effect on the resulting product distribution but heating the reaction to 60 °C increased the relative ratio of **14** to the other two.

Scheme 31: Synthesis of a Titanium complex bearing an imidazolidine-based inversely-polarized phosphaalkene-enolate ligand from **9**.
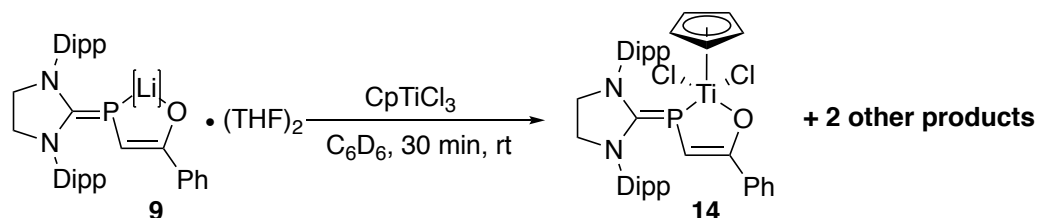
However, reaction of the silyl vinyl ether derivative **10** and CpTiCl$_3$ gives only one phosphorus-containing species, as determined by ^{31}P NMR spectroscopy (**Scheme 32**). After 5 days, the reaction is complete and isolation of the catalyst from the reaction mixture is obtained by removal of volatiles and subsequent washing with pentane. Drying the insoluble solids *in vacuo* gives **14** in 94% yield.

Scheme 32: Synthesis of a Titanium complex bearing an imidazolidine-based inversely-polarized phosphaalkene-enolate ligand from **10**.
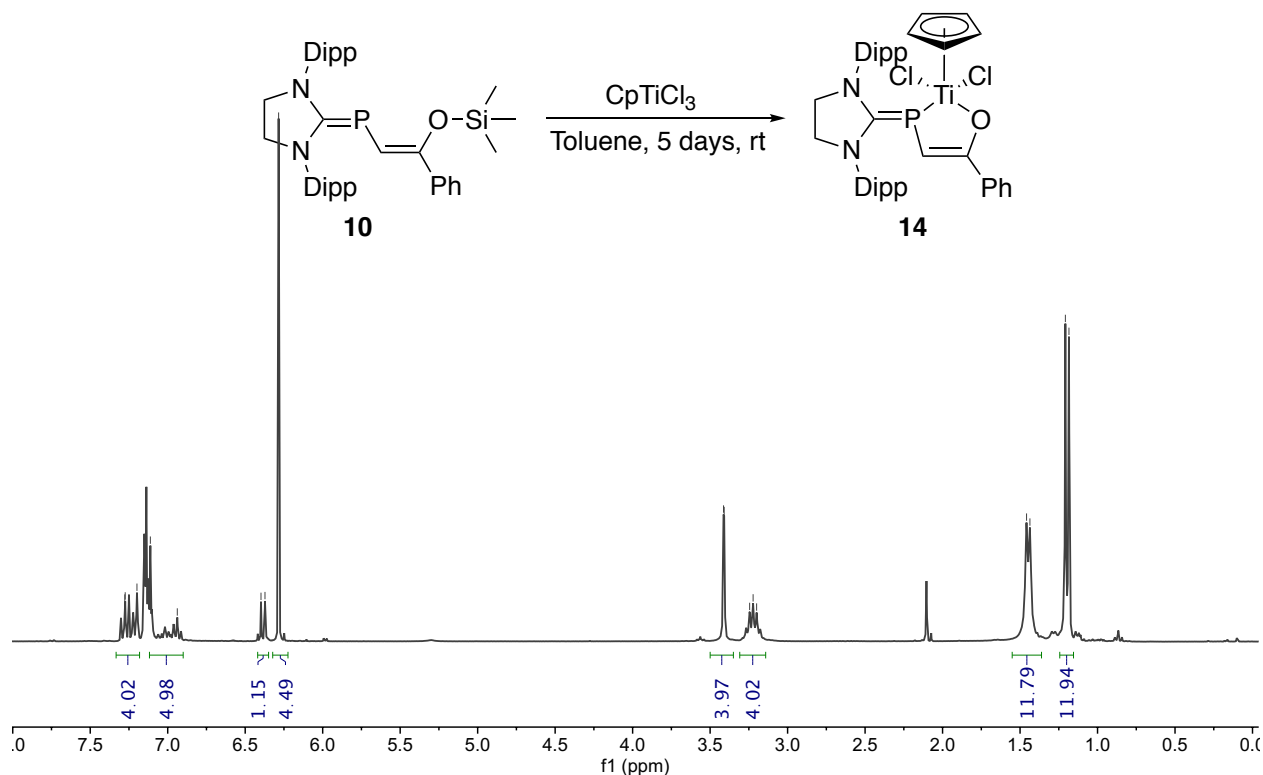
Figure 21: ^{1}H NMR spectrum of titanium complex bearing an imidazolidine-based IPP-enolate ligand, **14**, taken in C$_6$D$_6$ (300 MHz).

The NMR spectra of this product is also consistent with the complex of the related imidazole-based ligand. The signal for the cyclopentadienyl ligand is observed as a singlet at 6.29 ppm in the ^{1}H NMR spectrum (**Figure 21**). The vinylic proton for the ligand is observed at 6.37 ppm with $^2J_{HP}$ = 7.8 Hz. In contrast to the neutral and TMS-protected ligand, there is only one single magnetic environment observed for the methine groups and two for the methyl groups of the diisopropylphenyl rings of the bound ligand. The signal for the phosphorus atom of **14** is observed as a doublet at −23.6 with $^2J_{PH}$ = 7.7 Hz.

Notably, the reaction of **10** and CpTiCl$_3$ is much slower than the reaction of its imidazole-based counterpart. Complete conversion to **14** is observed after 5 days at room temperature, where the imidazole complex is accessed within 10 minutes as observed in the synthesis of the titanium complex bearing an IPP-enolate prepared by Juan E. R. Villanueva during his MSc studies in the Lavoie group. The slow reaction time with the imidazolidine-based ligand is attributed to the reduced nucleophilicity and slightly increased steric crowding of the phosphorus atom caused by the saturated backbone.[4,54] In attempt to increase the rate of reaction, the reaction mixture was heated to 60 °C. However, upon heating an additional species is produced, observed by ^{31}P NMR spectroscopy.

Thermostability studies were performed on **14** in C$_6$D$_6$ at 60 °C over five days (**Figure 22**). The experiment was set up using residual toluene as an internal standard for the relative concentration of **14** in solution. Each data point is the ratio of relative integration value of the signal for the saturated backbone of **14** at the respective time to the value obtained at 1 hour. Thus, at t = 122 h, approximately 6% of **14** has been consumed. However, the experiment was performed only once. Therefore, it is not known if this data could be reproduced to produce the exact amount of decomposition. Thus, a half-life of this complex in benzene-d$_6$ at 60 °C cannot be obtained. The titanium complex bearing the imidazolidine-based ligand is more stable than the imidazole counterpart as it has an observed decomposition of 15% over 24 hours at 60 °C in C$_6$D$_6$ using a comparable method. A thermally stable catalyst is a critical property in commercial reactions.
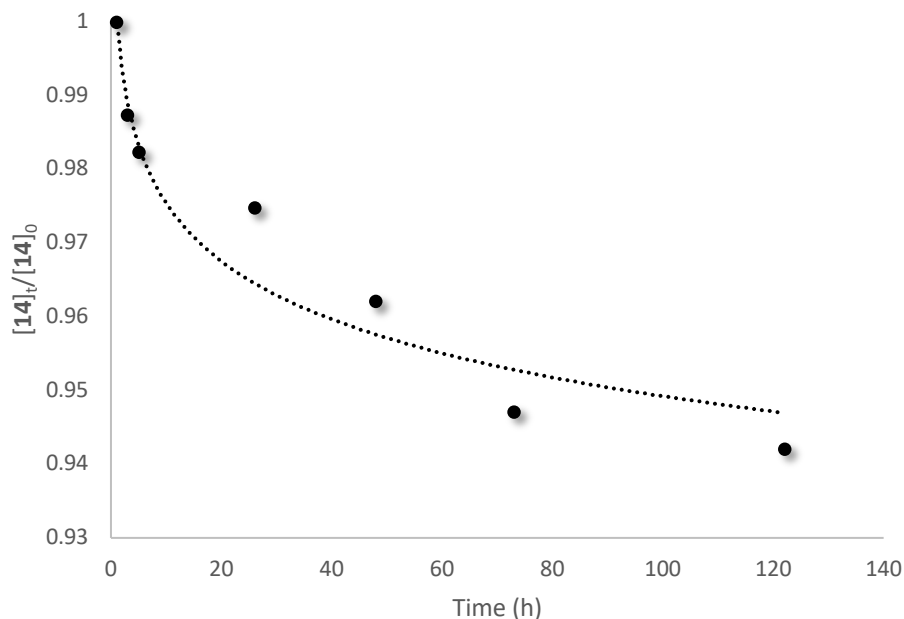
Figure 22: Thermostability study of **14** performed in C_6D_6 at 60 °C over five days.

Computational studies were performed to rationalize this increase in stability using the B3LYP functional and 6-31G++ basis set (**Figure 23**). There is a slightly shorter Ti–O bond length in **14** (1.938 Å) than the imidazole counterpart, **15** (1.947 Å), which is likely contributing to the increased stability of the complex. The C–P bond is also slightly shorter in **14** than **15** with bond lengths of 1.812 and 1.826 Å respectively, consistent with a more π-acidic carbenoid carbon in **14**. However, the Ti–P bond is shorter in **15** (2.699 Å) than it is **14** (2.737 Å). The ligand also is capable of sharing electron density from the ethenolate carbon-carbon double bond in a similar fashion of how ethylene binds a metal centre. This is supported by the elongated C–C double bond length of 1.375 Å, slightly longer than a typical C–C double bond.[55] The distance from the C–C double bond of the IPP-enolate ligand of **14** to the titanium centre is 2.469 Å, which is shorter than the distance calculated for Ti(IV) complexes bearing a bound ethylene molecule.[56] This phenomenon is also observed in the case of the imine-ethenolate ligand bound to group

4 metals.[12] The ability of the phosphaalkene-enolate ligand in **14** to donate electron density from multiple centres may contribute to the thermostability of the complex, which may result in a more stable active catalyst.
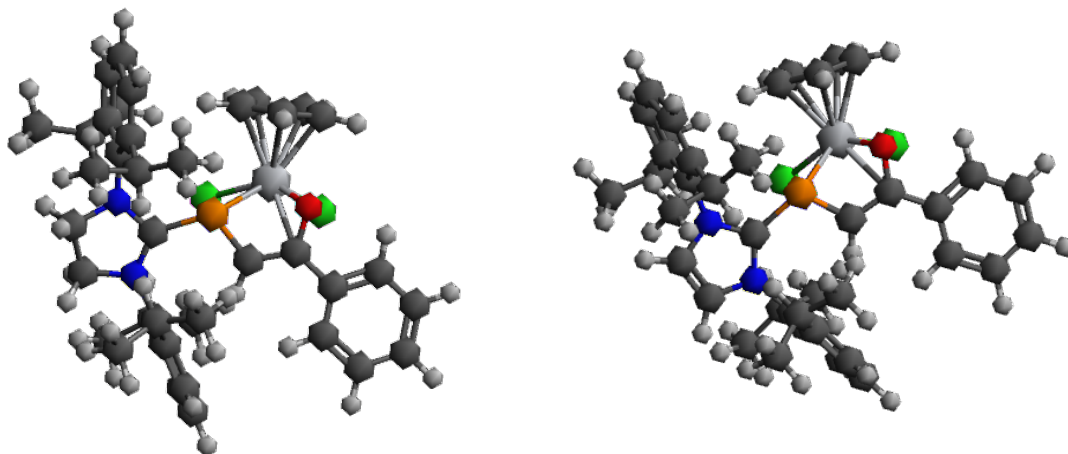
Figure 23: Optimized structures of **14** (left) and **15** (right).

With the success of the reaction between **10** and CpTiCl$_3$, the analogous reaction with **10Cl** was attempted (**Scheme 33**). Initially, the reaction was set up with only a small excess of CpTiCl$_3$ in toluene and after 16 hours less than 20% of **10Cl** and CpTiCl$_3$ had reacted. In order to drive the reaction forward, four additional equivalents of CpTiCl$_3$ were added. Immediately, more of **10Cl** was consumed and converted to **14Cl**, but still only half of the ligand precursor had converted. To drive the reaction forward, the temperature was increased to 60 °C. After two hours at 60 °C with 5.1 equivalents of CpTiCl$_3$ the full conversion of **10Cl** to **14Cl** was observed. Surprisingly, the reaction produced only the complex **14Cl** at 60 °C as the reaction of **11** and CpTiCl$_3$ at 60 °C gave multiple products. Alternatively, the full conversion of **10Cl** to **14Cl** occurs after 24 h at room temperature with 5 equivalents of CpTiCl$_3$. In attempts to isolate the desired complex and remove

54

excess CpTiCl₃, several extractions and crystallization experiments were performed using

pentane, toluene or a mixture of the two solvents. However, isolation of **14Cl** was not

successful as the removal of unreacted CpTiCl₃ was not achieved (**Figure 24**).

Scheme 33: Synthesis of titanium complex bearing an inversely-polarized phosphaalkene-enolate ligand with an additional electron withdrawing group.
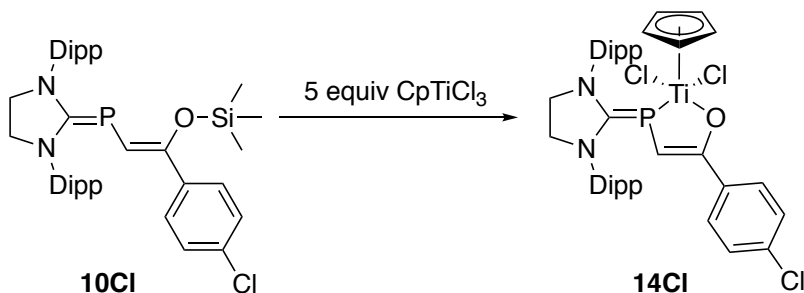
The ^{1}H NMR spectrum of **14Cl** obtained with residual CpTiCl₃ is similar to **14**,

where the vinylic proton is observed at 6.34 ppm with $^2J_{PH}$ = 7.7 Hz and the signal for the

cyclopentadienyl ligand is observed as a singlet at 6.28 ppm (**Figure 24**). Furthermore,

there is only one signal for the methine protons and two for the methyl protons of the

diisopropylphenyl rings. The ^{31}P NMR spectrum yields a doublet with $^2J_{PH}$ = 7.7 Hz

centred at −23.1 ppm. Unreacted CpTiCl₃ is observed in the spectrum as a singlet at 6.04

ppm.
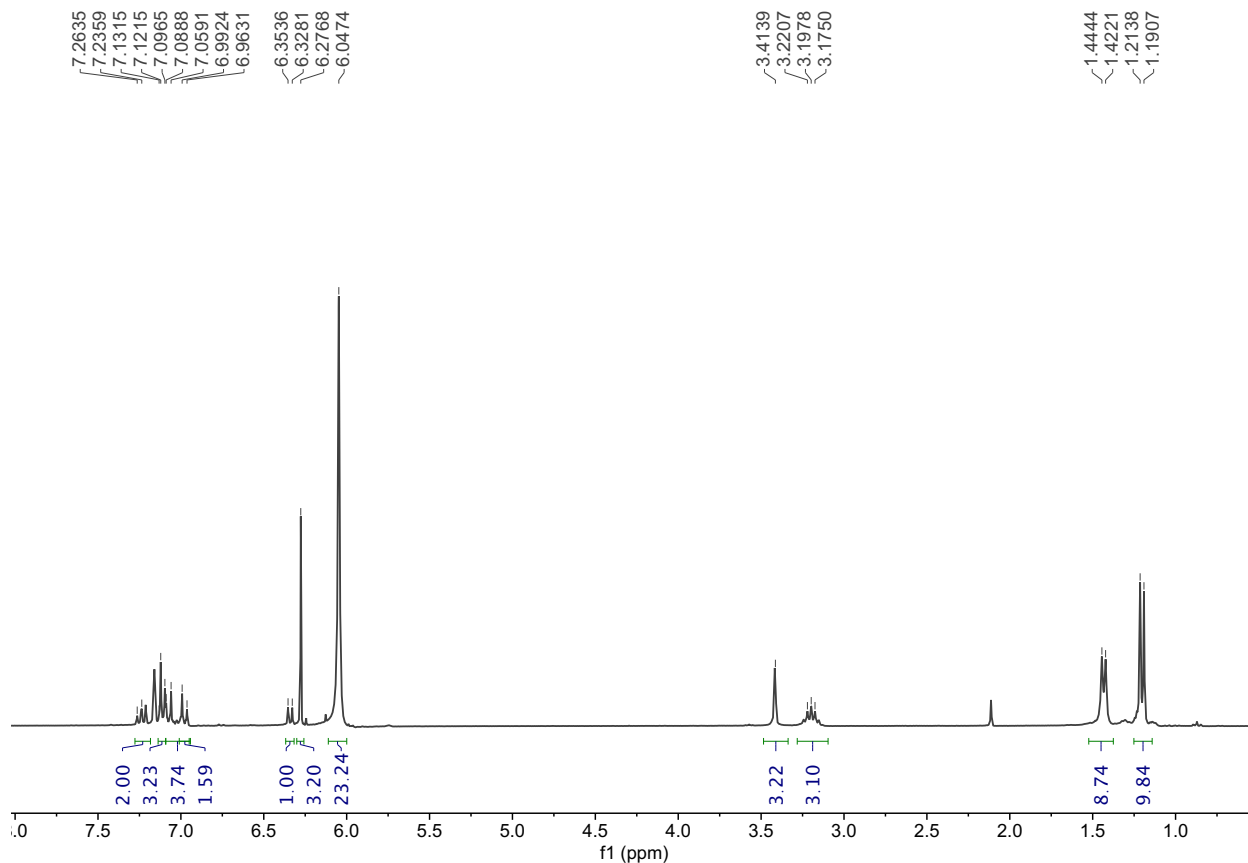
Figure 24: ^{1}H NMR spectrum of complex with an IPP-enolate ligand bearing an electron withdrawing group, **14Cl**, taken in C_6D_6 (300 MHz). Spectrum shows unreacted CpTiCl$_3$ at 6.05 ppm.

2.5 Activity in Olefin Polymerization

The ability of **14** to polymerize ethylene in toluene at room temperature in the presence of 220 equivalents of MMAO-12 and one atmosphere of ethylene gas was assessed in duplicates at time intervals from 30 minutes to five hours (**Table 1**). It was found that **14** gave turnover frequency (TOF) values as high as 5.64 kg$_{PE}$ • mol$_{Ti}^{-1}$ • h^{-1}, based on the cumulative amount of polyethylene (PE) produced at the given time. This value is thus not a representation of the instantaneous production rate of polyethylene at any given time. These values have an average relative standard deviation of 8%,

determined by the deviation in the amount of polyethylene produced between duplicate trials at each time interval.

Table 1: Ethylene polymerization activity of **14** in the presence of MMAO-12.

Time (h)	Mass of PE produced (g)	TON $(mol_{C2H4} \bullet mol_{Ti}^{-1})$	TOF $(kg_{PE} \bullet mol_{Ti}^{-1} \bullet h^{-1})$
0.5	0.144	100	5.64
1	0.181	127	3.54
2	0.252	177	2.47
3	0.325	228	2.13
5	0.667	468	2.62

Polymerization experiments performed under 1 atm of ethylene gas in a total volume of 30 mL of toluene at room temperature with vigorous stirring with 0.0509 mmol of precatalyst (**14**) and 11.2 mmol of MMAO.

The polyethylene was characterized by differential scanning calorimetry (DSC) and high-temperature NMR spectroscopy. Thus, the polyethylene has a melting temperature (T_m) of 131 °C with an onset of melting at 105 °C. The heat capacity of the crystals was determined to be 170 J/g which indicated a polymer with 58.0% crystallinity. For obtaining the average molecular weight and qualitatively assigning the linearity of the polymer, ^{1}H and ^{13}C NMR spectra were obtained of the polymer in 1,2-dichlorobenzene-d4 at 145 °C. The ^{1}H NMR spectrum revealed that the polymer has an average of 628 repeating units giving a number average molecular weight of 17.6 kDa. In the ^{13}C NMR spectrum only one signal is observed for the main polymer chain meaning the polymer is highly linear. Thus, with the data obtained it can be concluded that the polymer produced from a polymerization using **14** as the precatalyst is highly linear HDPE with a T_m of 131 °C and molecular weight of 17.6 kDa.

This catalyst is outperformed by the imidazole counterpart **15**, as well as CpTiCl₃, and the analogous guanidine, **16**, (**Figure 25**) with TOF values as high as 9.2, 39, and 170 kg_PE•mol_Ti⁻¹•h⁻¹ respectively obtained under comparable reaction conditions (**Table 2**). It was expected that **14** would have higher activity than the imidazole counterpart due to the reduced electron donating ability of the phosphorus atom. However, this is not the case.
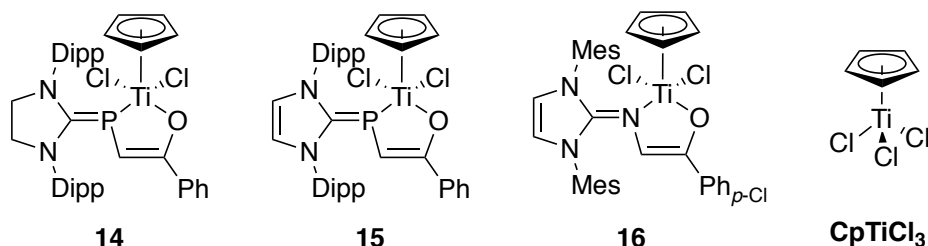
Figure 25: Half-metallocene titanium complexes comparable to **14** with known activities in olefin polymerization.

The reduced catalytic activity of **14** is possibly due to the increased steric crowding of the phosphorus atom caused by the saturated backbone of the azole ring.[57] The increase in bulk of the saturated compared to the unsaturated backbone of the carbene is reflected in the percent buried volume of the respective Au(I) complexes. Buried volume is the measure of the relative amount of volume that is occupied by a ligand within the coordination sphere of a coordination compound.[57] When bound to AuCl, the carbene with the saturated backbone (analogous to **14**) has a buried volume of 47% while the unsaturated carbene (analogous to **15**) has a buried volume of 44.5%.[57] This may contribute to the longer Ti–P bond computed for **14** (2.737 Å) than **15** (2.699 Å), as the more sterically demanding imidazolidine fragment will prevent the phosphorus atom from binding the titanium centre more closely. This also results in a greater computed distance of titanium from the C–C double bond of the P^O⁻ ligand to the metal centre in **14** (2.469 Å) than **15** (2.447 Å). Consequently, the first coordination sphere will be more open,

which will result in slower insertion of bound ethylene into the growing polymer. Thus, the activity of the active species of **14** is possibly lower as a result of a slower rate of propagation.

Table 2: Turnover frequencies (TOF) obtained for precatalysts **14**, **15**, CpTiCl$_3$, and **16**. Turnover frequencies are reported in kg$_{PE}$•mol$_{Ti}^{-1}$•h^{-1}

Time (h)	14	15	16	CpTiCl$_3$
0.25	–	–	170	38.8
0.5	5.64	9.24	–	25.4
1	3.54	7.56	–	21.9
2	2.47	3.50	–	19.5
3	2.13	3.83	–	13.9
5	2.62	2.97	–	–

TOF values for **15** and CpTiCl$_3$ obtained from results by Juan E. R. Villanueva in the Lavoie Group. TOF value for **16** obtained from T. G. Larocque et al.[30] All experiments were performed at room temperature with 1 atm of ethylene gas. Experiments for **14**, **15** and CpTiCl$_3$ performed with 220 equivalents of MMAO, experiment for **16** performed with 1000 equivalents of MAO.

The polymerization experiments with **14** indicate the active species is relatively stable over the time of the polymerization experiments (**Figure 26**). The data point at t = 5 hours is unexpectedly high for the TOF of **14**, however this can be attributed to the error associated with small-scale polymerization experiments. These errors include the time of addition of reagents, the exact amounts of reagent added, the stir rate, and the concentration of monomer in solution. The slope of the linear regression obtained for the TON of **14** over 5 hours is 80.1 mol$_{C2H4}$ • mol$_{Ti}^{-1}$ • h^{-1} with very little deviation from this upwards trend (R^2 = 0.949). The lack of deviation suggests the active species has a slow decay in the polymerization conditions as the production of polyethylene follows a linear

trend against time. This is reflected in the TOF values obtained for **14**. The initial drop in activity can be attributed to the bimolecular deactivation of the active species, as seen in polymerizations using single-site group 4 catalysts.[58,59] However, this reaction becomes less prominent as the polymerization experiment progresses over time due to the decreasing relative concentration of the catalyst. This is observed from the lower rate of decay in activity observed after two hours. The initial drop in activity of **15** is steeper than the drop in activity for **14**, suggesting that the active species of **14** has greater stability than **15** (**Figure 26**). Otherwise, the same general trend is observed for the TON and TOF values of **15**. The stability of the active species of **14** is likely related to the thermostability of **14** itself.

The polymer produced using **15** as the precatalyst is also highly linear HDPE, but is only 48.7% crystalline and has a molecular weight of 6.01 kDa. Thus, while the activity of **14** for olefin polymerization is lower, the material produced is larger in size and is more crystalline than the polymer produced by olefin polymerization using **15** under comparable reaction conditions.
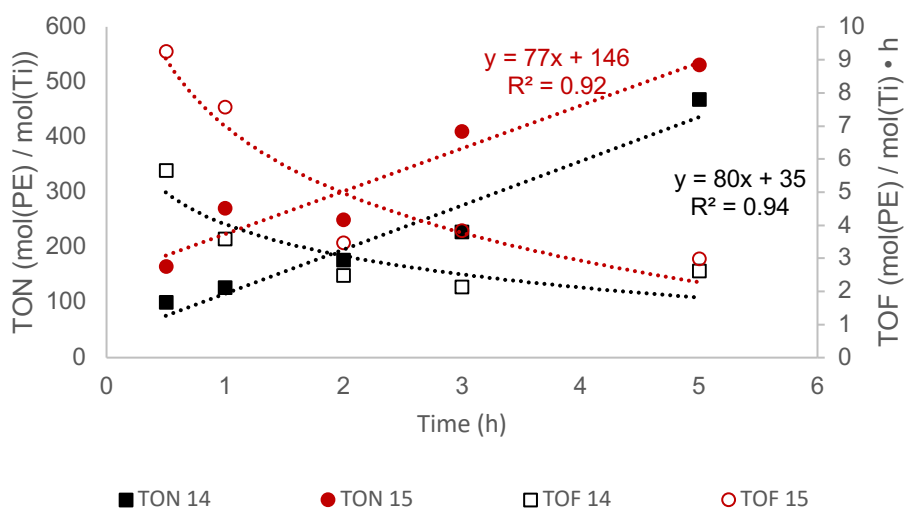
Figure 26: Activity of **14** (black) and **15** (red) in the polymerization of ethylene.

In comparison to the imine-ethenolate titanium catalysts studied previously in the Lavoie group, the titanium complexes bearing inversely-polarized phosphaalkene-enolates have lower activities. The imine-ethenolate catalysts exhibited activity as high as 170 $kg_{PE} \cdot mol_{Ti}^{-1} \cdot h^{-1}$ (**Table 2**).[30] The difference in activity can be attributed to the double bond character of the guanidine fragment compared to the inversely-polarized phosphaalkene fragment as this dictates the number of lone pairs available for bonding from the pnictogen centre. In the case of guanidine ligands, a strong double bond exists between the carbenoid carbon and the imine nitrogen, yielding a single lone pair available for coordination to a metal centre (**Figure 27**). However, inversely-polarized phosphaalkenes have less double bond character and will have two lone pairs available for bonding at the phosphorus atom.[13] This will result in a less electropositive metal centre and produce a less active catalyst. Additionally, the titanium complexes bearing an imine-ethenolate ligand may be more stable as a product of a stronger exocyclic $C_{carbenoid}$–N

bond. However, no studies into polymerizations at longer times nor studies into the thermal stability of the precursors or precatalyst (**16**) were performed.[12]
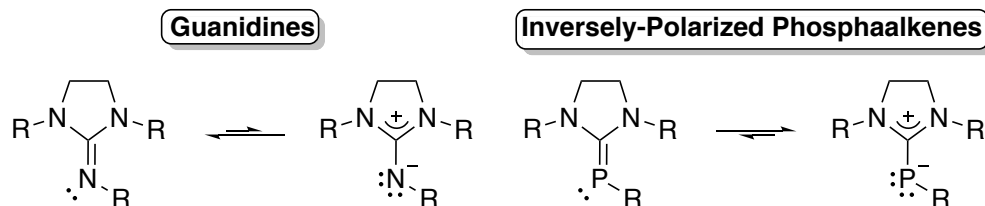

Figure 27: Favored canonical forms of guanidines and inversely-polarized phosphaalkenes.

The Wiberg bond indices for the carbenoid carbon of the ligand precursors were computed to confirm the increased double bond character (**Table 3**). The Wiberg bond index value is computed from a set of orthogonal natural atomic orbitals that are routinely obtained from a natural bonding orbital (NBO) computation. The values obtained are a sum of squared density matrix elements between the two atoms and are a good representation of bond order.[60] Generally, a single bond will have a calculated Wiberg bond index value of one and a double bond will have a bond index value of two. The computations for **8**, **17**, and **18** were performed using the B3LYP functional and 6-31G++ basis set. It was confirmed that there is significantly more double bond character for the guanidine **18**, favoring the structure with one pair of electrons available for bonding. This is supported by the high bond index for the nitrogen-carbenoid carbon bond and low bond index values for the carbon-nitrogen bonds of the azole ring. The phosphaalkenes, **8** and **17** have less double bond character, as they have slightly larger bond index values for the C–N bonds of the azole ring and a lower bond index value for the P–C bond. Additionally, **8** shows more double bond character than **17** which is consistent with the NMR spectroscopy studies on the ligand precursors. The reduced double bond character

in these phosphaalkenes results in a structure that has two lone pairs available at phosphorus.

Table 3: Computed Wiberg bond indices for neutral ligand precursors.

Compound	N^1-$C_{Carbenoid}$	N^2-$C_{Carbenoid}$	E-$C_{Carbenoid}$
8	1.129	1.131	1.391 (E = P)
17	1.112	1.117	1.326 (E = P)
18	1.068	1.049	1.627 (E = N)
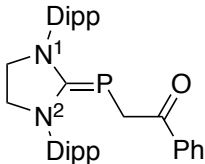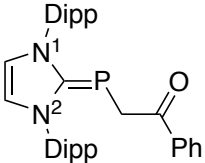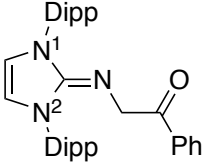
Computations performed using the B3LYP functional and 6-31G++ basis set. The Wiberg bond index values were obtained directly from the output file.

The number of lone pairs available at the donor atom in these ligands has a large impact on the reactivity of the Lewis acidic metal centre. Typically, the active species in group 4 metallocene and single-site olefin polymerization catalysts is a 14-valence electron complex that readily binds an alkene. In the case of inversely-polarized phosphaalkenes, the additional lone pair at the phosphorus atom can potentially be donated to the Lewis acidic metal centre, stabilizing the active species and reducing the activity in olefin polymerization (**Figure 28**). This is supported by the second-order perturbation theory analysis of the Fock matrix of the NBO analysis of **14**. The second-

order perturbation theory analysis of the Fock matrix is a routinely performed analysis from an NBO computation. This analysis samples Lewis acid and base interactions between filled and empty orbitals of an optimized structure and the resulting stabilization energy of these interactions are listed in a table when a cutoff energy is met.
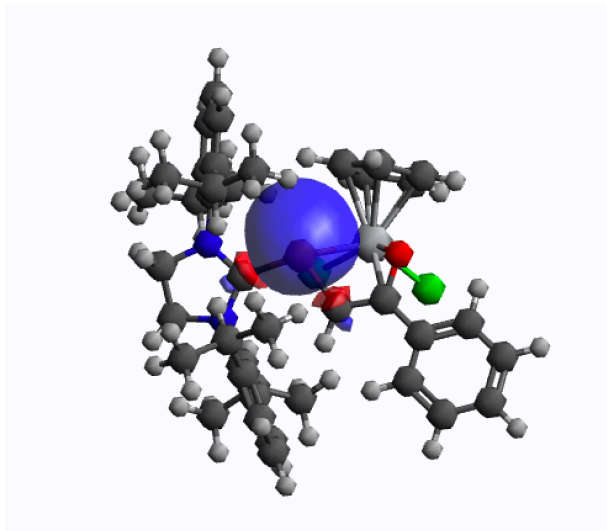

Figure 28: NBO containing lone pair of electrons on the phosphorus atom of **14**.

For example, in **14** the stabilization due to resonance of the diisopropylphenyl rings is between 17 and 23 kcal•mol^{-1}. This means in the optimized structure, which is a snapshot of the lowest energy structure, the donation of the filled π-orbital of one C–C double bond to the π*-orbital of an adjacent C–C double bond causes a stabilization of the structure of a value between 17 and 23 kcal • mol^{-1}. The donation of this additional lone pair on phosphorus to an empty orbital on titanium has a stabilization corresponding to 18.24 kcal • mol^{-1}. As a further comparison, the stabilization due to the donation of the lone pair in visualized in **Figure 28** to the carbenoid carbon is 6.12 kcal • mol^{-1}. Assuming

the ligand structure remains intact upon activation, it is reasonable that the same donor-acceptor relationship is sustained in the active species of **14**.

Thus, not only does the ligand have a structure that favors the presence of two lone pairs at phosphorus, there is evidence of donation of this additional lone pair to the resulting metal complex. However, the computed Ti–P bond is unusually long (2.737 Å, compared to 2.47 Å for the average Ti–P single bond) considering there is donation of multiple lone pairs to titanium. This bond length is a product of the sterically demanding imidazolidine fragment, preventing the close coordination of the phosphorus atom to titanium. This increase in steric bulk may kinetically stabilize the reactive metal centre.

As the P^O ligand of **14** adopts a structure in which two lone pairs are available for donation to the metal centre, the phosphorus atom should be negatively charged. However, there is a slightly positive natural population analysis charge computed for the phosphorus atom (0.401 a.u.). This is a result of the low occupancy of several natural atomic orbitals participating in bonding, yielding a total occupancy on phosphorus of 14.593 electrons with a valence shell occupancy of 4.554 electrons. These values are lower than expected (16 and 6 for total and valence occupancy, respectively) due to the strong donation of electron density to the metal centre and delocalization throughout the ligand.[60]

Despite the low activity of **14** in the polymerization of ethylene, the inversely-polarized phosphaalkene-enolate ligand may be capable of producing a catalyst that is capable of performing copolymerization with further tuning of the ligand structure. The current activity of the titanium complexes bearing inversely-polarized phosphaalkene-enolate ligands is too low to be efficient catalysts for the polymerization of larger olefins,

including those containing polar functional groups.[61] The current data suggests that avoiding an excess of steric bulk from the carbene fragment will benefit catalyst activity, as seen in the activity between **14** and **15**. Furthermore, addition of electron-withdrawing groups to the phenyl ring of the acetophenone moiety should increase the activity of the resulting catalyst, as observed in the imine-ethenolate analogs.[30] Unfortunately, this was not tested with the IPP-enolate ligand bearing an electron withdrawing group as the pre-catalyst **14Cl** was not isolated from the metal precursor, $CpTiCl_3$.

3. Conclusions

Several new inversely-polarized phosphaalkenes have been prepared en route to the successful expansion of the library of monoanionic bidentate inversely-polarized phosphaalkene-enolate ligand precursors, including the first ring-expanded hydrido-inversely-polarized phosphaalkene. NMR spectroscopy studies on the ligand precursors reveal that the degree of C–P double bond character of the parent phosphaalkene used in the synthesis of the ligand precursor is carried through to the ligand precursor itself.

The coordination of the imidazolidine-based inversely-polarized phosphaalkene-enolates was successful in producing new group 4 transition metal complexes. The titanium complex **14** is stable for several days at elevated temperatures, a critical property for commercial reactions. Compound **14** polymerizes ethylene over several hours, with an initial rate of 5.64 $kg_{PE} \cdot mol_{Ti}^{-1} \cdot h^{-1}$.

Computational studies performed on the complexes and ligand precursors confirm that there is less $C_{Carbenoid}$–P double bond character in the inversely-polarized phosphaalkenes than the $C_{Carbenoid}$–N bond in the corresponding guanidines. Thus, the phosphorus atom of these inversely-polarized phosphaalkene-enolates adopt a structure in which two lone pairs are available for donation to titanium from a partially negative phosphorus atom, stabilizing the metal centre of the precatalyst and potentially the active species.

The synthesis of new ligand precursors bearing electron-withdrawing substituents on the acetophenone moiety, the preparation of new group 4 and 10 complexes bearing inversely-polarized phosphaalkene-enolate ligands and studies of their activity in olefin

polymerization and copolymerization are proposed to further expand our understanding

of this new class of highly tunable phosphorus-based ligands.

4. Methods

4.1 General Remarks

All transformations described herein were performed using glassware dried at 160 °C overnight and occurred in a nitrogen atmosphere MBraun glovebox, or under an atmosphere of argon. Solvents used were dried using a solvent purification system fitted with alumina columns, degassed with argon and stored over molecular sieves under an argon atmosphere. 1,3-Dimesityl-3,4,5,6-tetrahydro-pyrimidin-1-ium tetrafluoroborate, 1,3-bis(2,6-diisopropylphenyl)-2-phosphinylideneimidazolidine, and Na_3P_7 was prepared according to literature procedures.[62,11] 2-Bromoacetophenone was purchased from Sigma Aldrich and purified by recrystallization from methanol. Trimethylsilyl chloride was purchased from Sigma Aldrich and purified by distillation. Lithium hexamethyldisilazide, sodium hexamethyldisilazide, 2-bromo-4'-chloroacetophenone, and MMAO-12 were purchased from Sigma Aldrich and used as received. Cyclopentadienyl titanium(IV) trichloride was purchased from Strem Chemicals and used as received. C_6D_6 and $CDCl_3$ were purchased from Sigma-Aldrich and dried over sodium/benzophenone and CaH_2, respectively. The dried solvents were then degassed through freeze-pump-thaw cycles and then vacuum transferred to a Schlenk tube. NMR spectra were obtained on a Bruker NEO 300 (^1H at 300 MHz, ^{13}C at 75 MHz, ^{31}P at 121 MHz), AV 400 (^1H at 400 MHz, ^{13}C at 100 MHz, ^{31}P at 162 MHz) or DRX600 (^1H at 600 MHz) spectrometer. ^1H NMR spectra were referenced to residual protio solvents and ^{13}C NMR spectra were referenced to their ^{13}C signals ($CDCl_3$ at δ=7.26 ppm for ^1H, 77.16 ppm for ^{13}C or C_6D_6 at δ=7.16 ppm for ^1H and 128.06 ppm for ^{13}C). ^{31}P NMR spectra are referenced to an external standard of H_3PO_4 with values of –58.14 and –61.73 for $CDCl_3$ and C_6D_6 respectively. Coupling

constants are reported in Hz and the multiplicity of signals are reported as singlet (s), doublet (d), triplet (t), quartet (q), quintet (quint), septet (sept), multiplet (m), broad (br) or a combination of any of these. Spectra were recorded at room temperature unless stated otherwise. Exact molar masses were determined at either University of Toronto using a mass spectrometer equipped with a time of flight ion selector and DART ionization apparatus or York University using a mass spectrometer equipped with an Orbitrap mass selector coupled to an electrospray ionization chamber. Elemental composition was determined at York University using a Vario EL cube instrument. Infrared spectra were collected on an Agilent Technologies Cary 630 FTIR-ATR. Differential scanning calorimetry was performed using a DSC Q20 V24.11 instrument.

4.2 Preparations:

Synthesis of 1,3-dimesityl-2-phosphinylidene-4,5,6-trihydropyrimidine (1):
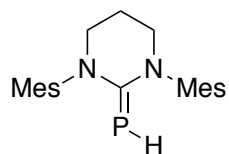
A 20 mL scintillation vial was charged with 1,3-dimesityl-4,5,6-trihydro-pyrimidinium tetrafluoroborate (313 mg, 0.768 mmol), Na_3P_7 (99.6 mg, 0.348 mmol) and 10 mL of THF. The reaction mixture was stirred at room temperature for 3 days followed by removal of solids by filtration and subsequent washing of the solids with THF (3×5 mL). The volatiles were removed from the filtrate *in vacuo.* The product was extracted with toluene and stirred for an additional three days for the full conversion of free carbene to the CH activated product. Then, the filtrate was dried under reduced pressure and the resulting solids were washed with pentane (3×5 mL) yielding **1** as a pale yellow powder (53.4 mg, 0.151 mmol, 19%). ^{1}H NMR (300 MHz, C_6D_6): δ= 6.81 (s, 2H, Ar-H), 6.78 (s, 2H, Ar-H), 2.90 (br s, 4H, NC**H$_2$**CH$_2$C**H$_2$**N), 2.39 (s, 6H, Ar-CH$_3$), 2.32 (s, 6H, Ar-CH$_3$), 2.29 (d, $^1J_{PH}$= 161 Hz, 1H, PH), 2.11 (s, 6H, Ar-CH$_3$), 1.55 (quint, $^3J_{HH}$ =

3.9 Hz, 2H, NCH$_2$CH$_2$CH$_2$N). ^{13}C NMR (101 MHz, C$_6$D$_6$) δ 189.54 (d, $^2J_{CP}$ = 75.3 Hz,

C=P), 143.45 (*ipso*-C$_{Mes}$), 141.84 (*ipso*-C$_{Mes}$), 137.72 (*p*-**C**(CH$_3$)), 137.21 (*p*-**C**(CH$_3$)),

136.36 (*o*-**C**(CH$_3$)), 136.17 (*o*-**C**(CH$_3$)), 130.46 (*m*-CH), 47.92 (NCH$_2$CH$_2$CH$_2$N), 23.29

(NCH$_2$**C**H$_2$CH$_2$N), 21.43 (*p*-C(**C**H$_3$)), 18.44 (*o*-C(**C**H$_3$)). ^{31}P NMR (121.5 MHz, C$_6$D$_6$): δ=

−99.7 (d, $^1J_{PH}$= 161 Hz). HRMS (DART-TOF+): mass [M+H] calc'd for C$_{22}$H$_{30}$N$_2$P

353.21451 *Da*, measured 353.21411 *Da.* FTIR-ATR (neat): ν$_{C=P}$: 1478 cm^{-1}, ν$_{P-H}$: 2290

cm^{-1}.

Synthesis of (1,3–bis(2,6–diisopropylphenyl)imidazolidin)(2–oxo–2–phenylethyl)phosphonium bromide (5):
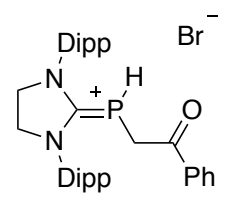
To a solution of 2–bromoacetophenone (199 mg, 1.25 mmol) in 4 mL of toluene at −40 °C was added a solution of 1,3-bis(2,6-diisopropylphenyl)-2-phosphinylideneimidazolidine (506 mg, 1.18 mmol) in 4 mL of toluene at −40 °C. This solution was stirred at −40 °C for 3 hours resulting in

the precipitation of **5**. The supernatant was decanted off and the solids were washed with

diethyl ether (3 × 5 mL). The solids were dried *in vacuo* yielding a light-green crystalline

product (586 mg, 0.942 mmol, 82%). ^{1}H NMR (400 MHz, CDCl$_3$): δ = 7.68 ppm (2H, d,

$^2J_{HH}$ = 8.0 Hz, *o*-CH$_{phenyl}$), 7.58 ppm (1H, t, $^2J_{HH}$ = 7.6 Hz *p*-CH$_{phenyl}$), 7.49 ppm (2H, t, $^2J_{HH}$

= 8.0 Hz, *p*-CH$_{Dipp}$), 7.42 ppm (2H, t, $^2J_{HH}$ = 7.6 Hz, *m*-CH$_{phenyl}$), 7.32 ppm (4H, d, $^2J_{HH}$ =

7.6 Hz, *m*-CH$_{Dipp}$), 4.82 ppm (4H, m, NCH$_2$CH$_2$N), 3.86 ppm (1H, dt, $^1J_{HP}$ = 241.2 Hz, $^2J_{HH}$

= 8.4 Hz, P**H**), 3.20 ppm (4H, sept, $^2J_{HH}$ = 6.8 Hz, C**H**(CH$_3$)$_2$), 3.03 ppm (2H, m,

PHC**H$_2$**C(O)Ph), 1.40 ppm (6H, d, $^2J_{HH}$ = 6.8 Hz, CH(C**H$_3$**)$_2$), 1.38 ppm (6H, d, $^2J_{HH}$ = 7.2

Hz, CH(C**H$_3$**)$_2$), 1.34 ppm (6H, d, $^2J_{HH}$ = 6.8 Hz, CH(C**H$_3$**)$_2$), 1.27 ppm (6H, d, $^2J_{HH}$ = 7.6

Hz, CH(C**H$_3$**)$_2$). ^{13}C NMR (100 MHz, CDCl$_3$): δ = 194.9 ppm (PHCH$_2$**C**(O)Ph), 177.4 ppm (d, $^1J_{CP}$ = 44.0 Hz, C=P) 146.9 ppm (o-C$_{Dipp}$), 146.4 (o-C$_{Dipp}$), 134.7 ppm (p-C$_{Ph}$), 131.8 ppm (m-C$_{Ph}$), 130.5 (ipso-C$_{Dipp}$), 129.1 ppm (p-C$_{Dipp}$), 128.5 ppm (o-C$_{Ph}$), 126.0 ppm (m-C$_{Dipp}$), 125.5 ppm (m-C$_{Dipp}$), 125.1 ppm (ipso-C$_{Ph}$), 55.9 ppm (N**C**H$_2$**C**H$_2$N), 29.2 ppm (**C**H(CH$_3$)$_2$), 28.8 ppm (d, $^1J_{CP}$ = 84 Hz, PH**C**H$_2$C(O)Ph), 26.4 (CH(**C**H$_3$)$_2$), 26.3 (CH(**C**H$_3$)$_2$), 25.5 ppm (CH(**C**H$_3$)$_2$), 23.9 ppm (CH(**C**H$_3$)$_2$), 23.8 ppm (CH(**C**H$_3$)$_2$), 23.8 ppm (CH(**C**H$_3$)$_2$), 23.6 ppm (CH(**C**H$_3$)$_2$), 23.6 ppm (CH(**C**H$_3$)$_2$). ^{31}P NMR (121 Hz, CDCl$_3$): δ = −95.8 ppm (dd, $^1J_{PH}$ = 241 Hz, $^2J_{PH}$ = 10.4 Hz). HRMS (ESI$^+$, Acetonitrile) Calculated for C$_{35}$H$_{46}$N$_2$OP$^+$ m/z = 541.3342 [M − Br]$^+$; Found: 541.3333 [M − Br]$^+$. FTIR-ATR (neat): ν$_{C=P}$: 1458 cm^{-1}, ν$_{C=O}$: 1670 cm^{-1}.

Synthesis of (1,3–bis(2,6–diisopropylphenyl)imidazolidin)(2–oxo–2–(4'–chlorophenyl)ethyl)phosphonium bromide (5Cl):
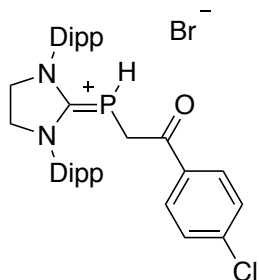

To a solution of 2-bromo-4'-chloroacetophenone (116 mg, 0.491 mmol) in 2 mL of toluene at −40 °C was added a solution of 1,3–bis(2,6-diisopropylphenyl)-2-phosphinylideneimidazolidin (201 mg, 0.468 mmol) in 2 mL of toluene at −40 °C. This solution was stirred at −40 °C for 5 hours resulting in the precipitation of **5Cl**. The solids were washed with diethyl ether (3 × 5 mL) and dried under reduced pressure yielding a light-yellow crystalline product (264 mg, 0.402 mmol, 86%). ^{1}H NMR (300 MHz, CDCl$_3$): δ = 7.73 ppm (2H, d, $^2J_{HH}$ = 9.0 Hz, o-CH$_{Ph}$), 7.49 ppm (2H, t, $^2J_{HH}$ = 6.0 Hz, p-CH$_{Dipp}$), 7.30 ppm (2H, d, $^2J_{HH}$ = 9.0 Hz, m-CH$_{Ph}$) 7.30 ppm (4H, d, $^2J_{HH}$ = 6.0 Hz, m-CH$_{Dipp}$), 4.68 ppm (4H, m, NC**H$_2$C**H$_2$N), 3.83 (1H, dt, $^1J_{PH}$ = 267.0 Hz, $^2J_{HH}$ = 9.0 Hz, PH), 3.21 (2H,

sept, $^2J_{HH}$ = 6.0 Hz, C**H**(CH$_3$)$_2$), 3.17 ppm (2H, dm, $^2J_{HP}$ = 117.0 Hz, PHC**H$_2$**C(O)Ph), 3.14 (2H, sept, $^2J_{HH}$ = 6.0 Hz, C**H**(CH$_3$)$_2$), 1.35 (12H, d, $^2J_{HH}$ = 6.0 Hz, CH(C**H$_3$**)$_2$), 1.27 (12H, d, $^2J_{HH}$ = 6.0 Hz, CH(C**H$_3$**)$_2$). ^{13}C NMR (75 MHz, CDCl$_3$): δ = 194.2 (C=O), 178.2 (d, $^1J_{CP}$ = 45.8 Hz, C=P), 147.0 (o-C$_{Dipp}$), 146.5 ppm (o-C$_{Dipp}$), 141.3 ppm (ipso-C$_{Ph}$), 133.3 (p-C$_{Ph}$), 131.9 ppm (p-CH$_{Dipp}$), 130.6 ppm (ipso-C$_{Dipp}$), 130.2 ppm (o-CH$_{Ph}$), 129.5 ppm (m-CH$_{Ph}$), 126.1 ppm (m-CH$_{Dipp}$), 125.6 ppm (m-CH$_{Dipp}$), 55.6 ppm (NCH$_2$CH$_2$N), 29.3 ppm (**C**H(CH$_3$)$_2$), 28.6 (d, $^2J_{CP}$ = 11.3 Hz, PH**C**H$_2$C(O)Ph), 26.5 ppm (CH(**C**H$_3$)$_2$), 26.4 ppm (CH(**C**H$_3$)$_2$), 23.8 ppm (CH(**C**H$_3$)$_2$), 23.7 ppm (CH(**C**H$_3$)$_2$). ^{31}P NMR (121 MHz, C$_6$D$_6$): δ = −94.2 ppm (dm, $^1J_{PH}$ = 267.0 Hz). HRMS (ESI$^+$, Acetonitrile) Calculated for C$_{35}$H$_{45}$N$_2$OPCl$^+$ m/z = 575.2952 [M − Br]$^+$; Found: 575.2966 [M − Br]$^+$. FTIR-ATR (neat): $\nu_{C=P}$: 1458.3 cm^{-1}, $\nu_{C=O}$: 1668 cm^{-1}.

2.3 Synthesis of Neutral Ligand precursor (8):
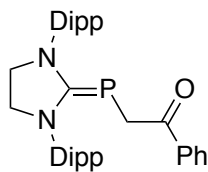
To a suspension of compound **5** (50 mg, 81 μmol) in 2 mL of tetrahydrofuran (THF) at −40 °C was added a solution of sodium hexamethyldisilazide (16 mg, 85 μmol) in 2 mL of THF at −40 °C. The reaction mixture was stirred for 30 minutes during which the suspension of **5** became a light-yellow solution. Volatiles were removed *in vacuo* and **8** was extracted with toluene (3 × 1 mL) and passed through Celite. The filtrate was dried under reduced pressure, washed with cold pentane (3 × 1 mL) and dried again *in vacuo* yielding **8** as a yellow powder (37 mg, 69 μmol, 85%). ^{1}H NMR (400 MHz, C$_6$D$_6$): δ = 7.94 ppm (2H, d, $^2J_{HH}$ = 6.0 Hz, o-CH$_{Ph}$), 7.06 ppm (6H, br d, Ar-H$_{Dipp}$), 6.97 ppm (3H, br s, 7.00 ppm, m,p-H$_{Ph}$), 3.57 ppm (2H, sept, $^2J_{HH}$ = 5.1 Hz, C**H**(CH$_3$)$_2$), 3.48 (4H, m, NC**H$_2$**C**H$_2$**N), 3.28 ppm (2H, $^2J_{HH}$ = 5.1 Hz, C**H**(CH$_3$)$_2$), 2.97 ppm (2H, d, $^2J_{HP}$ = 0.9 Hz, PC**H$_2$**C(O)Ph), 1.52 ppm (6H,

$^2J_{HH}$ =5.7 Hz, CH(C**H₃**)₂, 1.46 ppm (6H, $^2J_{HH}$ =5.1 Hz, CH(C**H₃**)₂), 1.22 ppm (6H, $^2J_{HH}$ =5.7 Hz, CH(C**H₃**)₂), 1.20 ppm (6H, $^2J_{HH}$ =5.7 Hz, CH(C**H₃**)₂). ^{13}C NMR (75 MHz, C₆D₆) δ 198.87 (d, $^2J_{CP}$ = 13.9 Hz, C=O), 188.08 (d, $^1J_{CP}$ = 90.9 Hz, C=P), 148.53 (*o*-C$_{Dipp}$), 148.49 (*o*-C$_{Dipp}$), 148.35 (*o*-CH$_{Ph}$), 138.23 (*ipso*-C$_{Dipp}$), 138.10 (*ipso*-C$_{Dipp}$), 135.50 (*ipso*-C$_{Ph}$), 132.30 (*m*-CH$_{Ph}$), 129.77 (m-CH$_{Dipp}$), 129.71 (m-CH$_{Dipp}$), 129.49 (m-CH$_{Dipp}$), 129.45 (m-CH$_{Dipp}$), 125.19 (*p*-CH$_{Dipp}$), 125.10 (*p*-CH$_{Dipp}$), 51.48 (d, $^3J_{CP}$ = 4.2 Hz, NCH₂CH₂N) 51.93 (NCH₂**C**H₂N), 31.52 (**C**H(CH₃)₂), 30.91 (**C**H(CH₃)₂), 29.37 (CH(**C**H₃)₂), 29.31 (CH(**C**H₃)₂), 26.07 (CH(**C**H₃)₂), 25.48 (CH(**C**H₃)₂), 25.05 (CH(**C**H₃)₂), 25.00 (CH(**C**H₃)₂), 23.84 (CH(**C**H₃)₂) *signal for p-CH$_{Ph}$ is buried under the solvent signal for C₆D₆.* ^{31}P NMR (162 MHz, C₆D₆): δ = −29.7 ppm. HRMS (ESI⁺, Acetonitrile) Calculated for C₃₅H₄₅N₂OPCl⁺ m/z = 575.2952 [M + H]⁺; Found: 575.2966 [M + H]⁺. FTIR-ATR (neat): ν$_{C=P}$: 1379 cm⁻¹, ν$_{C=O}$: 1655 cm⁻¹.

Synthesis of TMS-protected enolate (10):
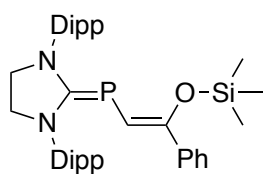
To a solution of **9** (124 mg, 0.218 mmol) in 2 mL of toluene was added trimethylsilyl chloride (118 mg, 1.09 mmol). The yellow reaction mixture was stirred for 30 minutes at room temperature, then passed through a Celite plug to remove the precipitate. Volatiles were removed *in vacuo* yielding **10** as a yellow oil (116 mg, 0.189 mmol, 83%). ^{1}H NMR: (600 MHz, C₆D₆): δ = 7.32 ppm (1H, t, $^2J_{HH}$ = 7.5 Hz, *p*-CH$_{Dipp}$), 7.25 ppm (1H, t, $^2J_{HH}$ = 7.2 Hz, *p*-CH$_{Dipp}$), 7.15 ppm (4H, d, $^2J_{HH}$ = 7.2 Hz *m*-CH$_{Dipp}$), 7.11 ppm (2H, t, $^2J_{HH}$ = 7.8 Hz, *m*-CH$_{Ph}$), 7.02 ppm (2H, d, $^2J_{HH}$ = 7.2 Hz, *o*-CH$_{Ph}$), 6.97 ppm (1H, t, $^2J_{HH}$ = 7.2, *p*-CH$_{Ph}$), 6.06 ppm (1H, d, 7.8 Hz, PC**H**C(O)Ph), 3.44 ppm (6H, br s, NC**H₂**C**H₂**N and C**H**(CH₃)₂), 3.28 ppm (2H, sept, $^2J_{HH}$ = 6.6 Hz, **C**H(CH₃)₂), 1.56 ppm (6H, d, $^2J_{HH}$ = 6 Hz, CH(C**H₃**)₂), 1.35 (6H, d, $^2J_{HH}$ =

6.6 Hz, CH(C**H₃**)₂), 1.23 Hz (12H, d, $^2J_{HH}$ = 5.4 Hz, CH(C**H₃**)₂), 0.17 ppm (9H, s,

OSi(C**H₃**)₃). ^{13}C NMR (75 MHz, C₆D₆): δ = 183.7 ppm (d, $^1J_{CP}$ = 78.0 Hz, C=P), 149.1 ppm

(*ipso*-C$_{Dipp}$), 149.0 ppm (*ipso*-C$_{Dipp}$), 146.8 ppm (d, $^2J_{CP}$ = 27 Hz, PCH**C**(OSiMe₃)Ph),

139.6 ppm (*ipso*-C$_{Ph}$), 129.0 ppm (*p*-CH$_{Dipp}$), 125.4 ppm (*o*-CH$_{Ph}$), 125.3 ppm (o-C$_{Dipp}$),

124.8 ppm (*m*-CH$_{Ph}$), 124.4 ppm (p-CH$_{Ph}$), 124.3 ppm (*m*-CH$_{Dipp}$), 109.8 ppm (d, $^1J_{CP}$ = 38.3

Hz), 53.8 ppm (NCH₂**C**H₂N), 51.0 ppm (N**C**H₂CH₂N), 28.7 ppm (**C**H(CH₃)₂), 24.8 ppm

(CH(**C**H₃)₂), 24.4 ppm (CH(**C**H₃)₂), 23.6 ppm (CH(**C**H₃)₂), 0.9 ppm (OSi(**C**H₃)₃). ^{31}P NMR

(121 MHz, C₆D₆): δ = –27.0 ppm (d, $^2J_{PH}$ = 7.3 Hz). HRMS (ESI⁺, Acetonitrile) Calculated

for C₃₈H₅₄ON₂PSi m/z = 613.3738 [M + H]⁺ ; Found: 613.3765 [M + H]⁺ . FTIR-ATR (neat):

ν$_{C=P}$: 1381 cm⁻¹.

Synthesis of TMS-protected enolate (10Cl):
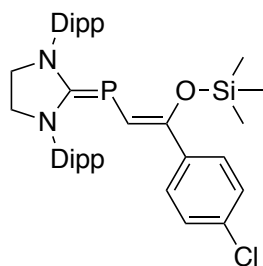
A solution of LiHMDS (87 mg, 0.52 mmol) in 2 mL of THF at –40 °C was added dropwise to a suspension of **5Cl** (162 mg, 0.247 mmol) in 4 mL of THF, resulting in a yellow solution. The reaction mixture was stirred at room temperature for 1 hour after which TMSCl (134 mg, 1.24 mmol) was added resulting in a precipitation of LiCl. After stirring for an

additional 30 minutes, volatiles were removed *in vacuo*. The product **10Cl** and side

product (TMS)₃N was extracted with toluene (3 × 1 mL) and passed through a Celite plug.

Subsequent removal of pentane and (TMS)₃N was performed under reduced pressure

yielding yellow solids (159 mg, 0.238 mmol, 96%). ^{1}H NMR (300 MHz, C₆D₆): δ = 7.21

ppm (2H, br s, *p*-CH$_{Dipp}$), 7.10 ppm (4H, br s, *m*-CH$_{Dipp}$), 7.06 ppm (2H, d, $^2J_{HH}$ = 8.7 Hz,

m-CH$_{Ph}$), 6.77 ppm (2H, d, $^2J_{HH}$ = 8.7 Hz, *o*-CH$_{Ph}$), 6.03 ppm (1H, d, $^2J_{HP}$ = 7.5 Hz,

PC**H**C(O)Ph), 3.414 ppm (4H, br s, NC**H₂CH₂**N) 3.414 ppm (2H, buried under previously

listed signal, C**H**(CH$_3$)$_2$), 3.25 ppm (2H, br m, C**H**(CH$_3$)$_2$), 1.54 ppm (6H, br d, $^2J_{HH}$ = 5.1 Hz, CH(C**H$_3$**)$_2$), 1.32 ppm (6H, br d, $^2J_{HH}$ = 5.1 Hz, CH(C**H$_3$**)$_2$), 1.22 ppm (12H, d, $^2J_{HH}$ = 6.9 Hz, CH(C**H$_3$**)$_2$), 0.125 ppm (9H, s, OSi(C**H$_3$**)$_3$). ^{13}C NMR (75 MHz, C$_6$D$_6$): δ = 184.2 (d, $^2J_{CP}$ = 55.5 Hz, C=P), 148.2 ppm (o-C$_{Dipp}$), 147.9 ppm (d, $^3J_{CP}$ = 22.5 Hz), 147.8 ppm (o-C$_{Dipp}$), 138.4 ppm (ipso-C$_{Ph}$), 137.8 ppm (ipso-C$_{Dipp}$), 135.3 ppm (ipso-C$_{Dipp}$), 131.2 ppm (o-CH$_{Ph}$), 129.4 ppm (o-CH$_{Dipp}$), 125.8 ppm (m-CH$_{Ph}$), 125.2 ppm (m-CH$_{Dipp}$), 124.8 ppm (m-CH$_{Dipp}$), 111.3 ppm (d, $^1J_{CP}$ = 39.8 Hz, P**C**HC(OSiMe$_3$)Ph), 54.2 ppm (N**C**H$_2$CH$_2$N), 51.4 ppm (NCH$_2$**C**H$_2$N), 29.1 ppm (**C**H(CH$_3$)$_2$), 25.1 ppm (CH(**C**H$_3$)$_2$), 24.7 ppm (CH(**C**H$_3$)$_2$), 24.0 ppm (CH(**C**H$_3$)$_2$), 1.2 ppm (OSi(**C**H$_3$)$_3$), m-C$_{Ph}$ shows HSQC correlation to a signal buried by the solvent peak in the ^{13}C NMR spectrum. ^{31}P NMR: (121 MHz, C$_6$D$_6$): δ = –27.2 ppm (d, $^2J_{PH}$ = 7.5 Hz). HRMS (ESI$^+$, Acetonitrile) Calculated for C$_{38}$H$_{53}$N$_2$OPClSi m/z = 647.3348 [M + H]$^+$; Found: 647.3359 [M + H]$^+$. FTIR-ATR (neat): ν$_{C=P}$: 1381 cm^{-1}.

Synthesis of Titanium Complex (14):
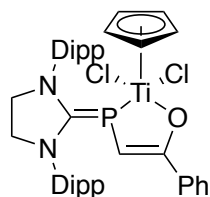
The ligand precursor **10** (100 mg, 0.161 mmol) and cyclopentadienyl titanium(IV) trichloride (38 mg, 0.17 mmol) were dissolved in toluene yielding a dark green solution. After stirring for 5 days, the solution had changed to a deep blue colour and volatiles were removed. The blue solids were washed with pentane and dried *in vacuo* yielding **14** (94% yield). ^{1}H NMR (300 MHz, Benzene-d$_6$) δ 7.28 (t, 2H, m-CH$_{Ph}$), 7.22 (d, J = 8.2 Hz, 2H, o-CH$_{Ph}$), 7.14 (d, J = 3.3 Hz, 4H, m-CH$_{Dipp}$), 7.12 (t, J = 4.4 Hz, 2H, p-CH$_{Dipp}$) 6.96 (t, J = 6.2 Hz, 1H, p-CH$_{Ph}$), 6.40 (d, J = 7.7 Hz, 1H, PC**H**C(O)Ph), 6.29 (s, Cp), 3.42 (br d, J = 1.2 Hz, 4H, NC**H$_2$**C**H$_2$**N), 3.23 (sept, J = 6.6 Hz, 4H, C**H**(CH$_3$)$_2$), 1.46 (d, J = 6.4 Hz, 12H, CH(C**H$_3$**)$_2$), 1.21 (d, J = 6.9 Hz, 12H,

CH(C**H**$_3$)$_2$). ^{13}C NMR (75 MHz, C$_6$D$_6$) δ 184.8 (d, $^1J_{CP}$ = 80 Hz C=P), 167.8 (d, $^2J_{CP}$ = 24.1 Hz, C-O) 148.28 (*o*-C$_{Dipp}$), 137.46 (*ipso*-C$_{Dipp}$), 137.41 (*ipso*-C$_{Dipp}$), 130.21 (*m*-CH$_{Ph}$), 128.90 (*p*-CH$_{Dipp}$), 126.81 (*p*-CH$_{Ph}$), 126.03 (*ipso*-C$_{Ph}$), 125.50 (*m*-CH$_{Dipp}$), 124.15 (*o*-CH$_{Ph}$), 121.10 (d, $^2J_{CP}$ = 5.0 Hz, Cp) 117.79 (d, $^1J_{CP}$ = 44.1 Hz, P**C**HC(O)Ph), 53.08 (NCH$_2$**C**H$_2$N), 29.55 (**C**H(CH$_3$)$_2$), 25.32 (CH(**C**H$_3$)$_2$), 24.70 (CH(**C**H$_3$)$_2$), 24.67 (CH(**C**H$_3$)$_2$). ^{31}P NMR (121 MHz, C$_6$D$_6$) δ −23.56 (d, $^2J_{PH}$ = 7.7 Hz). Anal. Calc'd for C$_{40}$H$_{49}$N$_2$OCl$_2$PTi (%): C, 66.40; H, 6.83; N, 3.87. Found (%): C, 66.17; H, 7.021; N, 3.63. FTIR-ATR (neat): ν$_{C=P}$:1457 cm^{-1}.

4.3 General Procedure for Ethylene Polymerization

Polymerization experiments were performed in a 200-mL polymerization flask equipped with a stirbar at room temperature and under 1 atmosphere of ethylene gas. First, 20 mL of toluene were degassed through freeze-pump-thaw cycles then saturated with ethylene gas for a minimum of 15 minutes with vigorous stirring during which 5 mL of a 7 wt% aluminum solution of MMAO-12 in toluene (11.5 mmol) was added. Afterwards, 4.5 mL of a 11 µM solution of precatalyst (0.0509 mmol) was added. Once complete, 20 mL of a solution containing equal parts methanol and hydrochloric acid was added, quenching the reaction. The polymer prepared was collected by gravity filtration and washed multiple times with water and methanol. The resulting polymer was oven dried under vacuum at 100 °C for a minimum of 3 hours. Characterization was performed using NMR spectroscopy and differential scanning calorimetry. The NMR spectra were recorded at 145 °C in 1,2-dichlorobenzene-d^4 in a J-Young NMR tube. For the DSC experiment the sample was weighed into an aluminum crucible, sealed, and heated over

a single ramp from 20 °C to 160 °C with a temperature increase rate of 10 °C/min with a purge gas flow rate of 50 mL/min.

4.4 Computational Details

Geometry optimizations and NBO analyses were carried out using Gaussian 16 and molecular visualization was performed on Avogadro version 1.2.0.[63,64,65] Values for Wiberg bond indices and stabilization energies were obtained directly from the output file. Computations were performed using the B3LYP functional and 6-31G(d,p) basis set.[66,67] Computations were performed on the Shared Hierarchical Academic Research Computing Network (SHARCNET: www.sharcnet.ca) and made possible by Compute Canada (www.computecanada.ca).

References

(1)   Crabtree, R. H. *The Organometallic Chemistry of the Transition Metals*, Fourth.; John Wiley & Sons, Inc.: Hoboken, New Jersey, 2005.

(2)   Perras, J. H.; Mezibroski, S. M. J.; Wiebe, M. A.; Ritch, J. S. Diverse Silver(I) Coordination Chemistry with Cyclic Selenourea Ligands. *Dalton Trans.* **2018**, *47* (5), 1471–1478. https://doi.org/10.1039/C7DT04243D.

(3)   Charette, B. J.; Ritch, J. S. A Selenium-Containing Diarylamido Pincer Ligand: Synthesis and Coordination Chemistry with Group 10 Metals. *Inorg. Chem.* **2016**, *55* (12), 6344–6350. https://doi.org/10.1021/acs.inorgchem.6b01203.

(4)   Back, O.; Henry-Ellinger, M.; Martin, C. D.; Martin, D.; Bertrand, G. 31P NMR Chemical Shifts of Carbene–Phosphinidene Adducts as an Indicator of the π-Accepting Properties of Carbenes. *Angew. Chem. Int. Ed.* **2013**, *52* (10), 2939–2943. https://doi.org/10.1002/anie.201209109.

(5)   Arduengo, A. J.; Harlow, R. L.; Kline, M. A Stable Crystalline Carbene. *J. Am. Chem. Soc.* **1991**, *113* (1), 361–363. https://doi.org/10.1021/ja00001a054.

(6)   Vummaleti, S. V. C.; Nelson, D. J.; Poater, A.; Gómez-Suárez, A.; Cordes, D. B.; Slawin, A. M. Z.; Nolan, S. P.; Cavallo, L. What Can NMR Spectroscopy of Selenoureas and Phosphinidenes Teach Us about the π-Accepting Abilities of N-Heterocyclic Carbenes? *Chem. Sci.* **2015**, *6* (3), 1895–1904. https://doi.org/10.1039/C4SC03264K.

(7)   Krachko, T.; Slootweg, J. C. N-Heterocyclic Carbene–Phosphinidene Adducts: Synthesis, Properties, and Applications. *Eur. J. Inorg. Chem.* **2018**, *2018* (24), 2734–2754. https://doi.org/10.1002/ejic.201800459.

(8) Tondreau, A. M.; Benkő, Z.; Harmer, J. R.; Grützmacher, H. Sodium
Phosphaethynolate, Na(OCP), as a "P" Transfer Reagent for the Synthesis of N-
Heterocyclic Carbene Supported P3 and PAsP Radicals. *Chem. Sci.* **2014**, *5* (4),
1545–1554. https://doi.org/10.1039/C3SC53140F.

(9) Arduengo, A. J.; Calabrese, J. C.; Cowley, A. H.; Dias, H. V. R.; Goerlich, J. R.;
Marshall, W. J.; Riegel, B. Carbene−Pnictinidene Adducts. *Inorg. Chem.* **1997**, *36*
(10), 2151–2158. https://doi.org/10.1021/ic970174q.

(10) Rodrigues, R. R.; Dorsey, C. L.; Arceneaux, C. A.; Hudnall, T. W. Phosphaalkene
vs. Phosphinidene: The Nature of the P–C Bond in Carbonyl-Decorated Carbene
→ PPh Adducts. *Chem. Commun.* **2013**, *50* (2), 162–164.
https://doi.org/10.1039/C3CC45134H.

(11) Cicač-Hudi, M.; Bender, J.; Schlindwein, S. H.; Bispinghoff, M.; Nieger, M.;
Grützmacher, H.; Gudat, D. Direct Access to Inversely Polarized Phosphaalkenes
from Elemental Phosphorus or Polyphosphides. *Eur. J. Inorg. Chem.* **2016**, *2016*
(5), 649–658. https://doi.org/10.1002/ejic.201501017.

(12) Larocque, T. G.; Lavoie, G. G. Reactivity Study of Low-Coordinate Phosphaalkene
IMesPPh with Grubbs First-Generation Ruthenium Benzylidene Complexes. *New
J. Chem.* **2014**, *38* (2), 499–502. https://doi.org/10.1039/C3NJ01416A.

(13) Doddi, A.; Bockfeld, D.; Nasr, A.; Bannenberg, T.; Jones, P. G.; Tamm, M. N-
Heterocyclic Carbene–Phosphinidene Complexes of the Coinage Metals. *Chem. –
Eur. J.* **2015**, *21* (45), 16178–16189. https://doi.org/10.1002/chem.201502208.

(14) Bockfeld, D.; Doddi, A.; Jones, P. G.; Tamm, M. Transition-Metal Carbonyl
Complexes and Electron-Donating Properties of N-Heterocyclic-Carbene–

Phosphinidene Adducts. *Eur. J. Inorg. Chem.* **2016**, *2016* (23), 3704–3713. https://doi.org/10.1002/ejic.201600483.

(15) Su, W.-F. *Principles of Polymer Design and Synthesis*; Lecture notes in chemistry; Springer: Heidelberg ; New York, 2013.

(16) Chum, P. S.; Swogger, K. W. Olefin Polymer Technologies—History and Recent Progress at The Dow Chemical Company. *Prog. Polym. Sci.* **2008**, *33* (8), 797–819. https://doi.org/10.1016/j.progpolymsci.2008.05.003.

(17) Carraher, C., E. *Introduction to Polymer Chemistry*, 2nd Ed.; Taylor and Francis Group, LLC: Boca Raton, Florida, 2010.

(18) Mardare, D.; Matyjaszewski, K. "Living" Radical Polymerization of Vinyl Acetate. *Macromolecules* **1994**, *27* (3), 645–649. https://doi.org/10.1021/ma00081a003.

(19) Bisht, H. S.; Chatterjee, A. K. Living Free-Radical Polymerization—a Review. *J. Macromol. Sci. Part C* **2001**, *41* (3), 139–173. https://doi.org/10.1081/MC-100107774.

(20) Kumar, A.; Gupta, R., K. *Fundamentals of Polymer Engineering*, 2nd Ed.; Marcel Dekker, Inc.: New York, New York, 2003.

(21) Su, W.-F. Ionic Chain Polymerization. In *Principles of Polymer Design and Synthesis*; Su, W.-F., Ed.; Lecture Notes in Chemistry; Springer Berlin Heidelberg: Berlin, Heidelberg, 2013; pp 185–218. https://doi.org/10.1007/978-3-642-38730-2_8.

(22) Aoshima, S.; Kanaoka, S. A Renaissance in Living Cationic Polymerization. *Chem. Rev.* **2009**, *109* (11), 5245–5287. https://doi.org/10.1021/cr900225g.

(23) Möhring, P. C.; Coville, N. J. Homogeneous Group 4 Metallocene Ziegler-Natta

    Catalysts: The Influence of Cyclopentadienyl-Ring Substituents. *J. Organomet.*

    Chem. **1994**, *479* (1), 1–29. https://doi.org/10.1016/0022-328X(94)84087-3.

(24) Peacock, A.; Calhoun, A. *Polymer Chemistry Properties and Applications*, 1st ed.;

    Hanser Gardner Publications, Inc.: Cincinnati, Ohio, 2006.

(25) Makio, H.; Terao, H.; Iwashita, A.; Fujita, T. FI Catalysts for Olefin Polymerization—

    A Comprehensive Treatment. *Chem. Rev.* **2011**, *111* (3), 2363–2449.

    https://doi.org/10.1021/cr100294r.

(26) Odian, G. *Principles of Polymerization*, Fourth.; John Wiley & Sons, Inc.: Hoboken,

    New Jersey, 2004.

(27) Cossee, P. Ziegler-Natta Catalysis I. Mechanism of Polymerization of α-Olefins

    with Ziegler-Natta Catalysts. *J. Catal.* **1964**, *3* (1), 80–88.

    https://doi.org/10.1016/0021-9517(64)90095-8.

(28) Galli, P.; Vecellio, G. Technology: Driving Force behind Innovation and Growth of

    Polyolefins. *Prog. Polym. Sci.* **2001**, *26* (8), 1287–1336.

    https://doi.org/10.1016/S0079-6700(01)00029-6.

(29) Furuyama, R.; Fujita, T.; Funaki, S. F.; Nobori, T.; Nagata, T.; Fujiwara, K. New

    High-Performance Catalysts Developed at Mitsui Chemicals for Polyolefins and

    Organic Synthesis. *Catal. Surv. Asia* **2004**, *8* (1), 61–71.

    https://doi.org/10.1023/B:CATS.0000015115.09940.4e.

(30) Larocque, T. G.; Dastgir, S.; Lavoie, G. G. Coordination and Reactivity Study of

    Titanium and Zirconium Complexes of the First Imidazol-2-Imine Ethenolate

Ligand. *Organometallics* **2013**, *32* (15), 4314–4320.

https://doi.org/10.1021/om4004708.

(31) Reddy, S. S.; Sivaram, S. Homogeneous Metallocene-Methylaluminoxane Catalyst

Systems for Ethylene Polymerization. *Prog. Polym. Sci.* **1995**, *20* (2), 309–367.

https://doi.org/10.1016/0079-6700(94)00035-Z.

(32) Kaminsky, W.; Külper, K.; Brintzinger, H. H.; Wild, F. R. W. P. Polymerization of

Propene and Butene with a Chiral Zirconocene and Methylalumoxane as

Cocatalyst. *Angew. Chem. Int. Ed. Engl.* **1985**, *24* (6), 507–508.

https://doi.org/10.1002/anie.198505071.

(33) Brintzinger, H. H.; Fischer, D.; Mülhaupt, R.; Rieger, B.; Waymouth, R. M.

Stereospecific Olefin Polymerization with Chiral Metallocene Catalysts. *Angew.*

Chem. Int. Ed. Engl. **1995**, *34* (11), 1143–1170.

https://doi.org/10.1002/anie.199511431.

(34) Spaleck, W.; Kueber, F.; Winter, A.; Rohrmann, J.; Bachmann, B.; Antberg, M.;

Dolle, V.; Paulus, E. F. The Influence of Aromatic Substituents on the

Polymerization Behavior of Bridged Zirconocene Catalysts. *Organometallics* **1994**,

13 (3), 954–963. https://doi.org/10.1021/om00015a032.

(35) Ewen, J. A.; Jones, R. L.; Razavi, A.; Ferrara, J. D. Syndiospecific Propylene

Polymerizations with Group IVB Metallocenes. *J. Am. Chem. Soc.* **1988**, *110* (18),

6255–6256. https://doi.org/10.1021/ja00226a056.

(36) Vyboishchikov, S. F.; Musaev, D. G.; Froese, R. D. J.; Morokuma, K. Density

Functional Study of Ethylene Polymerization Catalyzed by a Zirconium Non-

Cyclopentadienyl Complex, L2ZrCH3+. Effects of Ligands and Bulky Substituents. *Organometallics* **2001**, *20* (2), 309–323. https://doi.org/10.1021/om000705+.

(37) Makio, H.; Kashiwa, N.; Fujita, T. FI Catalysts: A New Family of High Performance Catalysts for Olefin Polymerization. *Adv. Synth. Catal.* **2002**, *344* (5), 477–493. https://doi.org/10.1002/1615-4169(200207)344:5<477::AID-ADSC477>3.0.CO;2-6.

(38) Terao, H.; Ishii, S.; Mitani, M.; Tanaka, H.; Fujita, T. Ethylene/Polar Monomer Copolymerization Behavior of Bis(Phenoxy–Imine)Ti Complexes: Formation of Polar Monomer Copolymers. *J. Am. Chem. Soc.* **2008**, *130* (52), 17636–17637. https://doi.org/10.1021/ja8060479.

(39) Kuhn, P.; Sémeril, D.; Matt, D.; Chetcuti, M. J.; Lutz, P. Structure–Reactivity Relationships in SHOP-Type Complexes: Tunable Catalysts for the Oligomerisation and Polymerisation of Ethylene. *Dalton Trans.* **2007**, *0* (5), 515–528. https://doi.org/10.1039/B615259G.

(40) Wang, C.; Friedrich, S.; Younkin, T. R.; Li, R. T.; Grubbs, R. H.; Bansleben, D. A.; Day, M. W. Neutral Nickel(II)-Based Catalysts for Ethylene Polymerization. *Organometallics* **1998**, *17* (15), 3149–3151. https://doi.org/10.1021/om980176y.

(41) Carrow, B. P.; Nozaki, K. Transition-Metal-Catalyzed Functional Polyolefin Synthesis: Effecting Control through Chelating Ancillary Ligand Design and Mechanistic Insights. *Macromolecules* **2014**, *47* (8), 2541–2555. https://doi.org/10.1021/ma500034g.

(42) Younkin, T. R.; Connor, E. F.; Henderson, J. I.; Friedrich, S. K.; Grubbs, R. H.; Bansleben, D. A. Neutral, Single-Component Nickel (II) Polyolefin Catalysts That

Tolerate Heteroatoms. *Science* **2000**, *287* (5452), 460–462.

https://doi.org/10.1126/science.287.5452.460.

(43) Drent, E.; Van Broekhoven, J. A. M.; Doyle, M. J. Efficient Palladium Catalysts for

the Copolymerization of Carbon Monoxide with Olefins to Produce Perfectly

Alternating Polyketones. *J. Organomet. Chem.* **1991**, *417* (1), 235–251.

https://doi.org/10.1016/0022-328X(91)80176-K.

(44) Drent, E.; Dijk, R. van; Ginkel, R. van; Oort, B. van; I. Pugh, R. Palladium

Catalysed Copolymerisation of Ethene with Alkylacrylates: Polar Comonomer Built

into the Linear Polymer Chain. *Chem. Commun.* **2002**, *0* (7), 744–745.

https://doi.org/10.1039/B111252J.

(45) Drent, E.; Budzelaar, P. H. M. Palladium-Catalyzed Alternating Copolymerization of

Alkenes and Carbon Monoxide. *Chem. Rev.* **1996**, *96* (2), 663–682.

https://doi.org/10.1021/cr940282j.

(46) Nakamura, A.; Anselment, T. M. J.; Claverie, J.; Goodall, B.; Jordan, R. F.;

Mecking, S.; Rieger, B.; Sen, A.; van Leeuwen, P. W. N. M.; Nozaki, K. Ortho-

Phosphinobenzenesulfonate: A Superb Ligand for Palladium-Catalyzed

Coordination–Insertion Copolymerization of Polar Vinyl Monomers. *Acc. Chem.

Res.* **2013**, *46* (7), 1438–1449. https://doi.org/10.1021/ar300256h.

(47) Nagai, Y.; Kochi, T.; Nozaki, K. Synthesis of N-Heterocyclic Carbene-Sulfonate

Palladium Complexes. *Organometallics* **2009**, *28* (20), 6131–6134.

https://doi.org/10.1021/om9004252.

(48) Zhou, X.; Jordan, R. F. Synthesis, Cis/Trans Isomerization, and Reactivity of

Palladium Alkyl Complexes That Contain a Chelating N-Heterocyclic-Carbene

Sulfonate Ligand. *Organometallics* **2011**, *30* (17), 4632–4642.

https://doi.org/10.1021/om200482a.

(49) Holdroyd, R. S.; Page, M. J.; Warren, M. R.; Whittlesey, M. K. Intramolecular C–H

Insertion in Ring-Expanded N-Heterocyclic Carbenes. *Tetrahedron Lett.* **2010**, *51*

(3), 557–559. https://doi.org/10.1016/j.tetlet.2009.11.090.

(50) Ryglowski, A.; Kafarski, P. Preparation of 1-Aminoalkylphosphonic Acids and 2-

Aminoalkylphosphonic Acids by Reductive Amination of Oxoalkylphosphonates.

Tetrahedron **1996**, *52* (32), 10685–10692. https://doi.org/10.1016/0040-

4020(96)00590-X.

(51) Bispinghoff, M.; Tondreau, A. M.; Grützmacher, H.; Faradji, C. A.; Pringle, P. G.

Carbene Insertion into a P–H Bond: Parent Phosphinidene–Carbene Adducts from

PH3 and Bis(Phosphinidene)Mercury Complexes. *Dalton Trans.* **2016**, *45* (14),

5999–6003. https://doi.org/10.1039/C5DT01741F.

(52) Wang, Y.; Hickox, H. P.; Xie, Y.; Wei, P.; Cui, D.; Walter, M. R.; Iii, H. F. S.;

Robinson, G. H. Protonation of Carbene-Stabilized Diphosphorus: Complexation of

HP2+. *Chem. Commun.* **2016**, *52* (33), 5746–5748.

https://doi.org/10.1039/C6CC01759B.

(53) Makio, H.; Terao, H.; Iwashita, A.; Fujita, T. FI Catalysts for Olefin Polymerization—

A Comprehensive Treatment. *Chem. Rev.* **2011**, *111* (3), 2363–2449.

https://doi.org/10.1021/cr100294r.

(54) Fantasia, S.; Petersen, J. L.; Jacobsen, H.; Cavallo, L.; Nolan, S. P. Electronic

Properties of N-Heterocyclic Carbene (NHC) Ligands: Synthetic, Structural, and

Spectroscopic Studies of (NHC)Platinum(II) Complexes. *Organometallics* **2007**, *26* (24), 5880–5889. https://doi.org/10.1021/om700857j.

(55) Pyykkö, P.; Atsumi, M. Molecular Double-Bond Covalent Radii for Elements Li–E112. *Chem. – Eur. J.* **2009**, *15* (46), 12770–12779. https://doi.org/10.1002/chem.200901472.

(56) Jensen, V. R.; Ystenes, M.; Waernmark, K.; Aakermark, B.; Svennson, M.; Siegbahn, P. E. M.; Blomberg, M. R. A. Strength of the Metal-Olefin Bond in Titanium Complexes Related to Ziegler-Natta Catalysis. A Theoretical Model Study of a Square-Pyramidal Active Center Postulated to Be Found in Titanium Halide-Based Catalysts. *Organometallics* **1994**, *13* (1), 282–288. https://doi.org/10.1021/om00013a041.

(57) Clavier, H.; Nolan, S. P. Percent Buried Volume for Phosphine and N-Heterocyclic Carbene Ligands: Steric Properties in Organometallic Chemistry. *Chem. Commun.* **2010**, *46* (6), 841–861. https://doi.org/10.1039/B922984A.

(58) Fischer, D.; Mülhaupt, R. Reversible and Irreversible Deactivation of Propene Polymerization Using Homogeneous Cp2ZrCl2/Methylaluminoxane Ziegler—Natta Catalysts. *J. Organomet. Chem.* **1991**, *417* (1), C7–C11. https://doi.org/10.1016/0022-328X(91)80182-J.

(59) Sarzotti, D. M.; Marshman, D. J.; Ripmeester, W. E.; Soares, J. B. P. A Kinetic Study of Metallocene-catalyzed Ethylene Polymerization Using Different Aluminoxane Cocatalysts. *J. Polym. Sci. Part Polym. Chem.* **2007**, *45* (9), 1677–1690. https://doi.org/10.1002/pola.21935.

(60) Glendening, E. D.; Weinhold, F. Natural Resonance Theory: II. Natural Bond Order and Valency. *J. Comput. Chem.* **1998**, *19* (6), 610–627. https://doi.org/10.1002/(SICI)1096-987X(19980430)19:6<610::AID-JCC4>3.0.CO;2-U.

(61) Kaminsky, W. Highly Active Metallocene Catalysts for Olefin Polymerization. *J. Chem. Soc. Dalton Trans.* **1998**, *0* (9), 1413–1418. https://doi.org/10.1039/A800056E.

(62) Iglesias, M.; Beetstra, D. J.; Knight, J. C.; Ooi, L.-L.; Stasch, A.; Coles, S.; Male, L.; Hursthouse, M. B.; Cavell, K. J.; Dervisi, A.; et al. Novel Expanded Ring N-Heterocyclic Carbenes: Free Carbenes, Silver Complexes, And Structures. *Organometallics* **2008**, *27* (13), 3279–3289. https://doi.org/10.1021/om800179t.

(63) Glendening, E. D.; Landis, C. R.; Weinhold, F. NBO 6.0: Natural Bond Orbital Analysis Program. *J. Comput. Chem.* **2013**, *34* (16), 1429–1437. https://doi.org/10.1002/jcc.23266.

(64) Hanwell, M. D.; Curtis, D. E.; Lonie, D. C.; Vandermeersch, T.; Zurek, E.; Hutchison, G. R. Avogadro: An Advanced Semantic Chemical Editor, Visualization, and Analysis Platform. *J. Cheminformatics* **2012**, *4* (1), 17. https://doi.org/10.1186/1758-2946-4-17.

(65) Gaussian 16, Revision C.01, Frisch, M. J.; Trucks, G. W.; Schlegel, H. B.; Scuseria, G. E.; Robb, M. A.; Cheeseman, J. R.; Scalmani, G.; Barone, V.; Petersson, G. A.; Nakatsuji, H.; Li, X.; Caricato, M.; Marenich, A. V.; Bloino, J.; Janesko, B. G.; Gomperts, R.; Mennucci, B.; Hratchian, H. P.; Ortiz, J. V.; Izmaylov, A. F.; Sonnenberg, J. L.; Williams-Young, D.; Ding, F.; Lipparini, F.;

Egidi, F.; Goings, J.; Peng, B.; Petrone, A.; Henderson, T.; Ranasinghe, D.;

Zakrzewski, V. G.; Gao, J.; Rega, N.; Zheng, G.; Liang, W.; Hada, M.; Ehara, M.;

Toyota, K.; Fukuda, R.; Hasegawa, J.; Ishida, M.; Nakajima, T.; Honda, Y.; Kitao,

O.; Nakai, H.; Vreven, T.; Throssell, K.; Montgomery, J. A., Jr.; Peralta, J. E.;

Ogliaro, F.; Bearpark, M. J.; Heyd, J. J.; Brothers, E. N.; Kudin, K. N.; Staroverov,

V. N.; Keith, T. A.; Kobayashi, R.; Normand, J.; Raghavachari, K.; Rendell, A. P.;

Burant, J. C.; Iyengar, S. S.; Tomasi, J.; Cossi, M.; Millam, J. M.; Klene, M.;

Adamo, C.; Cammi, R.; Ochterski, J. W.; Martin, R. L.; Morokuma, K.; Farkas, O.;

Foresman, J. B.; Fox, D. J. Gaussian, Inc., Wallingford CT, 2016.

(66) Lee, C.; Yang, W.; Parr, R. G. Development of the Colle-Salvetti Correlation-

Energy Formula into a Functional of the Electron Density. *Phys. Rev. B* **1988**, *37*

(2), 785–789. https://doi.org/10.1103/PhysRevB.37.785.

(67) Becke, A. D. A New Mixing of Hartree–Fock and Local Density-functional Theories.

J. Chem. Phys. **1993**, *98* (2), 1372–1377. https://doi.org/10.1063/1.464304.

Appendix

Figure A1: ^{1}H NMR spectrum of C–H activated (**1"**) product taken in C_6D_6 using the DRX600 spectrometer (600 MHz).
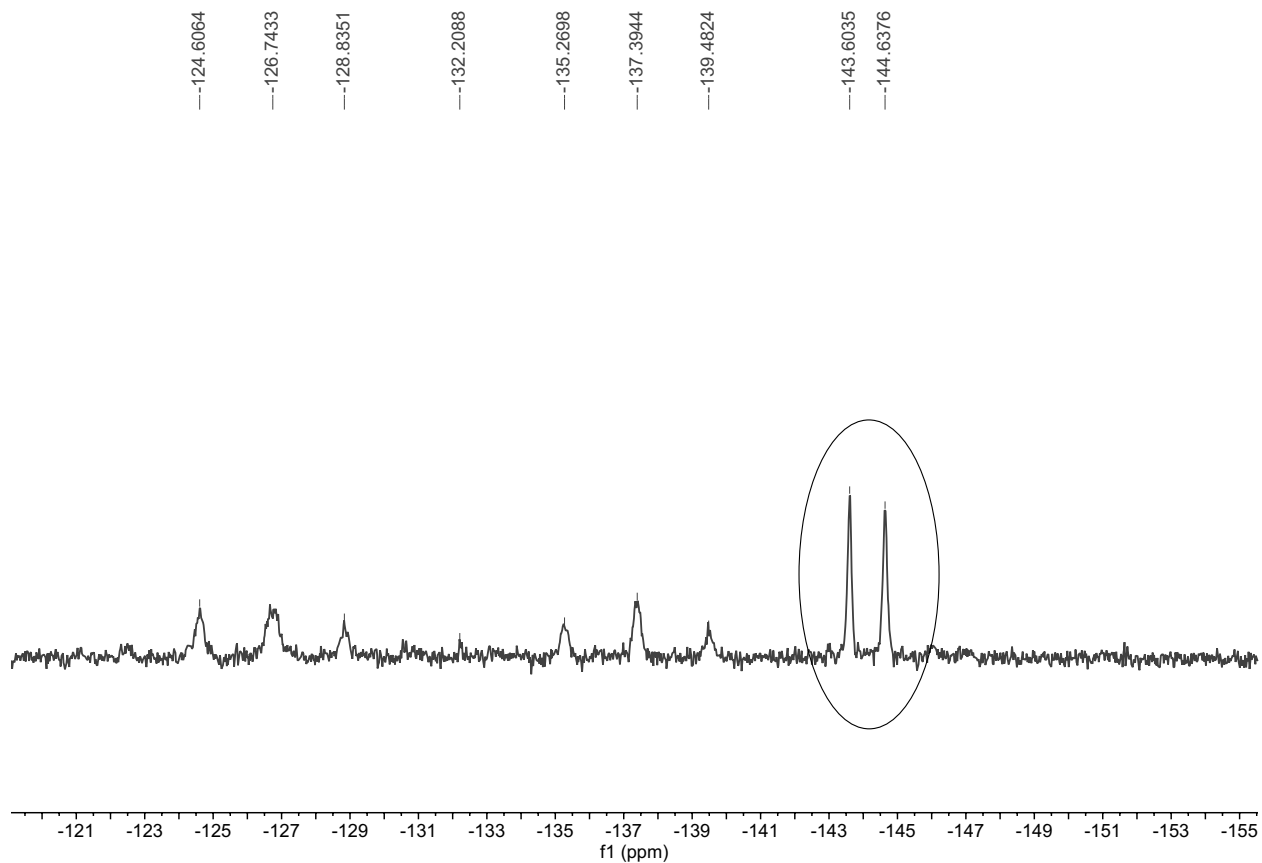
Figure A2: Signal assigned to **2** in ^{31}P NMR spectrum taken in DMSO using an AV400 spectrometer (162 MHz). Multiple other phosphorus containing species observed as this is a crude reaction mixture.
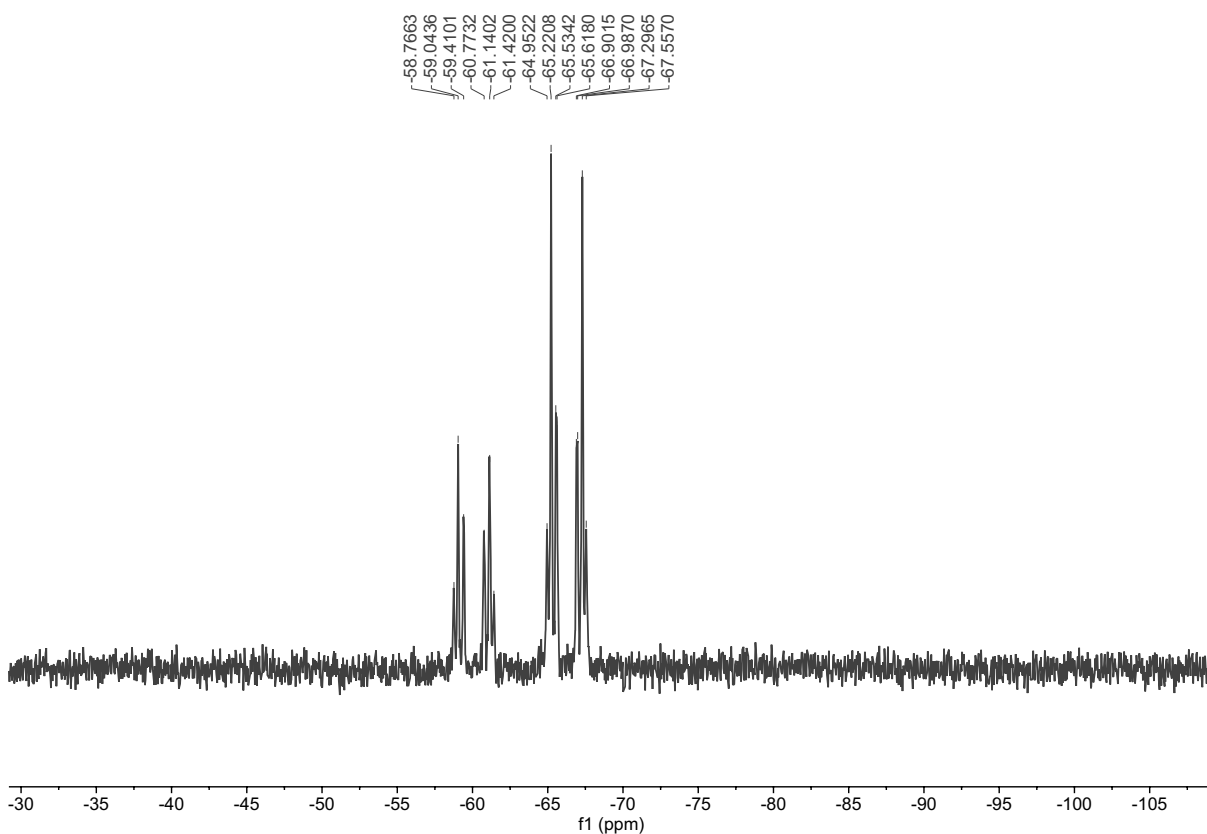
**Figure A3:** Signals assigned to the mixed salt product, **3** taken in CDCl$_3$ using an AV300 spectrometer (121 MHz).
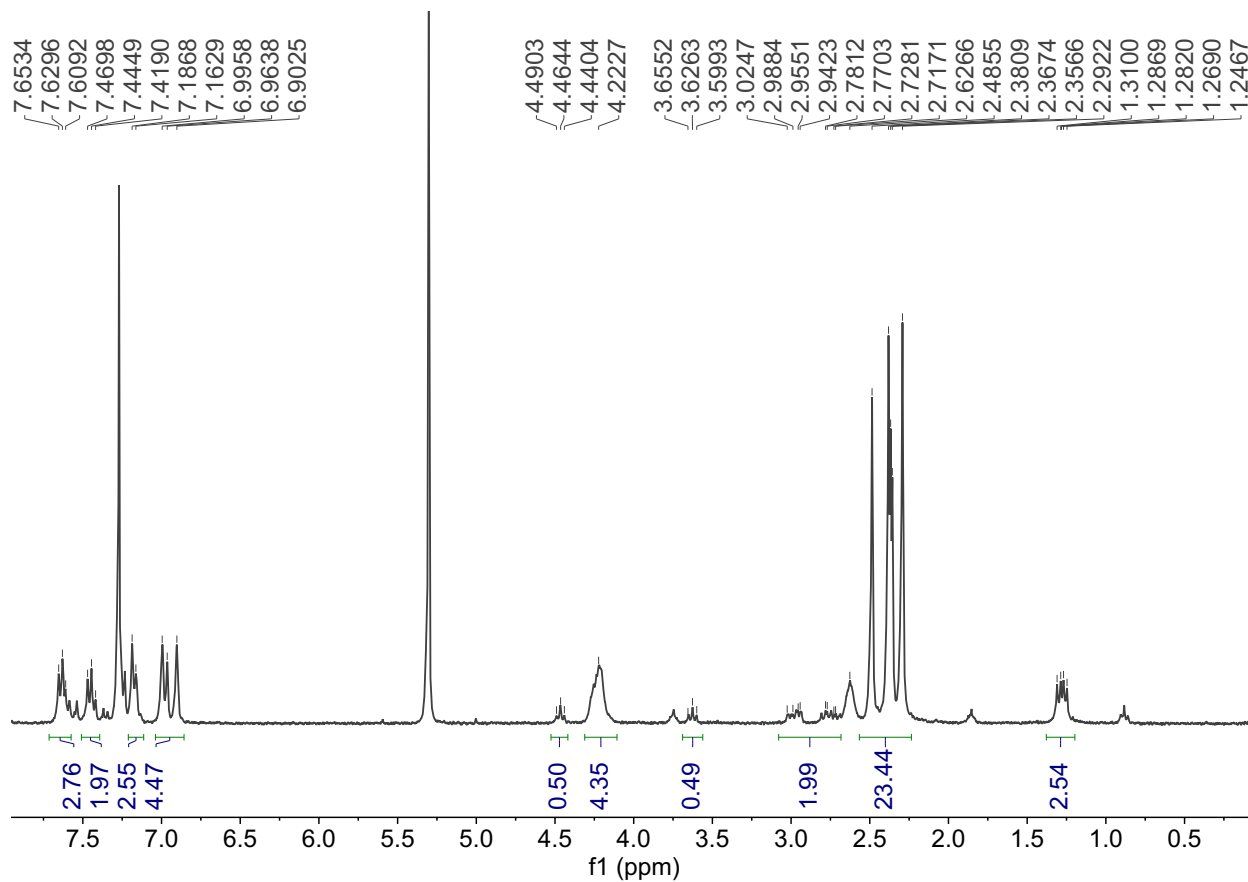
Figure A4: ^{1}H NMR spectrum of **4** taken in CDCl$_3$ using an AV300 spectrometer (300 MHz).
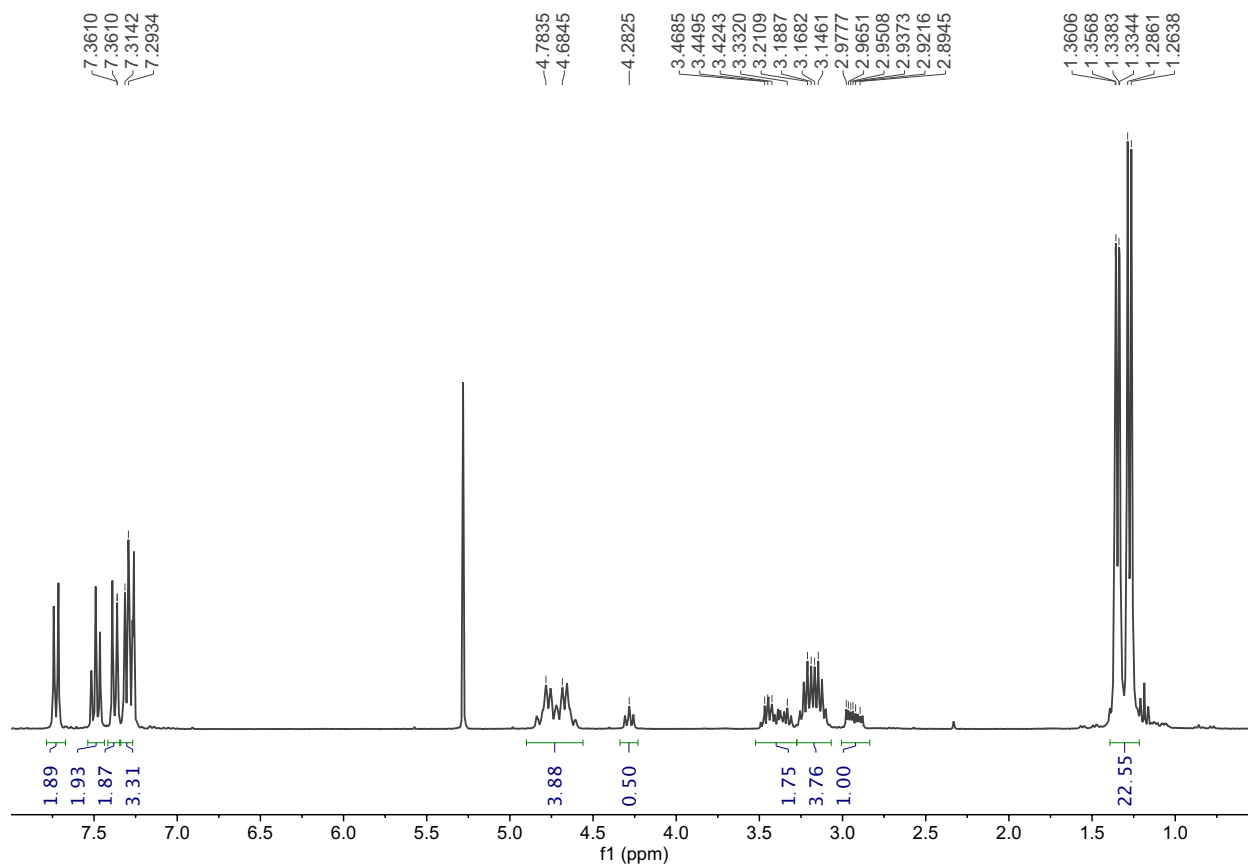
Figure A5: ^{1}H NMR spectrum of **5Cl** taken in CDCl$_3$ using the NEO300 spectrometer (300 MHz).
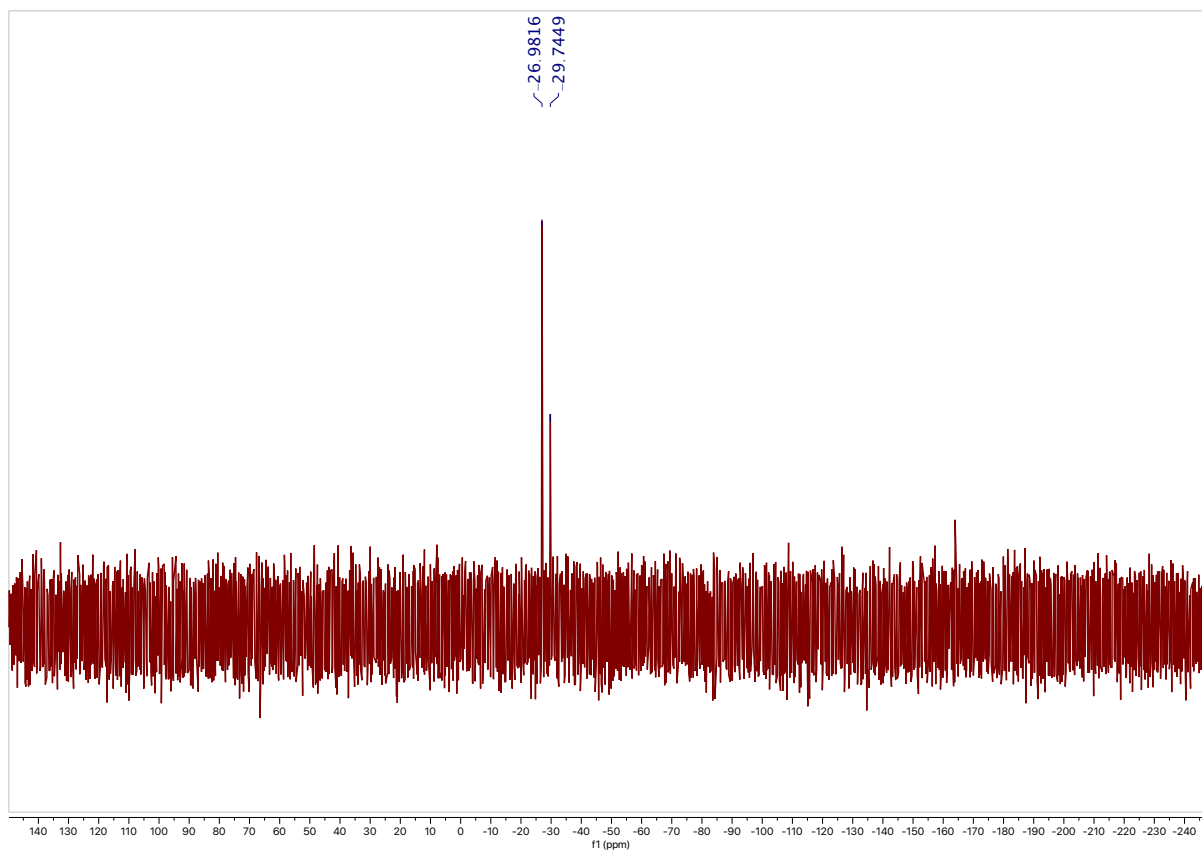
Figure A6: ^{31}P NMR spectrum of enol tautomer (–26.98 ppm) formed *in situ* from pentane soluble fraction taken on the NEO300 NMR spectrometer in benzene-d$_6$ (121 MHz).
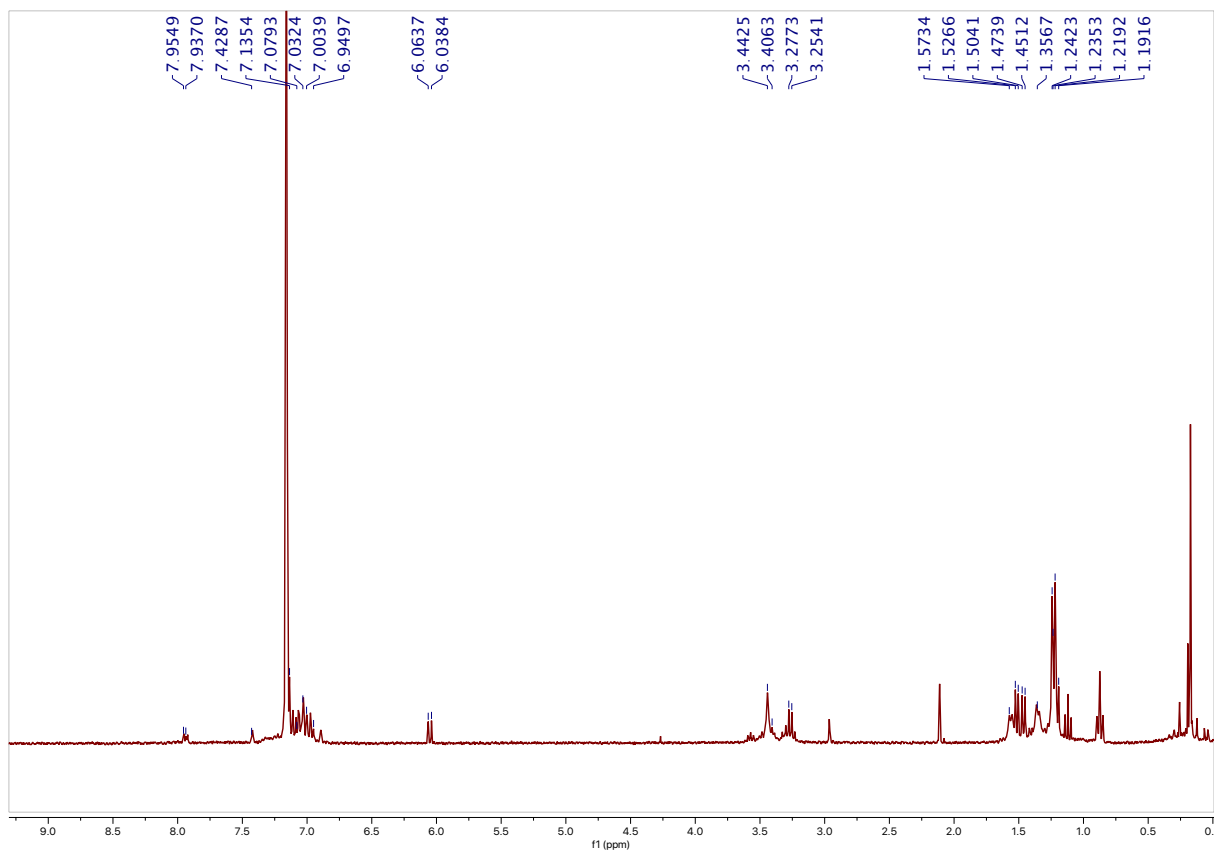
Figure A7: ^{1}H NMR evidence of enol tautomer formed *in situ* taken on NEO300 NMR spectrometer in benzene-d$_6$ (300 MHz). Residual HN(SiMe$_3$)$_2$ is observed in this spectrum.
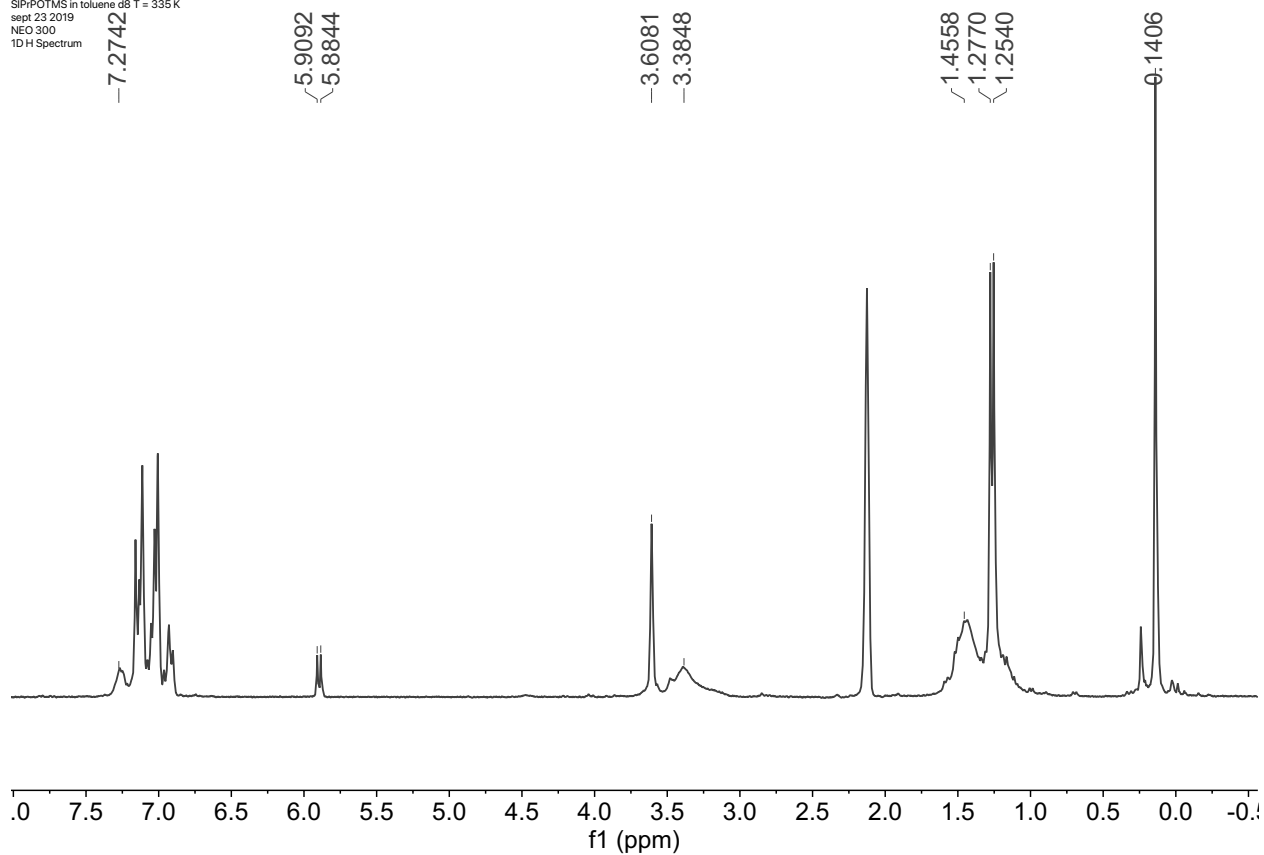
Figure A8: ^{1}H NMR spectrum of **10** taken at 335 K in toluene-d^8 using a NEO300 spectrometer (300 MHz).
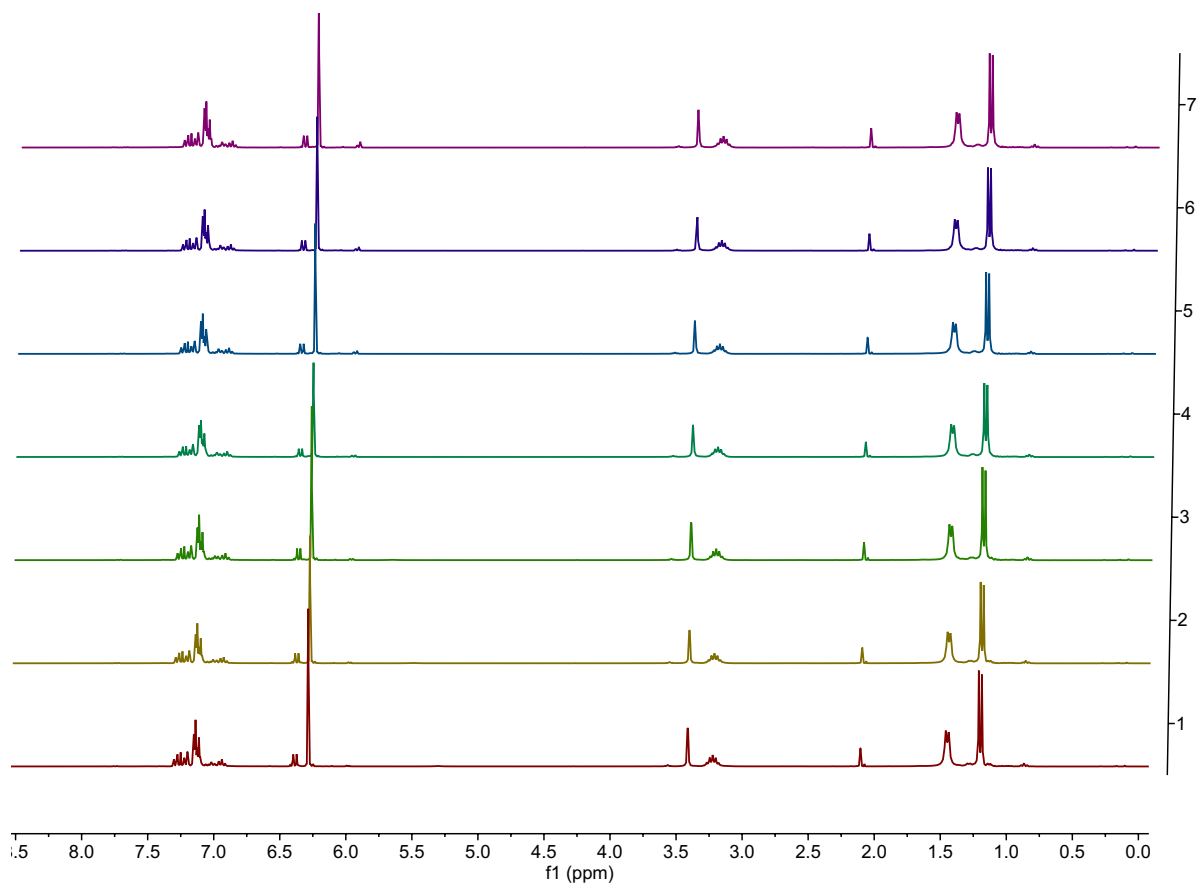
Figure A9: ^{1}H NMR spectra of complex taken for thermostability studies of **14** using a NEO300 spectrometer (300 MHz). Spectrum 1 through 7 are taken after 1, 3, 5, 26, 48, 73, and 122 hours at 60 °C respectively.
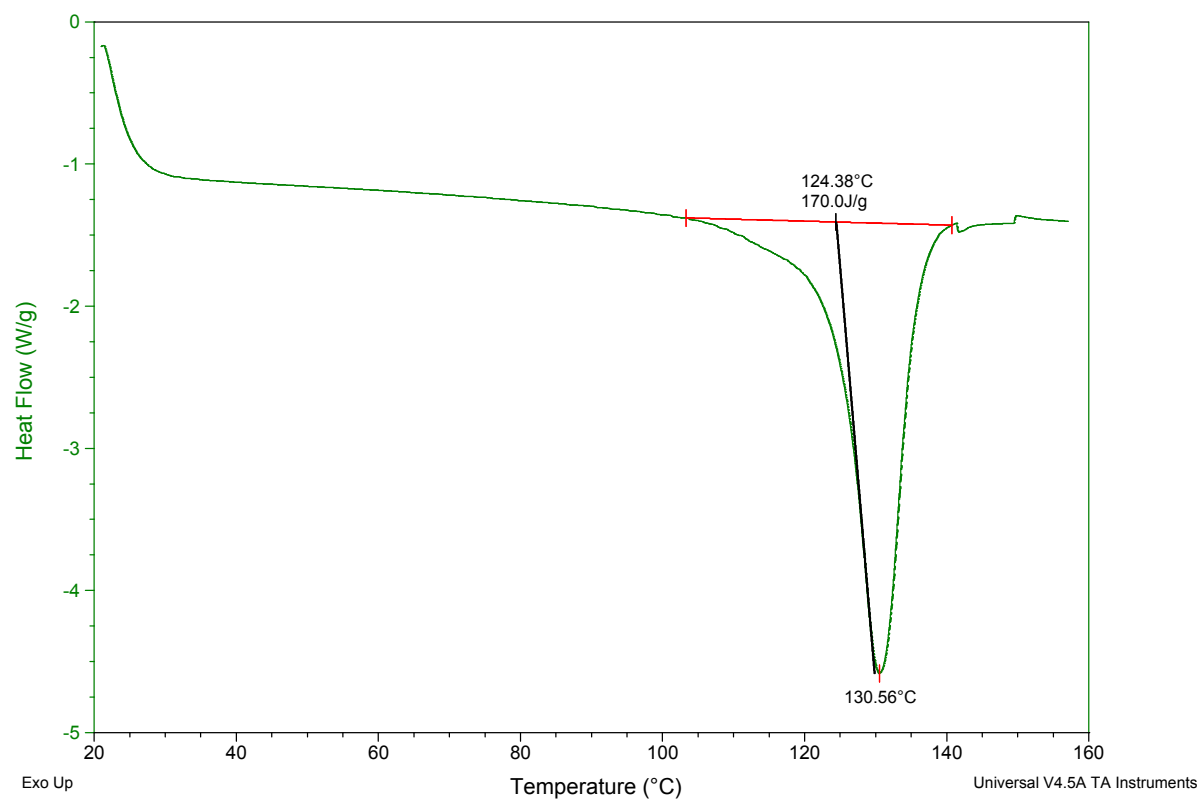
Figure A10: Thermogram of polymer produced by **14** giving melting point and heat capacity of the polyethylene produced.
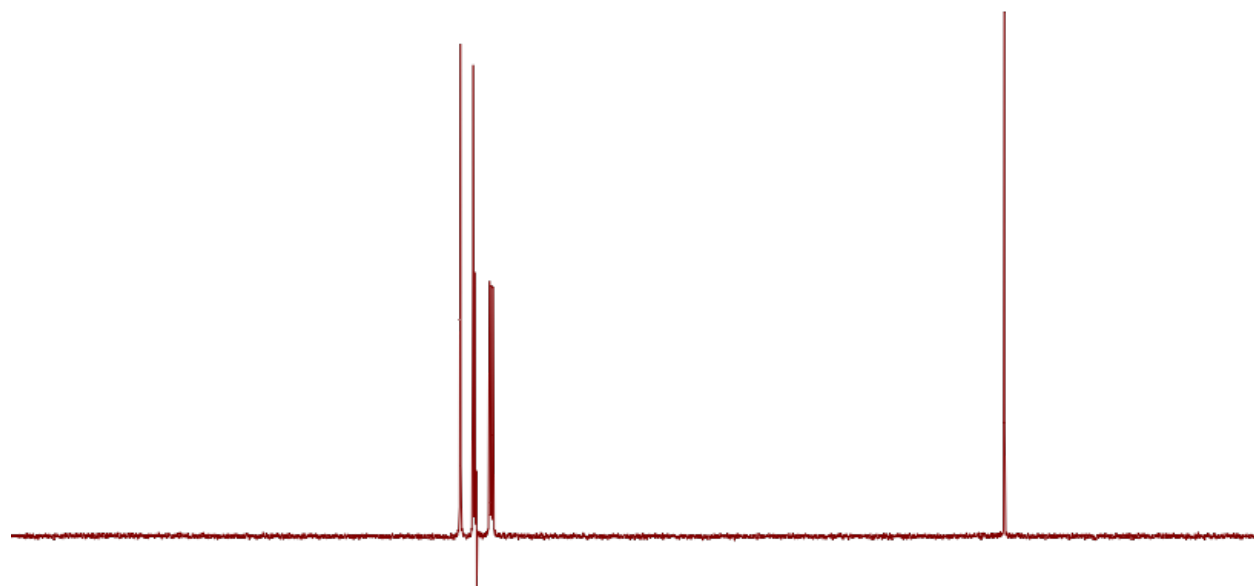
**Figure A11:** ^{13}C NMR of polyethylene produced by **14** taken in 1,2-dichlorobenzene-d4 at 145 °C using the NEO300 spectrometer (300 MHz).

1H NMR spectrum of PE (no. of scans = 128, d1 = 5s)
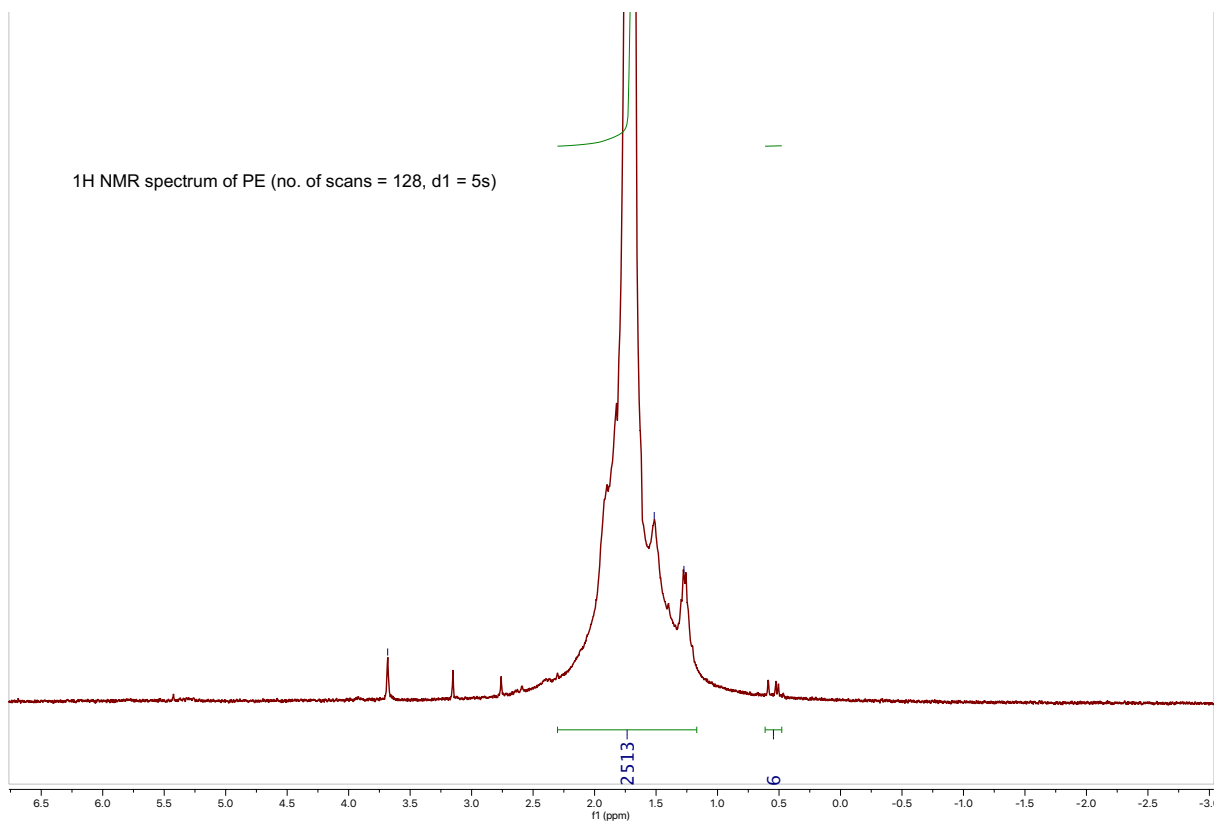
Figure A12: ^{1}H NMR of polyethylene produced by **14** taken in 1,2-dichlorobenzene-d4 at 145 °C using the 300 spectrometer (300 MHz).